CHALMERS

UNIVERSITY OF TECHNOLOGY

From pair-wise interactions
to triplet dynamics

Master's thesis in Engineering Mathematics and Computational Science

Björn Vessman

From pair-wise interactions to triplet dynamics

BJÖRN VESSMAN

Department of Mathematical Sciences
Chalmers University of Technology
Gothenburg, Sweden 2015

From pair-wise interactions to triplet dynamics
BJÖRN VESSMAN

From pair-wise interactions to triplet dynamics
Björn Vessman
Department of Mathematical Sciences
Chalmers University of Technology

Abstract

The present thesis investigates the properties of a system of ordinary differential equations, that describes cross-feeding in two- and three-species systems of bacteria. The system is studied statistically and the probability of permanence — a stable state where no species is driven extinct — is computed under the assumption that the energy-uptake parameters of the system are either independent or organised in a hierarchy where any excreted metabolites carry less energy than previous nutrients. For a system of two species, we derive the probability of permanence analytically. For three-species systems, we differentiate between different modes of coexistence with respect to boundary behaviour of the system. We are able to show that the affine fitness function described by Lundh & Gerlee (Lundh, T., Gerlee, P., *Bull Math Biol*, **75**, 2013) is equivalent to the linear fitness function investigated by Bomze (Bomze, I. M., *Biol Cybern*, **48**, 1983) and hence that the dynamics derived by Bomze holds for the cross-feeding paradigm of Lundh & Gerlee. For the question implicit in the title of the thesis, the pair-wise interactions of a three-species system are not enough to draw any deterministic conclusions on permanence of the triplet. We find, however, that the probability of permanence is close to 50% for systems with three coexistent pairs on the boundary and for so-called intransitive systems. Systems with two and one coexistent pairs on the boundary are more likely to exist for random interactions parameters, but are not as likely to be permanent.

Acknowledgements

Contents

Contents

x

1

Introduction

Many bacterial species interact by exchanging nutrients in a process called cross-feeding or syntrophy. Typically, one of the present bacterial strains consumes a primary nutrient, degrading it partially or fully into a secondary metabolite which is then processed by one or more of the other species [8]. The degradation process may be non-sequential, in the sense that the involved species may consume and further degrade metabolites from any step in the chain starting with the primary nutrient. The change in the proportion of a given species in a population — denoted the species frequency — depends on the rate of replication, i.e., the fitness of the species, which in turn depends on the frequencies of other species that produce nutrients. If the species of an ecosystem do not go extinct, then we may say that the species are co-existent, a concept that is made more precise in Section 1.3.1. Important examples of real-world systems that exhibit cross-feeding are the human gut flora [1], the interactions between sulfate-reducing bacteria and methane oxidisers in the deep sea [12, 17], the degradation of pesticides [15], and in soil nitrification [5]. When considering experimental set-ups or the design of plants for degradation of toxins that consist of multiple species, one needs to know if the species are coexistent and at what frequencies. Furthermore, it is important to study how coexistence in a population is affected when the environment changes.

The dynamics of infinite and well-mixed populations of cross-feeding bacteria can be described by a system of coupled non-linear autonomous ordinary differential equations (ODEs) known as replicator equations [16]. The assumption well-mixedness allows us to disregard any spatial dependencies of the population and in an infinite population, the births and deaths of individuals would need to be considered, prompting a stochastic model. The replicator system of equations has its origin in game theory [14] where it describes an evolutionary game of n strategies and d players [10]. The dynamics of the game consists of the change of the relative amount of the involved strategies. In species populations, the equations model the rate of change of species frequencies based on their fitness in an environment [2, 14]. In the present setting, the fitness of a species is based on the amount of energy that the species may extract from the available nutrients, so that the dynamics of the system of equations is determined by the interactions parameters that describe how much energy a given species can extract from a nutrient excreted by another species. Comparison to the game-theoretical framework shows that the n strategies and d players correspond to n species and d steps in the metabolic process. Cross-feeding systems for two species have been studied by Lundh & Gerlee [16], where the authors derive conditions for permanence, a stable co-existence where no involved species will go extinct.

The dynamics of a cross-feeding ecosystem need not be modelled in the game-theoretical framework of the replicator system [16]. Other ODE systems have been based on cross-feeding proportional to the frequency of the reciprocal species [4, 7],

on the difference of nutrient uptake and mortality [15], or on adaptive dynamics [6]. Agent-based models have been investigated by Gerlee & Lundh [8], whereas Pfeiffer & Bonhoeffer [18] have studied the evolution of cross-feeding as a result of optimal ATP energy production.

1.1 Purpose

The aim of this Master's thesis is to study qualitative and quantitative features of replicator systems of two and three species, and in particular to establish properties of the three-species system based on properties of pair-wise interactions between the constituent species. The first part of the thesis investigates how different random models for the interactions parameters affect the qualitative dynamics of two species, i.e., if one species dominates or if co- existence occurs. When considering three species, the general properties of permanent systems will be outlined before a few special cases are discussed. So-called pair-wise intransitive dynamics are of special interest since a subset of these systems are known to form co-existing triplets [2, 14]. Pair-wise intransitivity for a triplet of species x, y and z means that the species form pairs similar to those in a game of rock-paper-scissors, i.e., that species x has a competitive advantage over species y which has an advantage over z, and finally that species z has an advantage over x [16]. The other special cases is known as pair-wise coexistence and involves one more coexistent pairs of the species triplet.

The analysis of the three-species systems is based on statistical simulations on the same random models that are used in the investigation of two-species systems. In particular, we look at how qualitative features of the two-species system map to three-species dynamics. If three species co-exist pairwise, how likely are they to co-exist in unison? Also, is it possible to find interactions parameters for which this is guaranteed? The answer to these questions are important in bacterial ecology where it is of interest to be able to predict multi-species dynamics from pair-wise experiments.

Lundh & Gerlee [16] considers five different scenarios for the behaviour of the two-species system whereas Bomze [2] investigates similar properties of three-species systems based on the number of fixed points, their location and stability. The project at hand will also study how these two classifications correspond.

The thesis will not consider dynamics for populations greater than three and will not consider more than two levels of metabolisation as described by Lundh & Gerlee [16]. Furthermore, the strategies that define the species will be considered fixed and static. The project will not consider evolution of strategies.

1.2 Methods

Theory on the stability of solutions to replicator systems that model species interactions [2, 14, 10, 16] will be followed in order to determine properties of the replicator systems for different parameter models. Primarily, the interactions parameters will be modelled in two ways: either as independent or according to a model that is hierarchical in the sense that energy gains further down in the metabolisation chain will be lower than energy gains from primary metabolites. For this model, coexis-

tence criteria similar to those for independent and arbitrary parameters [16] will be derived.

The series expansion [16] for the replicator fitness function is implemented for simulations of two- and three-species systems, in order to estimate the probability that the derived criteria for coexistence hold. For a given parameter model, random interactions parameters are drawn according to the independent or hierarchical model and the probability of permanence is estimated from the coexistence criteria.

1.3 Preliminaries

Before delving into the analysis of coexistent two- and three-species systems, let us review the model. We largely follow the notation of Lundh & Gerlee [16] while using methods and notations of Bomze [2] where convenient.

1.3.1 Replicator system of equations

The replicator system of equations for a population $\mathbf{x} = (x_1, x_2, \ldots, x_n)$ of species $i = 1, 2, \ldots, n$ with individual frequencies, i.e., fractions of the whole population, x_i is defined as

$$\begin{cases} \dot{x}_i & = (\phi_i(\mathbf{x}) - \bar{\phi}(\mathbf{x}))x_i, \\ \bar{\phi}(\mathbf{x}) & = \sum_{k=1}^{n} x_k \phi_k(\mathbf{x}), \end{cases} \tag{1.1}$$

where $\dot{x}_i$ denotes the derivative with respect to time of a species frequency, $\phi_i(\mathbf{x})$ is the species fitness function and $\bar{\phi}(\mathbf{x})$ is the average fitness in the population. Intuitively, this means that a species that is fitter than the population average will increase in proportion to its current frequency and a species less fit than the average will decrease correspondingly. In order to discuss coexistence between species, we need to properly define permanence of a system [16].

Definition 1. A replicator system (1.1) is considered *permanent* if for all initial states $\mathbf{x}^0 > 0$, we have that $x_i(t) > 0$ for all species $i = 1, 2, \ldots, n$ and all $t \geq 0$.

The fitness function models, in its simplest state, how populations change in an environment based on their frequency and fitness in the current population. In the present thesis, we will consider the fitness of a species to be the amount of energy that a species can extract from the available nutrients. Bomze [2] describes the fitness function as

$$\phi_i = \sum_{j=1}^{n} a_{ij} x_j, \tag{1.2}$$

where the payoff matrix $A = [a_{ij}]_{i,j=1}^n$ describes the outcome of the game when species i meet species j. An evolutionary game described by a linear fitness function based on a payoff matrix, as above, is said to be given on normal form [14] and the replicator system with such a fitness function can be called homogenous [9]. The elements of a general normal-form payoff matrix are

$$A = \begin{cases} 0, & i = j \\ k_{ij} \in \mathbb{R}, & i \neq j \end{cases}, \tag{1.3}$$

i.e., a game where any strategy played against itself will yield nothing. If a payoff matrix is not given in this zero-diagonal form, it may be transformed as such since the dynamics of the replicator system (1.1) does not change under column-wise addition of constants to the replicator system [2].

A fixed point of a system of ordinary differential equations $\dot{\mathbf{x}} = \mathbf{f}(\mathbf{x})$ is a point $\mathbf{x}^*$ in the domain of $\mathbf{f}$ such that $\mathbf{f}(\mathbf{x}^*) = 0$. For the replicator system, the domain of definition for $\mathbf{f}$ is the simplex

$$S_{n-1} = \left\{ \mathbf{x} \in \mathbf{R}^n | x_i \geq 0, \ \sum_{i=1}^{n} x_i = 1 \right\}, \tag{1.4}$$

due to the requirement that the species frequencies are positive and defined as fractions of the whole population. The stability of the fixed points is determined [14] by the eigenvalues of the Jacobian

$$J(\mathbf{x}^*) = \left[\frac{\partial f_i(\mathbf{x})}{\partial x_j} |_{\mathbf{x}=\mathbf{x}^*} \right]_{i,j}. \tag{1.5}$$

The number of fixed points, their location and stability is the basis for the classification of solutions to the system (1.1). Whether a fixed point is located on the boundary of the domain of $\mathbf{f}$ or in the interior of the domain of $\mathbf{f}$ is of special interest, since a permanent system is characterised by either a stable interior fixed point or a non-edge cyclic trajectory around a center fixed point. In the permanent case, we have $x_i > 0$ for all species i and thus that the interior fixed point $\mathbf{x}^*$ must satisfy $\phi_i(\mathbf{x}^*) - \bar{\phi}(\mathbf{x}^*) = 0$, which means

$$\phi_1(\mathbf{x}^*) = \phi_2(\mathbf{x}^*) = \ \dots \ = \phi_n(\mathbf{x}^*). \tag{1.6}$$

1.3.2 Replicator system for cross-feeding

For the cross-feeding model at hand, we use the series expansion fitness function [16], where it is assumed that the fitness of a species depends on its capacity to metabolise the available nutrients. To derive the fitness function, assume that the uptake $r(s_j)$ of a nutrient s_j is the same for all species and proportional to the available amount of the substance so that

$$r(s_j) = \kappa s_j, \tag{1.7}$$

for all metabolites j and species $i = 1, 2, \ldots, n$. Furthermore, it is assumed that metabolism is faster than population dynamics and that the nutrient uptake κ is the same for all species, so that the steady-state nutrient concentrations are

$$s_0 = \frac{\gamma}{\gamma + \kappa}, \tag{1.8}$$

for the primary resource s_0, and

$$s_i = \frac{\kappa \gamma}{(\gamma + \kappa)^2} x_i, \tag{1.9}$$

for the derived metabolites s_i, where γ is the inflow of the primary nutrient into the system. The fitness of a species i in a cross-feeding population is assumed to be dependent on how much energy $\mathcal{E}_i$, $\mathcal{E}_{ij}$ the species can extract from the primary nutrient s_0 and the derived metabolites s_i. For an illustration of the hierarchy of metabolites and energy extraction, see Figure 1.1. Any interactions of higher order than two are assumed small so that the fitness of a species i is considered to be the total energy uptake,

$$\phi_i(\mathbf{x}) = \eta\gamma\mathcal{E}_i + \eta^2\gamma\sum_j \mathcal{E}_{ji}x_j. \tag{1.10}$$

where the quantity

$$\eta = \frac{\kappa}{\kappa + \gamma}, \tag{1.11}$$

that describes the relation of the nutrient uptake coefficient κ to the nutrient inflow rate γ, is introduced so that $\kappa s_0 = \eta\gamma$ and $\kappa s_j = \eta^2\gamma x_j$. Note that (1.10) implies that a general form of the fitness functions is conveniently written in matrix-vector form as

$$\phi(\mathbf{x}) = \eta\gamma\mathcal{E} + \eta^2\gamma\underline{\mathcal{E}}^T\mathbf{x}, \tag{1.12}$$

where $\phi : \mathbb{R}^n \to \mathbb{R}^n$ is the vector-valued fitness function dependent on the individual fractions $\mathbf{x}$, $\mathcal{E}$ denotes the vector of first-order energy uptake and $\underline{\mathcal{E}} = [\mathcal{E}_{ij}]_{i,j}$ is the matrix of second-order energy uptake. All elements of $\mathcal{E}$ and $\underline{\mathcal{E}}$ are positive, as they model the energy extracted from a nutrient.
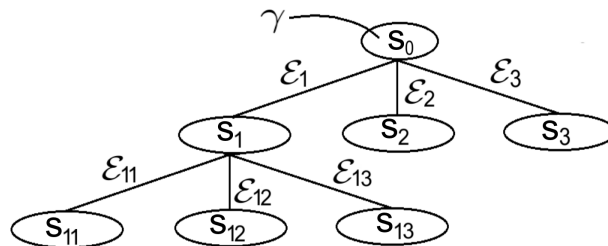
Figure 1.1: First-order energy uptake $\mathcal{E}_i$ for species i from the primary nutrient S_0 that flows into the system at a rate γ, second-order metabolism $\mathcal{E}_{ij}$ for species j from nutrient S_i.

1.3.3 Two-species system

For two bacterial species α, β with frequencies $\mathbf{x} = [x, 1-x]^T$ and $x \in [0, 1]$, the fitness functions are

$$\phi_\alpha(x) = \eta\gamma\mathcal{E}_\alpha + \eta^2\gamma(\mathcal{E}_{\alpha\alpha}x + \mathcal{E}_{\beta\alpha}(1-x)), \text{ and} \tag{1.13}$$
$$\phi_\beta(x) = \eta\gamma\mathcal{E}_\beta + \eta^2\gamma(\mathcal{E}_{\alpha\beta}x + \mathcal{E}_{\beta\beta}(1-x)), \tag{1.14}$$

with the corresponding average fitness

$$\bar{\phi}(\mathbf{x}) = x\phi_\alpha(\mathbf{x}) + (1-x)\phi_\beta(\mathbf{x}). \tag{1.15}$$

The two-species replicator system with fitness functions (1.13) and (1.14) is scalar due to the requirement that the frequencies sum to unity and may be written as

$$\frac{dx}{dt} = x(1-x)(\phi_\alpha(x) - \phi_\beta(x)). \tag{1.16}$$

The right hand side $f(x) = x(1-x)(\phi_\alpha(x) - \phi_\beta(x))$ of this replicator equation has a Jacobian

$$f'(x^*) = (1-2x)(\phi_\alpha(x) - \phi_\beta(x)) + x(1-x)(\phi'_\alpha(x) - \phi'_\beta(x))|_{x=x^*}. \qquad (1.17)$$

This derivative is a second-order polynomial, which allows for at most one stable fixed point in the interior of the domain $S_1 = [0,1]$. The system will have a stable interior fixed point when the boundary points $x_1^* = 0$ and $x_2^* = 1$ are unstable, i.e., when $f'(x_k^*) > 0$, $k = 1, 2$ [16]. If a replicator system has a stable interior fixed point it is said to exhibit permanence, since no species present at the initial state $\mathbf{x}(0) = \mathbf{x}_0$ will go extinct. Hence, using (1.17) we may put the conditions for permanence of the two-species system as

$$f'(0^+) = \phi_\alpha(0) - \phi_\beta(0) = \eta\gamma(\mathcal{E}_\alpha - \mathcal{E}_\beta - \eta(\mathcal{E}_{\beta\beta} - \mathcal{E}_{\beta\alpha})) > 0, \text{ and} \qquad (1.18)$$
$$f'(1^-) = -(\phi_\alpha(1) - \phi_\beta(1)) = \eta\gamma(\mathcal{E}_\beta - \mathcal{E}_\alpha - \eta(\mathcal{E}_{\alpha\alpha} - \mathcal{E}_{\alpha\beta})) > 0. \qquad (1.19)$$

For convenience, the following coordinates are introduced to give a comprehensive illustration of the two conditions (1.18) and (1.19),

$$\xi_\alpha = \eta(\mathcal{E}_{\alpha\beta} - \mathcal{E}_{\alpha\alpha}) - (\mathcal{E}_\alpha - \mathcal{E}_\beta), \text{ and} \qquad (1.20)$$
$$\xi_\beta = \eta(\mathcal{E}_{\beta\alpha} - \mathcal{E}_{\beta\beta}) - (\mathcal{E}_\beta - \mathcal{E}_\alpha), \qquad (1.21)$$

meaning that the conditions (1.18) and (1.19) can be stated as $\xi_\alpha > 0$, $\xi_\beta > 0$.

1.3.4 Three-species system

In a three-species replicator system, the discussion of permanence is somewhat more involved than in the two-species case since there is the possibility of stable interior fixed points as well as stable and unstable fixed points anywhere on the boundary of the system. Bomze [2, 3] characterises no less than 49 different types of phase portraits for a three-species replicator system, with the main division being the number of fixed points in the interior [2] of the simplex

$$S_2 = \left\{ x \in \mathbb{R}^3 | x_i \geq 0, \ \sum_{i=1}^{3} x_i = 1 \right\}. \qquad (1.22)$$

A sketch of the state space S_2 of the three-species replicator system is shown in Figure 1.2 a). In the following sections, any example and simulated systems will be visualised by their trajectories on the state space, which will be shown as the example in Figure 1.2 b) and called phase portraits.
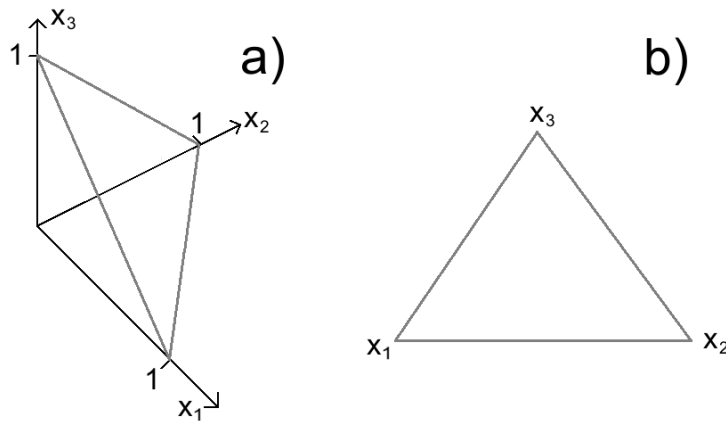
Figure 1.2: a) Sketch of state space (1.22) of the three-species replicator system. b) state space view as used for example systems.

Out of the phase portraits described by Bomze [2], nine exhibit permanence as of Definition 1 and five of these have a unique interior fixed point. The trajectories of the systems with phase portrait numbers 7, 9, 15 and 17 converge to the stable fixed point regardless of initial state [2]. We will also consider phase portrait number 16 — which describes a set of trajectories cycling a center fixed point, independently of the initial state — to be permanent. Of the other phase portraits, we have that nine are conditionally permanent, meaning that there are initial states in the interior of the simplex such that trajectories converge to fixed points on the simplex boundary — and one portrait with cyclic trajectories that may be reached from some initial states [2].

A replicator system of more than two species may exhibit pair-wise intransitivity, per Definition 2 of Lundh & Gerlee [16]. The definition being that the pair-wise fixed points $(x_i, x_{i+1}) = (1, 0)$ and $(x_i, x_{i+1}) = (0, 1)$, for $i = 1, 2, \ldots, n$ and $i + 1$ modulo n, and are unstable and stable, respectively. This means that the three-species system have no non-corner fixed points on the edges of S_2 and, as each corner is semi-stable, that trajectories along the edge between corners tend from one corner to another only to continue along the next edge at any perturbation. For an illustration, see Figure 1.3. This is interpreted as species $i + 1$ outcompetes species i in isolation from the third species. Furthermore, it is proven [16] to be equivalent to the criteria

$$\mathcal{E}_i - \mathcal{E}_j + \eta(\mathcal{E}_{ji} - \mathcal{E}_{jj}) > 0 \tag{1.23}$$
$$\mathcal{E}_i - \mathcal{E}_j + \eta(\mathcal{E}_{ii} - \mathcal{E}_{ij}) > 0 \tag{1.24}$$

for all pairs $(i, i + 1)$ where we consider $i + 1$ modulo n.

7
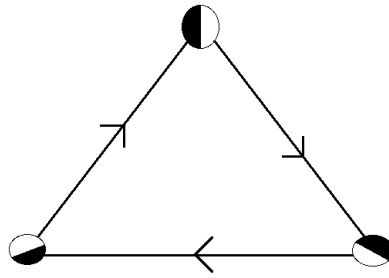
Figure 1.3: Sketch of pair-wise intransitive system. Each corner is semi-stable — where a filled dot denotes the stable side and an empty denotes the unstable side — so that trajectories on the boundary are cyclic.

Another form of coexistence is formed from pair-wise coexistence in the population. In this scenario, each pair of species are coexistent when isolated from the third species, so that there exists a stable or semi-stable fixed point on one or more of the non-corner boundaries of the simplex. This case is studied in Section 3.5.

2

Two-species coexistence

In this chapter, we study the two-species system in detail. The permanence conditions are due to Lundh & Gerlee [16] and the analytical investigation is based on modeling the unknown energy uptake parameters $\mathcal{E}_i$, $\mathcal{E}_{ij}$ as random variables and computing the probability of permanence. The analytical probability is compared to numerical simulations of replicator systems in Section 4.1, where the parameters are sampled randomly from two example distributions, the Uniform and the Exponential distribution. We will consider two models for the relation of $\mathcal{E}_i$, $\mathcal{E}_{ij}$, namely, that the parameters are either independent or exhibits a tree-like dependence, where for a given species i we have that any second-order uptake $\mathcal{E}_{ij}$ is required to be less than the corresponding first-order uptake $\mathcal{E}_i$, i.e., $\mathcal{E}_{ij} < \mathcal{E}_i$. The analytical results are then to be compared to simulations, where we classify the systems as either being permanent with a stable fixed point in the interior $\mathbf{x} \in (0,1)$ or non-permanent, where there are no fixed points but $\mathbf{x} = 0$, $\mathbf{x} = 1$ or a fixed point that is (formally) located outside $[0,1]$.

2.1 Independent model

The independent model for the energy uptake parameters $\mathcal{E}_i$ and $\mathcal{E}_{ij}$ assume that there is no dependence between the parameters, but does not specify how the parameters are distributed, when viewed as random variables. The conditions for permanence of the two-species replicator system are

$$\xi_\alpha = \eta(\mathcal{E}_{\alpha\beta} - \mathcal{E}_{\alpha\alpha}) - (\mathcal{E}_\alpha - \mathcal{E}_\beta) > 0 \tag{2.1}$$

$$\xi_\beta = \eta(\mathcal{E}_{\beta\alpha} - \mathcal{E}_{\beta\beta}) - (\mathcal{E}_\beta - \mathcal{E}_\alpha) > 0 \tag{2.2}$$

from which we may compute analytically the probability $\mathrm{P}(\xi_\alpha > 0, \; \xi_\beta > 0)$ of having a permanent two-species replicator system.

The criteria of permanence for the two example distributions are described in Sections 2.1.1-2.1.2 below. The Uniform distribution models the scenario where the energy extraction parameters are evenly distributed and normalised onto the interval $(0,1)$. In order to take non-uniformity into account, the Exponential distribution is used as an alternative. In the Exponential model, any amount of energy may be extracted in a given metabolism step, but the probobolity of a level of energy uptake decreases exponentially with the energy at a rate λ.

2.1.1 Uniformly distributed parameters

Consider the metabolism parameters $\mathcal{E}_i$ of (1.13) and $\mathcal{E}_{ij}$ of (1.14) as a collection of six random variables $\mathcal{E}_i \sim \mathrm{Uni}(0,1)$ and $\mathcal{E}_{ij} \sim \mathrm{Uni}(0,1)$ for $i = \alpha, \beta$ and $j = \alpha, \beta$. Then ξ_α of (1.20) and ξ_β of (1.21) are functions mapping the probability states

onto the interval $[-1-\eta, 1+\eta]$ according to a certain distribution and we have the probability of permanence

$$P(\xi_\alpha > 0, \xi_\beta > 0) = \int_\Omega f_{\mathbf{X}}(\mathbf{x}) \mathcal{I}_{\{\xi_\alpha > 0, \xi_\beta > 0\}} d\Omega, \tag{2.3}$$

for the indicator function $\mathcal{I}$ defined on the hypercube $\Omega = \{\mathbf{x} \in [0,1]^6\}$ and the joint density $f_{\mathbf{X}}(\mathbf{x})$ for the vector $\mathbf{X}$ of random variables. For simplification, note that for $\mathcal{E}_\alpha, \mathcal{E}_\beta \sim \text{Uni}(0,1)$ we have that $Z = \mathcal{E}_\alpha - \mathcal{E}_\beta \sim \text{Tri}(-1,1)$, where $\text{Tri}(-1,1)$ denotes the triangle distribution with density function

$$f_{Tri}(z) = \begin{cases} 0 & \text{if } z \notin [-1,1) \\ 1+z & \text{if } z \in [-1,0) \\ 1-z & \text{if } z \in [0,1) \end{cases}. \tag{2.4}$$

The derivation of this distribution can be found in Appendix B.1.1 and its distribution function is shown in Figure 2.1.
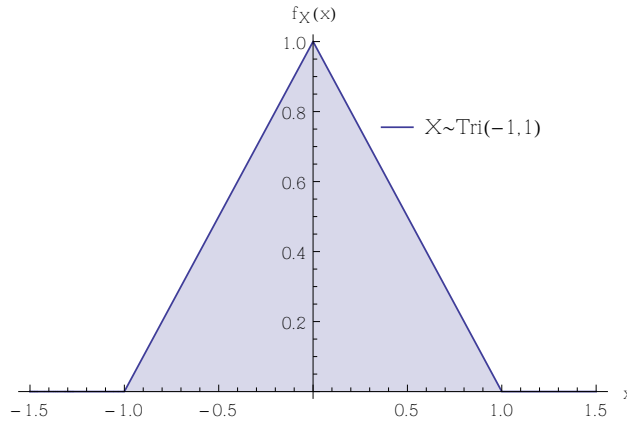
Figure 2.1: Triangle probability density function (2.4).

Similarly, we denote $X = \mathcal{E}_{\alpha\beta} - \mathcal{E}_{\alpha\alpha}$ and $Y = \mathcal{E}_{\beta\alpha} - \mathcal{E}_{\beta\beta}$, both of which are distributed as Tri(-1,1) for the same reason as Z. With these substitutions, we can express ξ_α and ξ_β as

$$\xi_\alpha = \eta X - Z, \text{ and} \tag{2.5}$$
$$\xi_\beta = \eta Y + Z. \tag{2.6}$$

The probability (2.3) can now be expressed as

$$P(\xi_\alpha > 0, \xi_\beta > 0) = \int_{\mathbb{R}} \int_{\mathbb{R}} \int_{\mathbb{R}} f_{X,Y,Z}(x,y,z) \mathcal{I}_{\{\eta x - z > 0\}} \mathcal{I}_{\{\eta y + z > 0\}} \, dz \, dy \, dx, \tag{2.7}$$

where $\mathcal{I}_S$ is the indicator function of the set S. By assumption, the joint distribution

$$f_{X,Y,Z}(x,y,z) = f_X(x) f_Y(y) f_Z(z) \tag{2.8}$$

due to independence, and the individual distribution functions $f_X(x)$, $f_Y(y)$, $f_Z(z)$ are the triangular distribution (2.4). The indicator functions are defined as

$$\mathcal{I}_{\{\eta x - z > 0\}}(x, z) = \begin{cases} 1 & \text{if } z < \eta x \\ 0 & \text{otherwise} \end{cases}, \tag{2.9}$$

and

$$\mathcal{I}_{\{\eta y + z > 0\}}(y, z) = \begin{cases} 1 & \text{if } z > -\eta y \\ 0 & \text{otherwise} \end{cases}. \tag{2.10}$$

The probability (2.3) is

$$P(\xi_\alpha > 0, \xi_\beta > 0) = \frac{\eta}{30}(7 - 2\eta), \tag{2.11}$$

and the calculation is found in Appendix B.2.1. The probability of permanence is a quadratic function of the parameter η (1.11) with a local maximum that is outside the domain of definition $D_{P(\eta)} = \{\eta \in [0, \ 1)\}$, so that the function is increasing as shown in Figure 2.2.
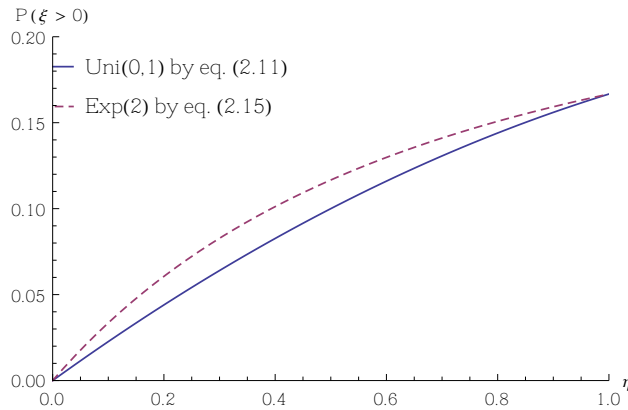
Figure 2.2: Probability of permanence $P(\xi_\alpha > 0, \xi_\beta > 0)$ as function of η for Uni(0, 1) and Exp(2)-distributed $\mathcal{E}_i$, $\mathcal{E}_{ij}$ by (2.11) and (2.15), respectively.

2.1.2 Exponentially distributed parameters

We now assume that the interactions parameters are random variables $\mathcal{E}_i$, $\mathcal{E}_{ij} \sim$ Exp(λ), where the density function for a random variable $X \sim$ Exp(λ) is

$$f_X(x) = \begin{cases} \lambda e^{-\lambda x}, & x \geq 0 \\ 0, & x < 0 \end{cases}. \tag{2.12}$$

Then the random variables that describe the differences $X = \mathcal{E}_{\alpha\beta} - \mathcal{E}_{\alpha\alpha}$, $Y = \mathcal{E}_{\beta\alpha} - \mathcal{E}_{\beta\beta}$ and $Z = \mathcal{E}_\alpha - \mathcal{E}_\beta$ of (2.1)-(2.2) are Laplace(0, λ)-distributed with mean 0 and rate λ [11]. The distribution function of $Z \sim$ Laplace(0, λ) is

$$f_Z(z) = \frac{\lambda}{2} e^{-\lambda|z|}, \tag{2.13}$$

and is defined for real z. The density functions of the corresponding X and Y have the same functional form. The derivation of this distribution is found in Appendix B.1.2, and the graph of the density function — where we have put the parameter $\lambda = 2$ as used in the simulations — is shown in Figure 2.3.
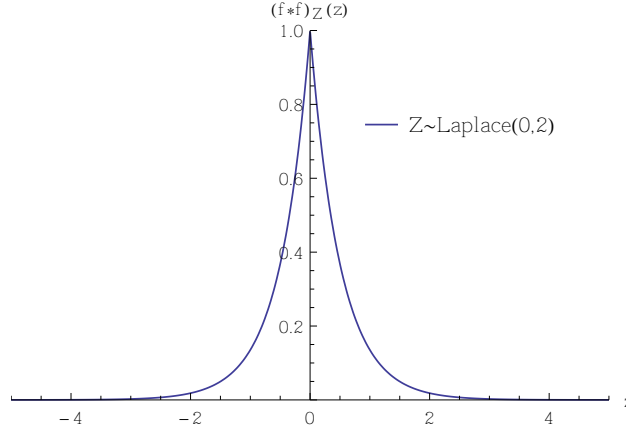
Figure 2.3: Laplace$(0, 2)$ density function (2.13).

With the Laplace-distributed variables X, Y and Z, we may again rewrite the coordinates ξ_α and ξ_β as (2.5)-(2.6) and define the probability of permanence as

$$\mathrm{P}(\xi_\alpha > 0,\ \xi_\beta > 0) = \int_{\mathbb{R}} \int_{\mathbb{R}} \int_{\mathbb{R}} f_{X,Y,Z}(x,y,z) \mathcal{I}_{\{\eta x - z > 0\}} \mathcal{I}_{\{\eta y + z > 0\}} \, dz\,dy\,dx, \qquad (2.14)$$

where we will once again use the assumption of independence of X, Y and Z so that (2.8) holds.

The computation of the probability of permanence is found in Appendix B.2.2 and found to be

$$\mathrm{P}(\xi_\alpha > 0,\ \xi_\beta > 0) = \frac{\eta(3 + \eta)}{2\lambda(1 + \eta)(2 + \eta)}. \qquad (2.15)$$

The graph of the probability, viewed as a function of η, is increasing for $\eta \in [0,\ 1)$ as shown in Figure 2.2, since the derivative

$$\frac{dP}{d\eta} = \frac{(3 + 2\eta)(2 - \eta)}{2\lambda(1 + \eta)^2(2 + \eta)^2}. \qquad (2.16)$$

is positive for $\eta \in [0,\ 1)$.

2.2 Coexistence, tree hierarchy model

The derivations of the coexistence criteria (1.18) and (1.19) put no requirements on the energy extraction parameters $\mathcal{E}_i$ and $\mathcal{E}_{ij}$ except the implicit $\mathcal{E}_i > 0\ \forall i$. Consider now the constraint that the amount of energy extracted at higher levels of cross-feeding is necessarily smaller than the amount extracted from the primary resource, i.e., that for a fixed species i, we have

$$\mathcal{E}_i > \mathcal{E}_{ij} > 0 \qquad (2.17)$$

for all species j. For a more specific hierarchical model, the higher-level interactions $\mathcal{E}_{ij}$ are proportional to $\mathcal{E}_i$ as

$$\mathcal{E}_{ij} = r_{ij}\mathcal{E}_i \tag{2.18}$$

for $r_{ij} \sim \mathrm{Uni}(0,1)$. For this model, we redefine (1.20) and (1.21) to

$$\xi_\alpha = \mathcal{E}_\beta - \mathcal{E}_\alpha[1 - \eta(r_{\alpha\beta} - r_{\alpha\alpha})], \tag{2.19}$$
$$\xi_\beta = \mathcal{E}_\alpha - \mathcal{E}_\beta[1 - \eta(r_{\beta\alpha} - r_{\beta\beta})]. \tag{2.20}$$

Hence, the system is permanent when $\xi_\alpha > 0$ and $\xi_\beta > 0$, i.e., when

$$\mathcal{E}_\beta > \mathcal{E}_\alpha[1 - \eta(r_{\alpha\beta} - r_{\alpha\alpha})], \text{ and} \tag{2.21}$$
$$\mathcal{E}_\alpha > \mathcal{E}_\beta[1 - \eta(r_{\beta\alpha} - r_{\beta\beta})]. \tag{2.22}$$

2.2.1 Uniformly distributed parameters

The probability of permanence (2.3) is defined in the same way as in the independent model for the parameters, with the addition that the relation (2.18) will make the indicator function $\mathcal{I}_{\{\xi_\alpha>0,\ \xi_\beta>0\}}$ behave differently. Define new variables for the differences as

$$S = \mathcal{E}_\alpha \sim \mathrm{Uni}(0,1), \tag{2.23}$$
$$T = \mathcal{E}_\beta \sim \mathrm{Uni}(0,1), \tag{2.24}$$
$$X = 1 - \eta\,(r_{\alpha\beta} - r_{\alpha\alpha}) \sim \mathrm{Tri}(1-\eta, 1+\eta), \tag{2.25}$$
$$Y = 1 - \eta\,(r_{\beta\alpha} - r_{\beta\beta}) \sim \mathrm{Tri}(1-\eta, 1+\eta). \tag{2.26}$$

In Section 2.1.1, the random variable that describes the difference of two uniformly distributed random variables is found to be triangularly distributed. The triangularly distributed random variable X may be scaled and translated by the constants η and 1, so that its scaled and translated distribution function is

$$f_X(x) = \eta^{-2} \begin{cases} 0 & \text{if } x \notin [1-\eta, 1+\eta] \\ \eta + x - 1 & \text{if } x \in [1-\eta, 1) \\ \eta - x + 1 & \text{if } x \in [1, 1+\eta] \end{cases}. \tag{2.27}$$

and an example graph of the distribution function for $\eta = \frac{25}{28}$ is shown in Figure 2.4
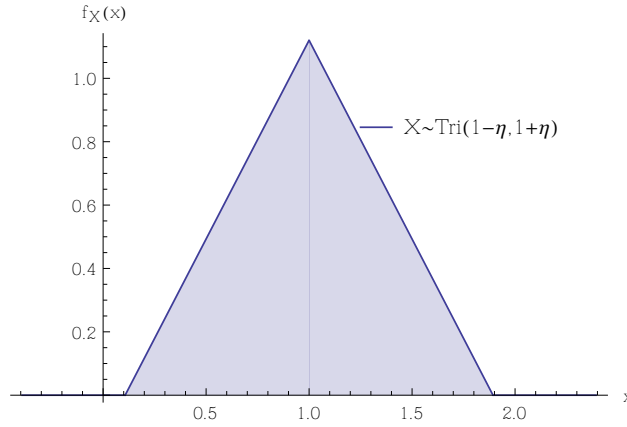
Figure 2.4: $\mathrm{Tri}(1-\eta,\ 1+\eta)$ density function (2.27) scaled by $\eta = \frac{25}{28}$ and translated a unit step.

Combining the permanence conditions (2.21)-(2.22) with the simplified variables (2.23)-(2.26) we have the indicator function

$$\mathcal{I}_{\{\xi_\alpha > 0,\ \xi_\beta > 0\}} = \mathcal{I}_{\{T > SX\}}\mathcal{I}_{\{S > TY\}}. \tag{2.28}$$

The joint distribution of S, T, X, Y can, under an assumption of independence similar to (2.8), be defined as

$$f_{S,T,X,Y}(s,t,x,y) = f_S(s)f_T(t)f_X(x)f_Y(y). \tag{2.29}$$

Both the distribution and the indicator functions are hence separable, meaning that we may define the probability of permanence as

$$\mathrm{P}(\xi_\alpha > 0, \xi_\beta > 0) = \int\limits_0^1 f_S(s) \int\limits_0^1 f_T(t) I_x(s,t) I_y(s,t)\ dt ds, \tag{2.30}$$

where we have the inner integrals

$$I_x(s,t) = \int\limits_{1-\eta}^{1+\eta} f_X(x)\mathcal{I}_{\{T>SX\}}\ dx \tag{2.31}$$

$$I_y(s,t) = \int\limits_{1-\eta}^{1+\eta} f_Y(y)\mathcal{I}_{\{S>TY\}}\ dy \tag{2.32}$$

The probability is

$$\mathrm{P}(\xi_\alpha > 0, \xi_\beta > 0) = \frac{-12 + 6\eta + 14\eta^2 - 6\eta^3 - \eta^4 + 2\eta^5}{12\eta^3(1+\eta)} + \frac{2 - 3\eta^2 + \eta^4}{2\eta^4(1+\eta)}\log(1+\eta). \tag{2.33}$$

and the details are found in Appendix B.2.3.

The graph of the probability as a function of $\eta \in (0,1)$ is shown in Figure 2.5, where one sees that the function is increasing on the interval and behaves to a large extent in a linear fashion.
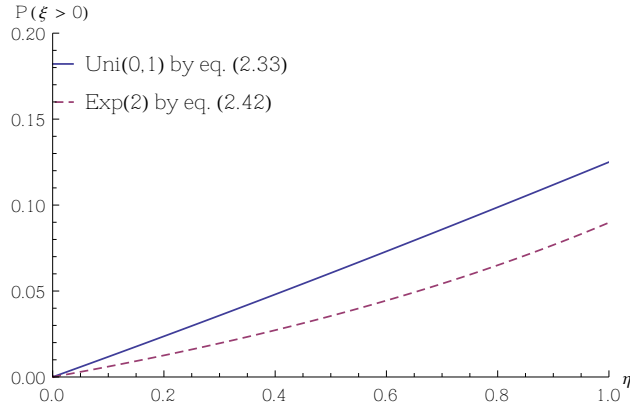
Figure 2.5: Probability of permanence $P(\xi_\alpha > 0, \xi_\beta > 0)$ as function of η for uniformly (2.33) and exponentially (2.41) distributed $\mathcal{E}_i$, $\mathcal{E}_{ij}$.

2.2.2 Exponentially distributed parameters

The model for the exponentially distributed energy uptake parameters is based on the conditions (2.21)-(2.22), so that we define the new set of variables as

$$S = \mathcal{E}_\alpha \sim \text{Exp}(\lambda), \tag{2.34}$$

$$T = \mathcal{E}_\beta \sim \text{Exp}(\lambda), \tag{2.35}$$

$$X = 1 - \eta\left(r_{\alpha\beta} - r_{\alpha\alpha}\right) \sim \text{Tri}(1 - \eta, 1 + \eta), \tag{2.36}$$

$$Y = 1 - \eta\left(r_{\beta\alpha} - r_{\beta\beta}\right) \sim \text{Tri}(1 - \eta, 1 + \eta), \tag{2.37}$$

where the $\text{Tri}(1 - \eta,\ 1 + \eta)$ distribution has the density function (2.27). The model uses the same form as the tree hierarchy with the uniformly distributed parameters for the indicator function

$$\mathcal{I}_{\{\xi_\alpha > 0,\ \xi_\beta > 0\}} = \mathcal{I}_{\{T > SX\}}\mathcal{I}_{\{S > TY\}} \tag{2.38}$$

and the joint density

$$f_{S,T,X,Y}(s, t, x, y) = f_S(s)f_T(t)f_X(x)f_Y(y). \tag{2.39}$$

With the indicator function (2.38) and the joint distribution (2.39), we may define the probability of permanence analogously to (2.30) as

$$P(\xi_\alpha > 0, \xi_\beta > 0) = \int_{\mathbb{R}+} f_S(s) \int_{\mathbb{R}+} f_T(t)I_x(s,t)I_y(s,t)\ dtds, \tag{2.40}$$

where $I_x(s,t)\ I_y(s,t)$ are the same inner integrals as in the Uniform case, (2.31) and (2.32), respectively.

Evaluating the integrals, we find that the probability of permanence for exponen-

tially distributed parameters in the tree-hierarchy model is

$$
\mathrm{P}(\xi_\alpha > 0, \xi_\beta > 0) = \frac{-12 + 6\eta + 8\eta^2 - 3\eta^3}{4\eta^3} + \frac{2(2 - \eta)}{\eta^2} \coth^{-1}\left(\frac{\eta^2 - 2\eta - 4}{\eta^2}\right)
$$
(2.41)
$$
+ \frac{1}{\eta^4}\bigg((3 + 4\eta - \eta^2)\log(1 + \eta) + \eta^2(2 - \eta)\log(2 - \eta)
$$
$$
- \eta(2 - \eta)(4 + \eta)\log(2 + \eta) + 4\eta(2 - \eta)\log(2)\bigg)
$$

The probability, when viewed as a function of η is shown in Figure 2.5. The function exhibits the interesting property of having an increasing derivative as well as being increasing, meaning that there is no maximum.

3

Three-species system

The dynamics of a three-species replicator system are complex, with possibilities of one or more fixed points in the interior of the state space as well as different combinations of the pair-wise dynamics (described in Section 2) on the boundaries of the state space. First, a classification of the systems based on the location of the fixed points in the simplex is outlined. A general criterion for permanence for three species is presented and we describe some systems of particular interest. Phase portraits or a few example trajectories, computed numerically with standard Runge–Kutta methods, will illustrate each case.

3.1   Classification of trajectories

The most interesting feature of a replicator system — from our point of view — is its permanence properties, as described in Section 1.3.1. Solutions to the replicator system (1.1) are classified according to the location and stability of any fixed points $\mathbf{x}^*$, which determines whether the system converges to a permanent state or not. We define four classes of fixed points:

Class I
> Corner fixed points, where only one species has a non-zero frequency.

Class II
> Non-corner boundary points, where two species have a non-zero frequency.

Class III
> Interior fixed points, where all frequencies are non-zero.

Class IV
> Cyclic trajectories described by interior fixed points with imaginary eigenvalues.

These may be compared to the phase portraits of Bomze [2]. As described in Section 1.3.4, there are five non–trivial phase portraits that are unconditionally permanent, meaning that any initial state in the interior of the state space simplex will remain in the interior. The present classification I-IV of replicator solutions does not take the initial state into account and as a result, the scheme may consider a conditionally permanent system as either permanent or not, depending on the initial state.

3.2   Comparison of replicator systems

In order to compare the investigation of evolutionary games by Bomze [2] to the cross-feeding model described by Lundh & Gerlee [16], we need to compare the

fitness functions (1.10) and (1.2). As a first step, we decompose the cross-feeding fitness (1.12) into first- and second-order metabolism as

$$\phi_i(\mathbf{x}) = \phi_i^{(I)}(\mathbf{x}) + \phi_i^{(II)}(\mathbf{x}), \tag{3.1}$$

where

$$\phi_i^{(I)}(\mathbf{x}) = \eta\gamma\mathcal{E}_i, \tag{3.2}$$

$$\phi_i^{(II)}(\mathbf{x}) = \eta^2\gamma\sum_{j=1}^{3}\mathcal{E}_{ji}x_j. \tag{3.3}$$

In the same spirit, we decompose the replicator system

$$\dot{x}_i = \Phi_i^{(I)}(\mathbf{x}) + \Phi_i^{(II)}(\mathbf{x}), \tag{3.4}$$

into its first- and second-order dynamics

$$\Phi_i^{(I)}(\mathbf{x}) = x_i(\phi_i^{(I)}(\mathbf{x}) - \bar{\phi}^{(I)}(\mathbf{x})), \tag{3.5}$$

$$\Phi_i^{(II)}(\mathbf{x}) = x_i(\phi_i^{(II)}(\mathbf{x}) - \bar{\phi}^{(II)}(\mathbf{x})), \tag{3.6}$$

with first- and second-order fitness functions (3.2) and (3.3).

3.2.1 First-order dynamics

The first-order metabolisation describes the energy uptake from the primary nutrient of a species, which means that the state $\mathbf{x}$ of the system will not change if all species have equal first-order parameters and are able to extract the same amount of energy from the primary nutrient. Consider the first-order metabolisation replicator system

$$\dot{x}_i = \Phi_i^{(I)}(\mathbf{x}) = \eta\gamma x_i(\mathcal{E}_i - \sum_{k=1}^{3}\mathcal{E}_k x_k), \tag{3.7}$$

which has a fixed point $\mathbf{x}^*$ if

$$\mathcal{E}_i - \sum_{k=1}^{3} x_k^*\mathcal{E}_k = 0 \ \vee \ x_i^* = 0 \tag{3.8}$$

for all species i. The first case,

$$\mathcal{E}_i = \sum_{k=1}^{3} x_k^*\mathcal{E}_k \tag{3.9}$$

says that the individual energy uptake $\mathcal{E}_i$ must be equal to the weighted population average, from which it holds that $\mathcal{E}_i = \mathcal{E}_j$ for all i, j. If the condition (3.9) does not hold for all species i, then there cannot be any interior fixed points, since the second case of (3.8), $x_i^* = 0$, does not hold for interior points where we by definition require non-zero frequencies. We may now define four possibilities for the first-order replicator system based on the number of species with equal energy uptake.

1) All species have equal energy uptake.

2) Two species have equal energy uptake.

    a) The third species has lower energy uptake than the other two.

    b) The third species has higher energy uptake than the other two.

3) The energy uptake parameters are all unequal.

Case 1) All points $\mathbf{x} \in S_2$ are fixed points, so that the classification I-III of a solution is determined by the starting point and a solution of Class IV is impossible. The case for equal energy uptake corresponds to the trivial phase portrait 1 of Bomze [2] that is shown in Figure 3.1.

Figure 3.1: Bomze phase portrait 1: First-order dynamics of Case 1 with the species ordered counter-clockwise from the lower left corner.

Case 2a) and 2b) If the energy uptake $\mathcal{E}_i = \mathcal{E}_j$ is equal for two species, then the third species will either dominate or perish depending on whether its energy uptake is greater or smaller than the population average. For motivation, assume without loss of generality that $\mathcal{E}_1 = \mathcal{E}_2 \neq \mathcal{E}_3$ so that

$$\sum_{k=1}^{3} x_k \mathcal{E}_k = \mathcal{E}_1(x_1 + x_2) + \mathcal{E}_3(1 - x_1 - x_2) = (\mathcal{E}_1 - \mathcal{E}_3)(x_1 + x_2) + \mathcal{E}_3. \qquad (3.10)$$

Then the replicator system (3.7) is

$$\begin{cases} \dot{x}_1 &= \eta\gamma x_1(1 - x_1 - x_2)(\mathcal{E}_1 - \mathcal{E}_3), \\ \dot{x}_2 &= \eta\gamma x_2(1 - x_1 - x_2)(\mathcal{E}_1 - \mathcal{E}_3), \\ \dot{x}_3 &= \eta\gamma(x_1 + x_2)(1 - x_1 - x_2)(\mathcal{E}_3 - \mathcal{E}_1), \end{cases} \qquad (3.11)$$

and thus that the fixed points are either the corner $\mathbf{x} = [0,\ 0,\ 1]$ or any point on the boundary $S_2 \cap \{x_3 = 0\}$. The stability of these fixed points are given by the relation between $\mathcal{E}_3$ and $\mathcal{E}_1 = \mathcal{E}_2$, if $\mathcal{E}_1 > \mathcal{E}_3$, then we have that $\dot{x}_3 < 0$ and $\dot{x}_1,\ \dot{x}_2 > 0$ so that the trajectories tend to a point on the boundary $S_2 \cap \{x_3 = 0\}$, a Class II solution. More specifically, the end state will be the state $[x_1,\ x_2,\ 0]$ with the same ratio of x_1 to x_2 as the initial state. If, on the other hand, $\mathcal{E}_1 < \mathcal{E}_3$, then the trajectories tend to the corner $\mathbf{x} = [0,\ 0,\ 1]$, which is a system of Class I. The systems in case

Figure 3.2: Bomze phase portrait 29: First-order dynamics of Case 2a with the species ordered counter-clockwise from the lower left corner.
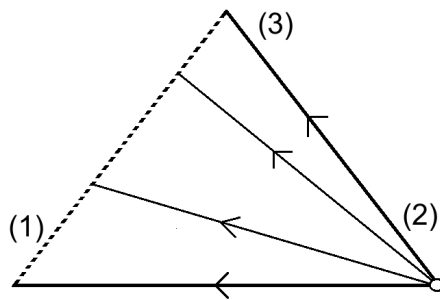
Figure 3.3: Reversal of Bomze phase portrait 29: First-order dynamics of Case 2b with the species ordered counter-clockwise from the lower left corner.

2a) and 2b) are shown in Figures 3.2 and 3.3, respectively, and correspond to the positive and negative of Bomze phase portrait 29 [2].

Case 3) All species have unequal energy uptake $\mathcal{E}_1 \neq \mathcal{E}_2 \neq \mathcal{E}_3$, by which the system will tend to the corner corresponding to the species with the highest energy uptake, once again a solution of Class I. The possible trajectories are determined by the relations between the energy parameters, if for instance two species have nearly equal parameters, we will have similar initial dynamics as in the cases 2a) and 2b) before either one species is nearly extinct (by which the relation between the two remaining species will be more important) or nearly dominant. This system corresponds to Bomze phase portrait 43 and is shown in Figure 3.4. When simulating systems, only the case of unequal interactions parameters, $\mathcal{E}_1 \neq \mathcal{E}_2 \neq \mathcal{E}_3$, is expected to be found from random parameters, as the probability of having equality between continuous random variables is of a zero measure.

3.2.2 Second-order dynamics

The matrix $\underline{\mathcal{E}}$ of second-order metabolism corresponds to the payoff matrix A of the homogenous evolutionary game described by (1.2), and if we subtract the diagonal elements from each corresponding column of $\underline{\mathcal{E}}$ we have

$$\widetilde{\mathcal{E}}_{ij} = \begin{cases} 0, & i = j \\ \mathcal{E}_{ij} - \mathcal{E}_{jj}, & i \neq j \end{cases}, \tag{3.12}$$
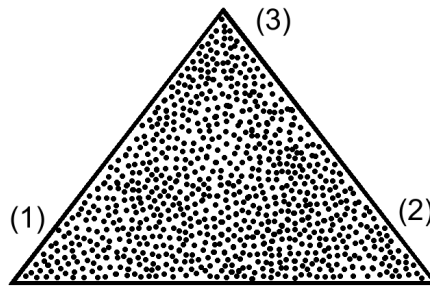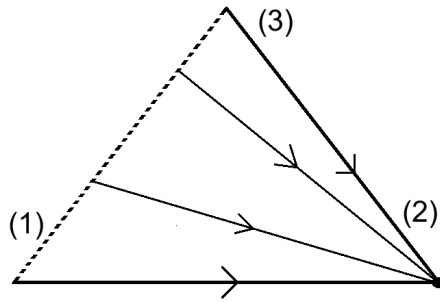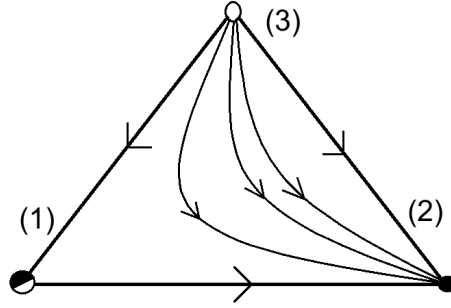
Figure 3.4: Bomze phase portrait 43: First-order dynamics of Case 3 with the species ordered counter-clockwise from the lower left corner.

i.e., that the metabolism matrix is on the form (1.3) with real (and possibly negative) elements. For the second-order dynamics, we have the homogenous replicator system

$$\dot{x}_i = \Phi_i^{(II)}(\mathbf{x}) = x_i(\mathbf{e}_i^T(\gamma\eta^2\underline{\mathcal{E}}^T)\mathbf{x} - \mathbf{x}^T(\gamma\eta^2\underline{\mathcal{E}}^T)\mathbf{x}), \tag{3.13}$$

which is equivalent to the homogenous replicator system with fitness (1.2).

3.2.3 Transformation of replicator systems

If it is not the case that the first-order energy uptake is equal among the species, then we may use a technique described by Gerstung et al. [9] and Stadler [20], namely that we define an alternative payoff matrix E with elements

$$E_{ji} = \gamma\eta\mathcal{E}_i + \gamma\eta^2\mathcal{E}_{ji} \tag{3.14}$$

so that the fitness function (1.2) may be constructed as

$$\widetilde{\phi}_i(\mathbf{x}) = \sum_{j=1}^{3} E_{ij}x_j \tag{3.15}$$

which is equivalent to the linear fitness function (1.2) when we define the entries of the payoff matrix A as $a_{ij} = E_{ij}$. The proof of the equality of the fitness (3.15) to the affine fitness (1.10) is straightforward, and relies on the fact that $\sum_{j=1}^{3} x_j = 1$, so that

$$\begin{aligned}
\widetilde{\phi}_i(\mathbf{x}) &= \sum_{j=1}^{3} E_{ij}x_j \\
&= \gamma\eta\sum_{j=1}^{3}(\mathcal{E}_i + \eta\mathcal{E}_{ji})x_j \\
&= \gamma\eta\sum_{j=1}^{3} x_j\mathcal{E}_i + \gamma\eta^2\sum_{j=1}^{3}\mathcal{E}_{ji}x_j \\
&= \gamma\eta\mathcal{E}_i + \gamma\eta^2\sum_{j=1}^{3}\mathcal{E}_{ji}x_j \\
&= \phi_i(\mathbf{x}).
\end{aligned}$$

Hence, the affine fitness function (1.10) is equivalent to the linear fitness function (1.2) so that the set of possible dynamics of the two corresponding replicator systems are the same. This is easily generalised to higher orders of interaction, as described in Appendix C.

3.3 A necessary criterion for permanence

We are now to derive general conditions for existence and stability of fixed points in the interior of the state space S_2 that do not depend on any pair-wise interactions. The conditions are necessary but not sufficient for permanence, as there are replicator systems with a stable fixed point in the interior of the simplex that can not be reached from all initial states. The method is due to Bomze [2] and also used by Stadler and Schuster [20] and is based on finding two coordinates p, q that define a unique fixed point

$$\mathbf{x}^* = \frac{1}{1+p+q}(1, \ p, \ q).$$
(3.16)

that lies in the interior of S_2 when p, q are positive. The coordinates are given by

$$p = \frac{\Delta_1}{\Delta_3}$$
(3.17)

$$q = \frac{\Delta_2}{\Delta_3}$$
(3.18)

where Δ_k are the 2×2 co-factors of the payoff matrix (A.5), defined as

$$\Delta_1 = (\lambda_{32} - \lambda_{31})(\lambda_{13} - \lambda_{11}) - (\lambda_{12} - \lambda_{11})(\lambda_{33} - \lambda_{31})$$
(3.19)

$$\Delta_2 = (\lambda_{12} - \lambda_{11})(\lambda_{23} - \lambda_{21}) - (\lambda_{22} - \lambda_{21})(\lambda_{13} - \lambda_{11})$$
(3.20)

$$\Delta_3 = (\lambda_{22} - \lambda_{21})(\lambda_{33} - \lambda_{31}) - (\lambda_{32} - \lambda_{31})(\lambda_{23} - \lambda_{21})$$
(3.21)

where $\lambda_{ij} = \mathcal{E}_i + \eta \mathcal{E}_{ij}$.

The criterion for existence of the fixed point (3.16) is that p, q are real and positive, which occurs when all of the Δ_i have the same sign,

$$\mathrm{sgn}(\Delta_1) = \mathrm{sgn}(\Delta_2) = \mathrm{sgn}(\Delta_3)$$
(3.22)

where $\mathrm{sgn}\,|\mathbb{R} \to \{-1, \ 0, \ 1\}$ denotes the sign function. The stability properties of the fixed point is based on its (non-zero) eigenvalues

$$\mu_{1, \ 2} = \frac{1}{2}\left(\alpha p + \beta q \pm \sqrt{(\alpha p + \beta q)^2 - 4pq\Delta_3}\right)$$
(3.23)

where we have defined, for convenience,

$$\alpha = \lambda_{22} - \lambda_{21}$$
(3.24)

$$\beta = \lambda_{33} - \lambda_{31}$$
(3.25)

as described in Proposition 6 of [2]. There are two non-trivial types of fixed points for a stable system. If the eigenvalues at the fixed point have negative real parts, the

fixed point is called a nodal or a spiral sink if the eigenvalues are real or complex, respectively. The real part of the eigenvalues will be negative if

$$\alpha p + \beta q < 0 \qquad (3.26)$$

since then we have by Corollary 7 (iii) [2] that the product $pq\Delta_3$ is positive so that

$$\left| \sqrt{(\alpha p + \beta q)^2 - 4pq\Delta_3} \right| < |\alpha p + \beta q|. \qquad (3.27)$$

The conditions for existence and stability of fixed points in the interior of the simplex are collected in Table 3.1.

Inner fixed point (3.16)	Existence (3.22)	Stability (3.26)
$\mathbf{x}^*$	$\text{sgn}(\Delta_1) = \text{sgn}(\Delta_2) = \text{sgn}(\Delta_3)$	$\alpha p + \beta q < 0$

Table 3.1: Criteria for permanent system, described by a stable fixed point in the interior of the simplex.

3.4   Centre fixed points and cyclic trajectories

As complex eigenvalues always come in conjugate pairs, a fixed point to the three-species system has at most two complex eigenvalues μ_k. If the eigenvalues to the payoff matrix of the replicator system (1.1) are strictly imaginary, i.e., with a zero real part, in a neighborhood of an inner fixed point, then all trajectories in the neighborhood will be cyclic corresponding to a solution of Class IV and we will call the fixed point a *center*. Note that a center fixed point does not necessarily need to be located in the barycenter of the simplex, "center" just means that it is circled by the periodic trajectories of the system. We will now discuss the conditions under which we can expect to find these trajectories.

Assume that the replicator system is determined by the fitness function (1.2), so that we have existence of the unique fixed point (3.16) to the replicator system (1.1) when the sign criterion (3.22) holds. If the eigenvalues (3.23) of the fixed point $\mathbf{x}^* = \frac{1}{1+p+q}(1, \ p, \ q)$ are strictly imaginary, then any trajectories of the system are cyclic. This occurs when

$$\Delta_3 > 0 \qquad (3.28)$$
$$\alpha p + \beta q = 0 \qquad (3.29)$$

as derived by Bomze [2]. Note that the criterion (3.28) means that the terms Δ_i of (3.19)-(3.21) are all positive for existence of the fixed point. A cyclic system is described in phase portrait 16 of Bomze, where the non-zero eigenvalues of the fixed point have the form

$$\mu_{1,2} = \pm i\sqrt{pq\Delta_3}, \qquad (3.30)$$

as seen when using the criteria (3.28)-(3.29) in the eigenvalues (3.23). An example of a system with the above properties is the rock-paper-scissors game with payoff

$$A_{rps} = \begin{bmatrix} 0 & -1 & 1 \\ 1 & 0 & -1 \\ -1 & 1 & 0 \end{bmatrix}, \tag{3.31}$$

and eigenvalues

$$\mu_{2,\,3} = \pm i\sqrt{3}. \tag{3.32}$$

The trajectory of the system for a random starting point is shown on the regular 2-simplex in $\mathbb{R}^3$ in Figure 3.5.

The center fixed point with imaginary eigenvalues is the limiting case between complex eigenvalues with negative and positive real parts. Teschl [21] defines the so-called center manifold as the set spanned by eigenvectors corresponding to purely imaginary eigenvalues of a dynamical system at a particular fixed point, and notes that the manifold is "generally not stable under small perturbations" and is for that reason oftentimes assumed empty. As an illustration, consider the case where a small perturbation $\delta \in \mathbb{R}$ is added to the imaginary eigenvalues

$$\mu_{2,\,3} = \delta \pm i\sqrt{pq\Delta_3}. \tag{3.33}$$

The phase portrait of the rock-paper-scissors example (3.32) is shown in the left subfigure of Figure 3.5. Three trajectories are shown: the Bomze phase portrait 17 (dotted) [2] that is characterised by eigenvalues (3.33) with a negative real part δ and converges to a stable fixed point, the corresponding portrait (dashed) with a positive real part δ of the eigenvalues where the trajectory diverges from the unstable fixed point, and the limiting case that is Bomze phase portrait 16 (solid) [2]. Note that the location of a center fixed point is dependent on the relative magnitude of the elements of the payoff matrix, which means that the fixed point need not be centered in the simplex. An example system is shown in the right subfigure of Figure 3.5.

Going back to the cross-feeding system, the question is: how likely is a Class IV solution with a center fixed point? To summarise the conditions above, we have existence of a fixed point $\mathbf{x}^* = \frac{1}{1+p+q}(1,\ p,\ q)$ in the interior of the simplex S_2, with strictly imaginary eigenvalues if

$$\Delta_1 > 0, \tag{3.34}$$
$$\Delta_2 > 0, \tag{3.35}$$
$$\Delta_3 > 0, \tag{3.36}$$
$$\alpha p + \beta q = 0. \tag{3.37}$$

As seen in the example in Figure 3.5, even a small disturbance to the condition of zero real part will change the stability of the fixed point to make it stable or unstable. This phenomenon, where a shift in a parameter causes a change in the stability of an ODE system is known as a bifurcation [21].
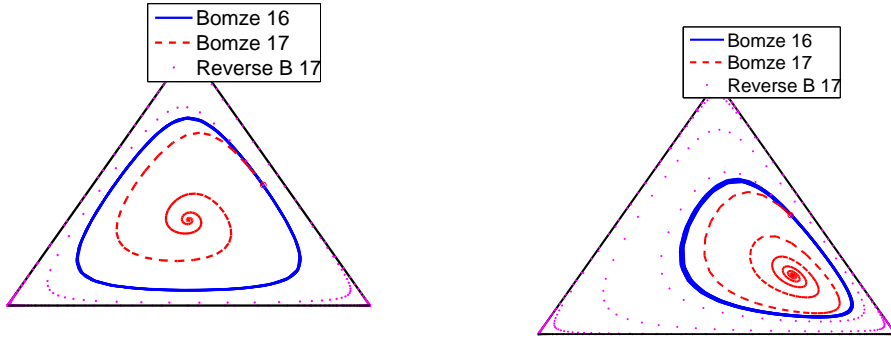
Figure 3.5: Intransitive rock-paper-scissors replicator system of Class IV. Pure system (solid) compared to system with unstable fixed point (dashed) with real part $\delta > 0$ of eigenvalues and a system with a stable fixed point (dotted) with a real part $\delta < 0$ as of (3.33).

To investigate the probability of having an interior fixed point, given that the system is cyclic, we assume that the criterion $\alpha p + \beta q = 0$ of (3.37) holds and use the definitions of p (3.17), q (3.17), α (3.24) and β (3.25) to rewrite it as

$$(\lambda_{33} - \lambda_{31}) = (\lambda_{13} - \lambda_{11})\frac{\lambda_{21} - \lambda_{22}}{\lambda_{11} - \lambda_{12}}\frac{\lambda_{32} - \lambda_{33}}{\lambda_{22} - \lambda_{23}} \tag{3.38}$$

Then, the conditions (3.34) to (3.36) may be rewritten as

$$-(\lambda_{22} - \lambda_{21})^2\frac{(\lambda_{13} - \lambda_{11})(\lambda_{32} - \lambda_{33})}{(\lambda_{11} - \lambda_{12})(\lambda_{22} - \lambda_{23})} - (\lambda_{32} - \lambda_{31})(\lambda_{23} - \lambda_{21}) > 0 \tag{3.39}$$

$$(\lambda_{12} - \lambda_{11})(\lambda_{23} - \lambda_{21}) - (\lambda_{22} - \lambda_{21})(\lambda_{13} - \lambda_{11}) > 0 \tag{3.40}$$

$$(\lambda_{13} - \lambda_{11})\left(\lambda_{32} - \lambda_{31} + \frac{(\lambda_{21} - \lambda_{22})(\lambda_{32} - \lambda_{33})}{\lambda_{22} - \lambda_{23}}\right) > 0 \tag{3.41}$$

These conditions for an interior fixed point are investigated in the numerical simulations in Section 4.2.3.

3.5 Pair-wise coexistence

In a permanent three-species system, it may be the case that two or more of the involved species are pair-wise coexistent when isolated from the third species, which is the case discussed in Section 2. In terms of dynamical systems, the criterion for pair-wise coexistence is that there exists a stable fixed point on the non-corner edges of the simplex. If the fixed point on a given edge is stable, any trajectories along that edge will converge to the fixed point as $t \to \infty$, as shown in the left subfigure of Figure 3.6. In the interior of the simplex near the fixed point there are however more than one possible behaviour. A semi-stable fixed point will repel the trajectories in the part of its neighborhood that lies in the interior of the simplex, shown as case (a) of Figure 3.6, whereas a stable fixed point will attract any trajectories in its neighborhood, shown as case (b) of Figure 3.6.
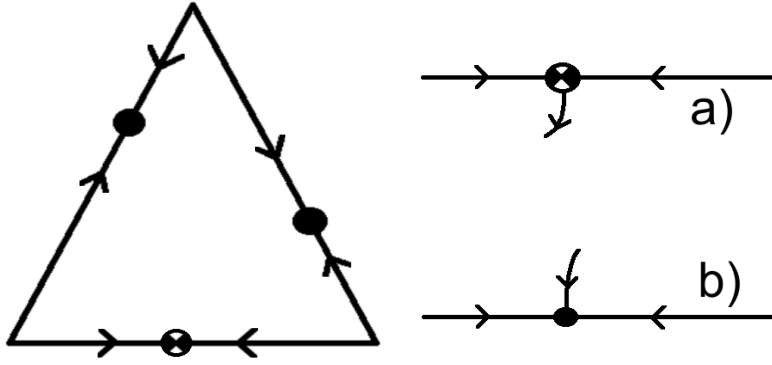
Figure 3.6: Left: Illustration of pair-wise coexistence in species triplets. Right: Differing behaviour between trajectories in neighborhood of semi-stable (a) and stable (b) fixed point.

A stable fixed point — as in the general case described in Section 3.3 — in the interior of the simplex S_2 is necessary for a permanent replicator system. For positive coordinates p, q, a general interior fixed point has the form

$$\mathbf{x}^* = \frac{1}{1 + p + q}(1, \ p, \ q) \tag{3.42}$$

where the coordinates p, q are defined as

$$p = \frac{\Delta_1}{\Delta_3} \tag{3.43}$$

$$q = \frac{\Delta_2}{\Delta_3} \tag{3.44}$$

and are positive if Δ_i have the same sign for $i = 1, \ 2, \ 3$. Recall the definition

$$\Delta_1 = (\lambda_{32} - \lambda_{31})(\lambda_{13} - \lambda_{11}) - (\lambda_{12} - \lambda_{11})(\lambda_{33} - \lambda_{31}) \tag{3.45}$$

$$\Delta_2 = (\lambda_{12} - \lambda_{11})(\lambda_{23} - \lambda_{21}) - (\lambda_{22} - \lambda_{21})(\lambda_{13} - \lambda_{11}) \tag{3.46}$$

$$\Delta_3 = (\lambda_{22} - \lambda_{21})(\lambda_{33} - \lambda_{31}) - (\lambda_{32} - \lambda_{31})(\lambda_{23} - \lambda_{21}) \tag{3.47}$$

as outlined in Section 3.3. For stability of the interior fixed point, the eigenvalues (3.23) of the linearisation of the system at the fixed point must have a negative real part. Condition (3.26) ensures this.

An interior fixed point is not sufficient for permanence and not enough for the present scenario. We also require the pair-wise coexistence of one to three of the species pairs, which is defined as stable fixed points on the non-corner boundary of the simplex S_2. We use the payoff matrix (3.14) on its normal form (A.4) that corresponds the homogenous replicator system of Bomze [2] as outlined in Appendix A and find that the non-corner edge fixed points are

$$\mathbf{x}_{12}^* = \frac{1}{\lambda_{12} - \lambda_{11} + \lambda_{21} - \lambda_{22}}(\lambda_{21} - \lambda_{22}, \ \lambda_{12} - \lambda_{11}, \ 0) \tag{3.48}$$

$$\mathbf{x}_{23}^* = \frac{1}{\lambda_{23} - \lambda_{22} + \lambda_{32} - \lambda_{33}}(0, \ \lambda_{32} - \lambda_{33}, \ \lambda_{23} - \lambda_{22}) \tag{3.49}$$

$$\mathbf{x}_{31}^* = \frac{1}{\lambda_{13} - \lambda_{11} + \lambda_{31} - \lambda_{33}}(\lambda_{31} - \lambda_{33}, \ 0, \ \lambda_{13} - \lambda_{11}) \tag{3.50}$$

under the conditions

$$(\lambda_{12} - \lambda_{11})(\lambda_{21} - \lambda_{22}) > 0 \tag{3.51}$$
$$(\lambda_{23} - \lambda_{22})(\lambda_{32} - \lambda_{33}) > 0 \tag{3.52}$$
$$(\lambda_{13} - \lambda_{11})(\lambda_{31} - \lambda_{33}) > 0 \tag{3.53}$$

which ensure that each pair of payoff elements, for example $\lambda_{21} - \lambda_{22}$ and $\lambda_{12} - \lambda_{11}$ of (3.48), have the same sign so that the coordinates of $\mathbf{x}_{12}^*$ are properly defined on the intervals $[0, 1)$ when normalised by the coordinate sum. We recall the definition that the parameters λ_{ij} are the elements of the 3×3 payoff matrix E (3.14). For a sketch of the fixed points, see Figure 3.7. The fixed points (3.48) and (3.50) are given by Proposition 2 of Bomze [2] and the fixed point on the edge $\{\mathbf{x} \in S_2|\ x_3 = 0\}$ is given by Proposition 5 of the same paper. Stadler & Schuster [20] give an alternative, although equivalent, formulation of the fixed points.
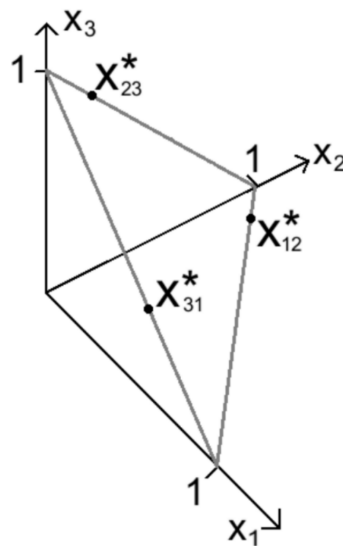
Figure 3.7: Pair-wise coexistence fixed points (3.48) through (3.50).

In order to have permanence, we require that the edge fixed points are so-called saddle points which attract trajectories on the edge and repel trajectories in the interior of the simplex (cf. Figure 3.6 a). For stability along the edges, we modify the conditions (3.51)-(3.53) to require positiveness for each element in the pairs of payoff elements

$$(\lambda_{12} - \lambda_{11}) > 0, \ (\lambda_{21} - \lambda_{22}) > 0 \tag{3.54}$$
$$(\lambda_{23} - \lambda_{22}) > 0, \ (\lambda_{32} - \lambda_{33}) > 0 \tag{3.55}$$
$$(\lambda_{13} - \lambda_{11}) > 0, \ (\lambda_{31} - \lambda_{33}) > 0 \tag{3.56}$$

so that edge-bound trajectories on both sides of the fixed point will tend to the fixed point. Three fixed points on the simplex boundary, combined with a stable fixed point in the interior of the simplex is a sufficient condition for permanence so that any trajectory near the edge in the interior of the simplex will tend towards the interior fixed point [2].

3.5.1 Three coexistent pairs

Bomze recognises one phase portrait of the replicator system of equations with semi-stable fixed points on each edge of the simplex, phase portrait 7, such that trajectories on the edges tend toward the fixed point and trajectories in the interior are repelled from the fixed points. This phase portrait has the properties that there is exactly one fixed point in the interior of the simplex and that there are three non-corner fixed points on the edges [2].
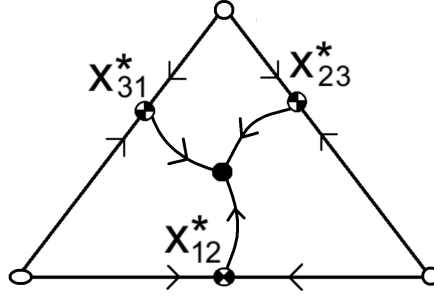
Figure 3.8: Illustration of Bomze phase portrait 7 [2] with pair-wise fixed points (3.48)-(3.50).

We have existence of unique fixed points $\mathbf{x}_{ij}^*$ as of (3.48)-(3.50) on the edges of the simplex when the conditions (3.51)-(3.53) are fulfilled. Furthermore, the fixed points are semi-stable when the conditions (3.54)-(3.56) hold and there exists a stable interior fixed point (3.42) and we note. We also note that the criteria for stability of the boundary fixed points imply existence of the interior fixed point. The conditions are collected in Table 3.2, where all conditions are necessary for a system with three pair-wise fixed points and one triplet fixed point in the interior of the state space.

Fixed point	Existence	Stability	
$\mathbf{x}_{12}^*$ (3.48)	$(\lambda_{12} - \lambda_{11})(\lambda_{21} - \lambda_{22}) > 0$ (3.51)	$(\lambda_{12} - \lambda_{11}) > 0$	$(\lambda_{21} - \lambda_{22}) > 0$
$\mathbf{x}_{23}^*$ (3.49)	$(\lambda_{23} - \lambda_{22})(\lambda_{32} - \lambda_{33}) > 0$ (3.52)	$(\lambda_{23} - \lambda_{22}) > 0$	$(\lambda_{32} - \lambda_{33}) > 0$
$\mathbf{x}_{31}^*$ (3.50)	$(\lambda_{31} - \lambda_{33})(\lambda_{13} - \lambda_{11}) > 0$ (3.53)	$(\lambda_{31} - \lambda_{33}) > 0$	$(\lambda_{13} - \lambda_{11}) > 0$
$\mathbf{x}^*$ (3.42)	$\text{sgn}(\Delta_i) = \text{sgn}(\Delta_j) \forall i,\ j$ (3.22)	$\alpha p + \beta q < 0$ (3.26)	

Table 3.2: Criteria for permanent system with semi-stable fixed points along boundary.

3.5.2 Two coexistent pairs

For a system with two pairs that are coexistent in isolation from the third species, we require that some — but not all — of the conditions in Table 3.2 hold. We will discuss which of the criteria that are relevant and also derive additional criteria.

If a system has stable non-corner fixed points on each edge of the boundary, as discussed in section (3.5.1), then the simplex corners must be unstable fixed points

as shown in the left subfigure of Figure 3.8. In the present case, where we have two semi-stable fixed points with the stable axes aligned with the simplex boundary, we will have that one of the semi-stable fixed points will have migrated to the remaining corner. The system is visualised by Bomze as phase portrait 9 and shown in Figure 3.9.

Figure 3.9: Illustration of Bomze phase portrait 9 [2] with pair-wise fixed points (3.48)-(3.50) where $\mathbf{x}_{12}^*$ have migrated to the left corner.

As before, we need a stable internal fixed point, where existence is given by the condition (3.22) and the stability is given by (3.26). Furthermore, we need that two out of the three conditions for existence and stability (3.54)-(3.56) of the edge fixed points hold. This means that for each case — where a specific edge fixed point does not exist — we need that one of the conditions

$$(\lambda_{12} - \lambda_{11})(\lambda_{21} - \lambda_{22}) \leq 0 \tag{3.57}$$

$$(\lambda_{23} - \lambda_{22})(\lambda_{32} - \lambda_{33}) \leq 0 \tag{3.58}$$

$$(\lambda_{13} - \lambda_{11})(\lambda_{31} - \lambda_{33}) \leq 0 \tag{3.59}$$

that negate (3.51)-(3.53) hold. The conditions for existence of such a system are shown in Table 3.3.

Edge fixed points[†]	Existent and stable if
$\neg \mathbf{x}_{12}^*$ (3.48)	$(\lambda_{12} - \lambda_{11})(\lambda_{21} - \lambda_{22}) \leq 0$ (3.57)
$\mathbf{x}_{23}^*$ (3.49)	$(\lambda_{23} - \lambda_{22}) > 0,\ (\lambda_{32} - \lambda_{33}) > 0$ (3.55)
$\mathbf{x}_{31}^*$ (3.50)	$(\lambda_{13} - \lambda_{11}) > 0,\ (\lambda_{31} - \lambda_{33}) > 0$ (3.56)
$\mathbf{x}_{12}^*$ (3.48)	$(\lambda_{12} - \lambda_{11}) > 0,\ (\lambda_{21} - \lambda_{22}) > 0$ (3.54)
$\neg \mathbf{x}_{23}^*$ (3.49)	$(\lambda_{23} - \lambda_{22})(\lambda_{32} - \lambda_{33}) \leq 0$ (3.58)
$\mathbf{x}_{31}^*$ (3.50)	$(\lambda_{13} - \lambda_{11}) > 0,\ (\lambda_{31} - \lambda_{33}) > 0$ (3.56)
$\mathbf{x}_{12}^*$ (3.48)	$(\lambda_{12} - \lambda_{11}) > 0,\ (\lambda_{21} - \lambda_{22}) > 0$ (3.54)
$\mathbf{x}_{23}^*$ (3.49)	$(\lambda_{23} - \lambda_{22}) > 0,\ (\lambda_{32} - \lambda_{33}) > 0$ (3.55)
$\neg \mathbf{x}_{31}^*$ (3.50)	$(\lambda_{13} - \lambda_{11})(\lambda_{31} - \lambda_{33}) \leq 0$ (3.59)
interior fixed point	Existent and stable if
$\mathbf{x}^*$ (3.42)	$\mathrm{sgn}(\Delta_1) = \mathrm{sgn}(\Delta_2) = \mathrm{sgn}(\Delta_3)$ (3.22) $\alpha p + \beta q < 0$ (3.26)

Table 3.3: Criteria for permanent system with two semi-stable fixed points along boundary. [†]Only one of the three sets of fixed points can occur, $\neg \mathbf{x}$ denotes that the fixed point is non-existent.

3.5.3 One coexistent pair

The final case of pair-wise coexistence occurs when two of the boundary fixed points have migrated onto corners of the simplex. In biological terms, we have one pair of coexistent species and an additional species that is dominant with respect to one species in the pair and dominated by the other. Figure 3.10 shows the phase portrait of an example system where species 1 and 3 are coexistent and where species 2 is dominant with respect to species 3 and recessive with respect to species 1. The system has phase portrait number 15 in Bomze [2].

For permanence of the system, we require the existence of a stable fixed point in the interior of the simplex S_2, by the conditions found in Table 3.1. In addition, one of the three sets of conditions in Table 3.4 need to hold.

Edge fixed points[†]	Existent and stable if
$\mathbf{x}_{12}^*$ (3.48)	$(\lambda_{12} - \lambda_{11}) > 0, \ (\lambda_{21} - \lambda_{22}) > 0$ (3.54)
$\neg\mathbf{x}_{23}^*$ (3.49)	$(\lambda_{23} - \lambda_{22})(\lambda_{32} - \lambda_{33}) \leq 0$ (3.58)
$\neg\mathbf{x}_{31}^*$ (3.50)	$(\lambda_{13} - \lambda_{11})(\lambda_{31} - \lambda_{33}) \leq 0$ (3.59)
$\neg\mathbf{x}_{12}^*$ (3.48)	$(\lambda_{12} - \lambda_{11})(\lambda_{21} - \lambda_{22}) \leq 0$ (3.57)
$\mathbf{x}_{23}^*$ (3.49)	$(\lambda_{23} - \lambda_{22}) > 0, \ (\lambda_{32} - \lambda_{33}) > 0$ (3.55)
$\neg\mathbf{x}_{31}^*$ (3.50)	$(\lambda_{13} - \lambda_{11})(\lambda_{31} - \lambda_{33}) \leq 0$ (3.59)
$\neg\mathbf{x}_{12}^*$ (3.48)	$(\lambda_{12} - \lambda_{11})(\lambda_{21} - \lambda_{22}) \leq 0$ (3.57)
$\neg\mathbf{x}_{23}^*$ (3.49)	$(\lambda_{23} - \lambda_{22})(\lambda_{32} - \lambda_{33}) \leq 0$ (3.58)
$\mathbf{x}_{31}^*$ (3.50)	$(\lambda_{13} - \lambda_{11}) > 0, \ (\lambda_{31} - \lambda_{33}) > 0$ (3.56)
Inner fixed point	Existent and stable if
$\mathbf{x}^*$ (3.42)	$\mathrm{sgn}(\Delta_1) = \mathrm{sgn}(\Delta_2) = \mathrm{sgn}(\Delta_3)$ (3.22) $\alpha p + \beta q < 0$ (3.26)

Table 3.4: Criteria for permanent system with one semi-stable fixed point along boundary. [†]Only one of the three sets of fixed points can occur, $\neg\mathbf{x}$ denotes that the fixed point is non-existent.
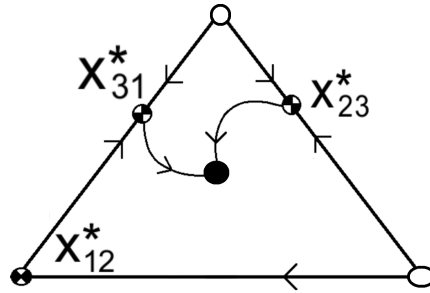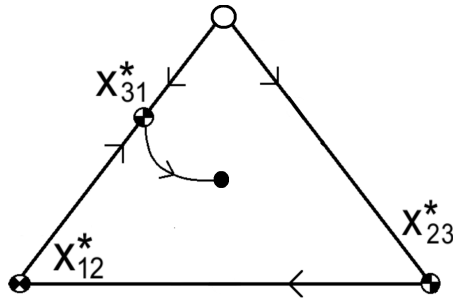

Figure 3.10: Illustration of Bomze phase portrait 15 [2] with pair-wise fixed points (3.48)-(3.50) where $\mathbf{x}_{12}^*$ and $\mathbf{x}_{23}^*$ have migrated to the bottom corners.

3.6 Intransitivity and permanence

The definition used in Section 1.3.4 for intransitivity does not consider the ordering of the species $i = 1, 2, \ldots N$, since the labels i are arbitrary. This theoretical setting does not differ between a right-handed intransitive system where species $i + 1$ outcompetes species i and a left-handed system where i outcompetes $i + 1$, see Figure 3.11 for an illustration. In the present section, we take all indices modulo n, so that the pair $(i, \ i + 1)$ is well defined also for $i = n$.

We first need to make sure that the definition of intransitivity, Definition 2 of Lundh & Gerlee [16], works both ways. The ordering of species in the numerical simulations

may be sorted with respect to which species outcompetes which, but the computational cost for this is high. Rather, the following paragraphs outline an argument to cover both possibilities for intransitivity when species' labeling is considered fixed.
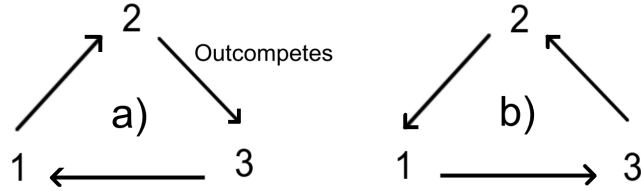
Figure 3.11: Illustration of the two possibilities for pair-wise intransitive triplets, left-handed (a) and right-handed (b).

The conditions for intransitivity (1.23), (1.24) for a pair $(i,\ i+1)$ may be expressed as

$$\lambda_{i+1,i} - \lambda_{i+1,i+1} > 0 \tag{3.60}$$
$$\lambda_{i,i} - \lambda_{i,i+1} > 0, \tag{3.61}$$

where λ_{ij} is the i-th row, j-th column element of the payoff matrix (3.14). These conditions follow from considering the ordered pairs $(i,\ i+1)$ such that the species $i+1$ outcompetes species i when no other species is present. In terms of the phase portrait of the replicator system, this means that the fixed point $(x_i^*,\ x_{i+1}^*) = (1,\ 0)$ is unstable and that the fixed point $(x_i^*,\ x_{i+1}^*) = (0,\ 1)$ is stable. Reversing the intransitivity, we have that $(x_i^*,\ x_{i+1}^*) = (1,\ 0)$ is *stable* and that the fixed point $(x_i^*,\ x_{i+1}^*) = (0,\ 1)$ is *unstable*, equivalent to the reversion of the conditions (3.60) and (3.61) as

$$\lambda_{i+1,i} - \lambda_{i+1,i+1} < 0 \tag{3.62}$$
$$\lambda_{i,i} - \lambda_{i,i+1} < 0. \tag{3.63}$$

So in conclusion, we may say that the system is pair-wise intransitive in both directions as long as

$$\lambda_{i+1,i} - \lambda_{i+1,i+1} = \mathcal{E}_i - \mathcal{E}_{i+1} + \eta(\mathcal{E}_{i+1,i} - \mathcal{E}_{i+1,i+1}) \tag{3.64}$$
$$\lambda_{i,i} - \lambda_{i,i+1} = \mathcal{E}_i - \mathcal{E}_{i+1} + \eta(\mathcal{E}_{i,i} - \mathcal{E}_{i,i+1}) \tag{3.65}$$

have the same sign for all pairs $(i,\ i+1)$ of species.
The criterion for permanence for an intransitive three-species replicator system is

$$\Gamma_{12}\Gamma_{23}\Gamma_{31} < 1, \tag{3.66}$$

as stated in Theorem 2 of Lundh & Gerlee [16]. The permanence factors Γ_{ij} are defined as

$$\Gamma_{ij} = \frac{\lambda_{ji} - \lambda_{jj}}{\lambda_{ii} - \lambda_{ij}}, \tag{3.67}$$

and are positive as long as the differences $\lambda_{ji} - \lambda_{jj}$ and $\lambda_{ii} - \lambda_{ij}$ have the same sign. In conclusion, the three-species replicator system (1.1) is pair-wise intransitive and

permanent if condition (3.66) holds together with either the conditions (3.60) and (3.61) or the conditions (3.62) and (3.63). The conditions are collected in Table 3.5.

Species pair	(1, 2)	(2, 3)	(3, 1)
Intransitive if (3.60), (3.61)	$\lambda_{21} - \lambda_{22} > 0$ $\lambda_{11} - \lambda_{12} > 0$	$\lambda_{32} - \lambda_{33} > 0$ $\lambda_{22} - \lambda_{23} > 0$	$\lambda_{13} - \lambda_{11} > 0$ $\lambda_{33} - \lambda_{31} > 0$
or if (3.62), (3.63)	$\lambda_{21} - \lambda_{22} < 0$ $\lambda_{11} - \lambda_{12} < 0$	$\lambda_{32} - \lambda_{33} < 0$ $\lambda_{22} - \lambda_{23} < 0$	$\lambda_{13} - \lambda_{11} < 0$ $\lambda_{33} - \lambda_{31} < 0$
Coexistent if (3.66)	$\Gamma_{12}\Gamma_{23}\Gamma_{31} < 1$		

Table 3.5: Criteria for existence of intransitive triplet.

4

Numerical simulations of replicator systems

For the three-species system, the derived criteria for existence and stability of fixed points in the 2-simplex are hard to interpret due to the high dimensionality of the parameters and are hence simulated rather than studied analytically. The statistical properties of both two- and three-species systems are evaluated numerically for random interactions parameters, which are drawn according to two distributions in the independent and hierarchical parameter model. The distributions under evaluation are the standard uniform Uni(0,1) with a probability density function

$$f_U(u) = \begin{cases} 1, & u \in [0,1] \\ 0, & \text{otherwise} \end{cases} \tag{4.1}$$

which is taken to model the case where any (finite) energy uptake is equally likely and normalised onto the $[0,1]$ interval. This is contrasted to the exponential Exp(λ)-distribution, with density function

$$f_X(x) = \begin{cases} \lambda e^{-\lambda x}, & x \geq 0 \\ 0, & \text{otherwise} \end{cases} \tag{4.2}$$

where the parameter $\lambda = 2$ is chosen to ensure that the mean is the same for both distributions. Any deviations from the standard values of the simulation parameters of Table 4.1 will be clearly noted.

Simulation parameters	Value	Explanation
N	10^6	Number of systems
λ	2	Exponential PDF rate
γ	0.03	Nutrient inflow [8]
κ	0.25	Nutrient uptake [16]
η	$\frac{\kappa}{\kappa+\gamma} \approx 0.89$	κ-γ quotient [16]

Table 4.1: Parameters used in most simulations, exceptions are stated when used.

4.1 Two-species coexistence

The data collected from the simulations on two-species systems are the coordinates ξ_α, ξ_β that form the coexistence criteria as outlined in Section 1.3.3. In the simulations, a system is formed from random interactions parameters $\mathcal{E}_i$, $\mathcal{E}_{ij}$ and the

coordinates ξ_i are computed according to the model used. The number of simulated systems that fulfil the criteria $\xi_\alpha > 0$, $\xi_\beta > 0$ divided by the total number of simulation runs is used as an estimate for the probability in question. The estimations are compared to the analytical probabilities (2.11), (2.15), (2.33) and (2.41).

The estimate probability of permanence from the simulations is presented in Table 4.2, where we see the expected correspondence of the numerical results to the analytical. Detailed investigations of the two distributions under the independent and hierarchical model follow in the subsections.

Probability of permanence		Analytic	$P(\xi_\alpha > 0, \xi_\beta > 0)$
			Simulated (2.1), (2.2)
$\mathcal{E}_i$ model	Uni$(0,1)$, Indep.	0.1552 [Eq. (2.11)]	0.1553
	Uni$(0,1)$, Tree	0.1109 [Eq. (2.33)]	0.1110
	Exp(2), Indep.	0.1585 [Eq. (2.15)]	0.1584
	Exp(2), Tree	7.591×10^{-2} [Eq. (2.41)]	7.606×10^{-2}

Table 4.2: Estimate probabilities for permanence for $N = 10^5$ simulated systems compared to derived analytical expressions.

4.1.1 Uni$(0, 1)$-distributed parameters

The parameters $\mathcal{E}_i$ and $\mathcal{E}_{ij}$ for species i, j are drawn either independently or according to the tree hierarchy (2.18) from a Uni(0,1) distribution. We recall that for the hierarchical model, the parameters $\mathcal{E}_i$ are drawn uniformly and then additional Uniform random numbers r_j were drawn to compute $\mathcal{E}_{ij} = r_j \mathcal{E}_i$ for species i, j. This assures that $\mathcal{E}_{ij} < \mathcal{E}_i$.

The empirical distribution of the fixed points in the system state space — which in the two-species case is the 1-simplex given as the interval $[0, 1]$ — is shown as a histogram in Figure 4.1 with the independent parameter model in the left subfigure and the tree hierarchy in the right. We note that there is a slight preference for fixed points in the center of the 1-simplex and that the probability of permanence is lower in the tree hierarchy model.

The condition for coexistence in two species is that the coordinates ξ_α, ξ_β are both positive by (2.1) and (2.2). The scatter plot of sampled (ξ_α, ξ_β) points in Figure 4.2 shows that the empirical distribution of the coordinates exhibits a negative correlation between the variables. More specifically, they are bounded by the ellipse

$$\left(\frac{x \cos(\theta) - y \sin(\theta)}{a} \right)^2 + \left(\frac{x \sin(\theta) + y \cos(\theta)}{b} \right)^2 = 1 \qquad (4.3)$$

with major axis of length a and minor axis of length b that is slanted by an angle θ

Figure 4.1: Histogram of empirical distribution over 1-simplex of interior fixed points x^*. Left: Independent Uni(0,1) parameter model. Right: Tree hierarchy

to the x-axis. For the independent parameters, we have

$$a = \sqrt{2}(1 + \eta) \tag{4.4}$$

$$b = \sqrt{2}\eta \tag{4.5}$$

$$\theta = -\frac{\pi}{4} \tag{4.6}$$

as derived in Appendix D.1. Furthermore, a larger section of the elliptical distribution is found in the second and fourth quadrant where the coordinates ξ_α and ξ_β have different signs. A majority of the sampled systems have (ξ_α, ξ_β) in the second or fourth quadrants, where $x^* = 1$ or $x^* = 0$, respectively, is a fixed point. These systems tend to dominance of one of the species, in accordance with the analytical results that show that only a small part of the two-species systems are coexistent. For the tree hierarchy model, the situation is somewhat different. We repeat the definitions (2.19), (2.20) for convenience

$$\xi_\alpha = \mathcal{E}_\beta - \mathcal{E}_\alpha \left(1 - \eta t_\alpha\right) \tag{4.7}$$

$$\xi_\beta = \mathcal{E}_\alpha - \mathcal{E}_\beta \left(1 - \eta t_\beta\right) \tag{4.8}$$

and see that for Uni(0,1)-distributed $\mathcal{E}_\alpha$, $\mathcal{E}_\beta$ and Tri(-1,1)-distributed t_α, t_β we have

$$\max \xi_\alpha = 1 \Rightarrow \xi_\beta = -(1 - \eta t_\beta) \sim \text{Tri}\Big(-(1+\eta), -(1-\eta)\Big) \tag{4.9}$$

$$\max \xi_\beta = 1 \Rightarrow \xi_\alpha = -(1 - \eta t_\alpha) \sim \text{Tri}\Big(-(1+\eta), -(1-\eta)\Big) \tag{4.10}$$

when $\mathcal{E}_\beta = 1$, $\mathcal{E}_\alpha = 0$ and $\mathcal{E}_\alpha = 1$, $\mathcal{E}_\beta = 0$, respectively. We note that due to the negative correlation, the minimum of one variable is obtained when the other is at its maximum and that . On the axis where $\xi_\alpha = \xi_\beta$ — corresponding to the minor axis of the ellipse in the independent case — we have from (4.7) and (4.8) that

$$\mathcal{E}_\alpha = \mathcal{E}_\beta \frac{2 - \eta t_\beta}{2 - \eta t_\alpha} \tag{4.11}$$

so that the maximum of ξ_α,

$$\max \xi_\alpha = \eta \tag{4.12}$$

is attained when $\mathcal{E}_\alpha = \mathcal{E}_\beta = 1$ and $t_\alpha = t_\beta = 1$. A similar argument shows that

$$\min \xi_\alpha = -\eta \qquad (4.13)$$

when $\mathcal{E}_\alpha = \mathcal{E}_\beta = 1$ and $t_\alpha = t_\beta = -1$. In conclusion, we have that the minor axis have the same length as in the independent model.
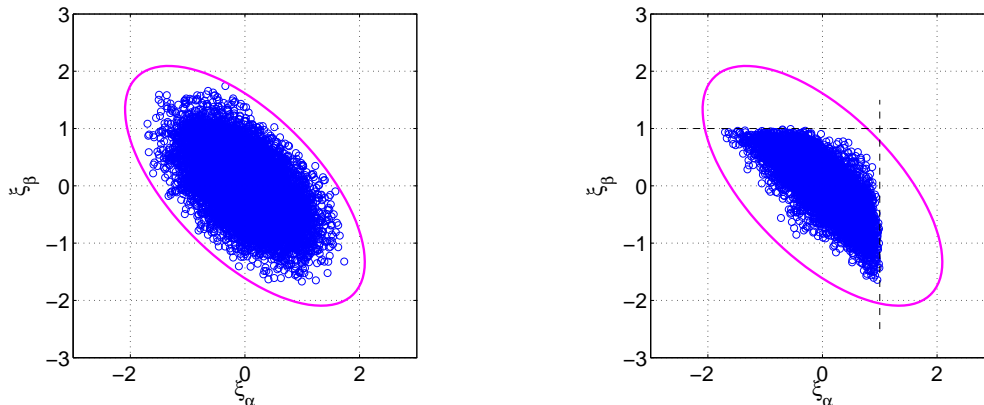
Figure 4.2: Scatter plot of $N = 10^5$ simulated points (ξ_α, ξ_β) with Uni(0,1)-distributed parameters with bounding ellipse (4.3). Left: Independent model. Right: Tree hierarchy model.

4.1.2 Exp(2)-distributed parameters

The energy extraction parameters $\mathcal{E}_i$, $\mathcal{E}_{ij}$ are assumed to be independently Exp(2)-distributed and the other simulation parameters are the same as in the Uniform case. The end state distribution have largely the same properties as in the Uniform case as seen in Figure 4.3, i.e., the fixed points are to a large extent located in the corners $(0, 1)$ or $(1, 0)$ and the interior fixed points show a small tendency of clustering in the middle of the interval. This is however not the case for the tree hierarchy, where the fixed points in the interior of the simplex are more likely to be located near the edges $\mathbf{x} = 0$ and $\mathbf{x} = 1$. As for the systems with Uni$(0, 1)$-distributed parameters, the number of interior fixed points is less in the hierarchical model and the clustering of fixed points near the edges is a likely explanation for the lower probability of permanence.

The scatter plot of the points (ξ_α, ξ_β) form an elliptic shape also when the parameters are Exp(λ)-distributed, as shown in Figure 4.5. Since the coordinates are not bounded in this case, the ellipse (4.3) is defined so that the probability of exceeding a certain range is less than a given threshold α, similar to a confidence level. For the major and minor axes of the ellipse, we define the quantiles ξ_m and ξ_M as the solutions to

$$(1 + \frac{\lambda}{\eta}\xi_m)e^{-\frac{2\lambda}{\eta}\xi_m} = 2\alpha \qquad (4.14)$$

$$e^{-\lambda \xi_M} - \eta^2 e^{-\frac{\lambda}{\eta}\xi_M} = 2\alpha(1 - \eta^2) \qquad (4.15)$$
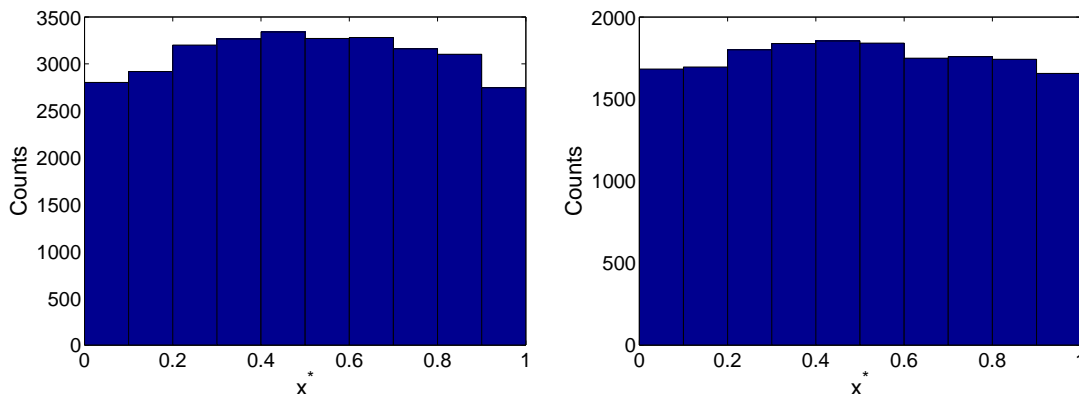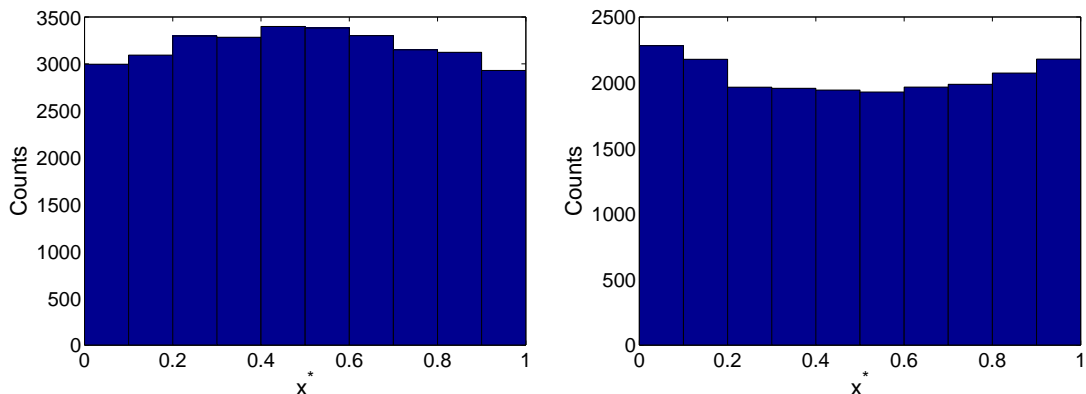
Figure 4.3: Histogram of empirical distribution over 1-simplex of interior fixed points x^*. Left: Independent Exp(2) parameter model. Right: Tree hierarchy

and we define the axes lengths as

$$b = \sqrt{2}\xi_m \tag{4.16}$$

$$a = \sqrt{2}\xi_M \tag{4.17}$$

The derivation of the equations can be found in Appendix D and the dependence of the quantiles ξ_m and ξ_M on η is shown in Figure 4.4. For a chosen confidence level $\alpha = 10^{-3}$, we have

$$b \approx 4.8 \tag{4.18}$$

$$a \approx 2.5 \tag{4.19}$$

which gives the bounding ellipse in Figure 4.5.

The scatter plot in the right subfigure of Figure 4.5 follow the same pattern as the one for the independent Uni[0, 1)-distributed parameters. The differences lie in that the coordinates are not bounded but rather have a probability $1 - \alpha$ of taking values in the interval $[0, z^*)$ for some arbitrary threshold z^*. We have that $\xi_\alpha \approx \mathcal{E}_\beta \sim \text{Exp}(\lambda)$ for small $\mathcal{E}_\alpha$ and analogously for ξ_β so that instead of reaching a max value, the coordinates are nearly Exp(λ)-distributed for small $\mathcal{E}_\alpha$ and $\mathcal{E}_\beta$. Also, we have that $\xi_\alpha \approx \mathcal{E}_\beta - \mathcal{E}_\alpha \sim \text{Laplace}(0, \lambda)$ for $t_1 \approx 1$ so that ξ_α and ξ_β each follow a distribution that is near the Laplace(0, λ)-distribution when the other is large.
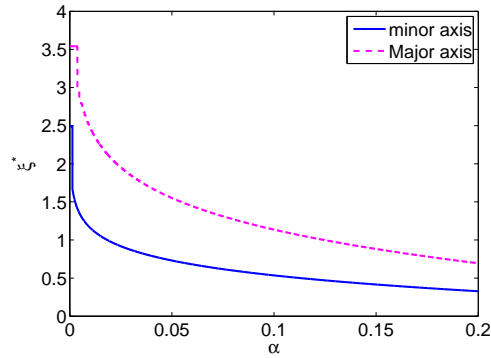
Figure 4.4: Quantile ξ^* dependence on probability threshold α on minor axis $\xi_\alpha = \xi_\beta$ and major axis $\xi_\alpha = -\xi_\beta$
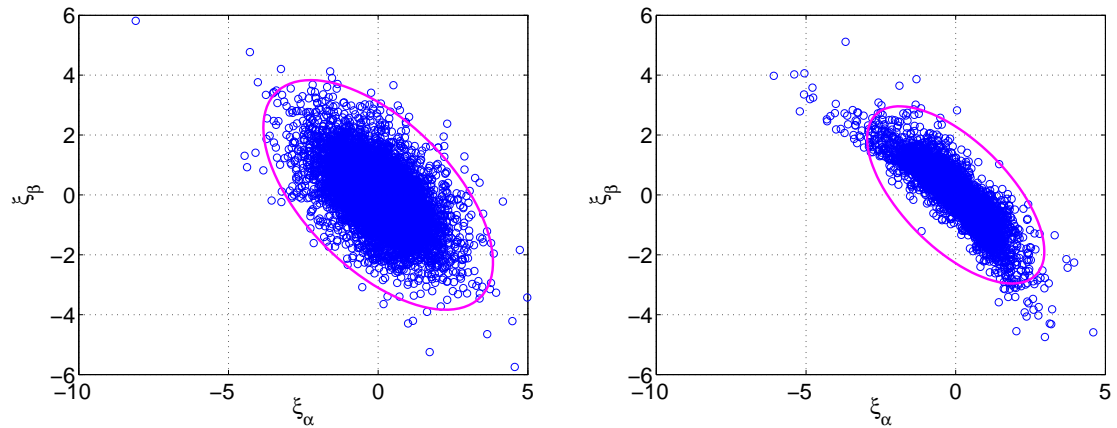
Figure 4.5: Scatter plot of (ξ_α, ξ_β) with Exp(2)-distributed parameters with 0.1% confidence ellipse (4.3). Left: Independent model. Right: Tree hierarchy model.

4.2 Three-species system

The three-species replicator system is defined from the interactions parameters $\mathcal{E}_i$ and $\mathcal{E}_{ij}$, which are drawn independently or according to the hierarchical model (2.17). The simulation parameters can be found in Table 4.1. The dynamics of the three-species system is more complex than the system with two species, and we will differentiate between fixed points in corners where there is exactly one species i with frequency $x_i = 1$ and the non-corner boundary where there is exactly one frequency $x_i = 0$.

4.2.1 Classification of end states

The fixed points of the simulated replicator systems may be categorised in the classes I-IV as described in Section (3.2), which we repeat for convenience

Class I
> Corner fixed points, where only one species has a non-zero frequency.

Class II
> Non-corner boundary points, where two species have a non-zero frequency.

Class III
> Interior fixed points, where all frequencies are non-zero.

Class IV
> Cyclic trajectories described by interior fixed points with imaginary eigenvalues.

The criteria for the fixed points $\mathbf{x}^* \in S_2$ that we use in the implementations are

Class I
> No interior fixed point by negation of the criteria in Table 3.1 and no fixed point on the S_2 boundaries by negation of criteria (3.51)-(3.53) of existence of boundary fixed points.

Class II
> Exactly one of the criteria (3.51)-(3.53) of existence of boundary fixed points hold.

Class III
> Existence of stable interior fixed point by Table 3.1.

Class IV
> Existence of interior fixed point with imaginary eigenvalues by (3.34)-(3.37).

Table 4.3 displays the fractions of systems that fall into the classes I-IV. A few properties are noteworthy: the systems with uniformly distributed parameters are likely to tend to a corner fixed point where all species but one will perish. This is not the case for the systems with exponentially distributed parameters, which tend toward fixed points on the non-corner edges. The probability of an Exponential system to

fall into the most likely Class II is more than 90%, which makes Exponential systems more homogenous in their behaviour than Uniform systems, which have a smaller probability (near 80%) of being Class I-systems. Also, Exponential systems are more likely to be permanent than to be dominated by a single species. Finally, note that the results of the last column are in agreement with the theory: the probability of having a cyclic trajectory is zero, since it requires eigenvalues with zero real part.

Fraction of solutions		Class I	Class II	Class III	Class IV
$\mathcal{E}_i$ model	Uni$(0, 1)$, Indep.	0.775	0.208	1.69×10^{-2}	0
	Uni$(0, 1)$, Tree	0.812	0.181	6.88×10^{-3}	0
	Exp(2), Indep.	0.004	0.928	6.80×10^{-2}	0
	Exp(2), Tree	0.002	0.926	7.22×10^{-2}	0

Table 4.3: Empirical distribution of $N = 10^5$ systems into classes I-IV as outlined in Section 3.2.

For a simulation of $N = 10^6$ systems, the results of Table 4.4 describes the empirical behaviour of the the triplets $\mathcal{E}_i$ of first-order energy uptake. The numerical results are in agreement with the theory, in that all the simulated systems fall into the third category, where one species is dominant. The theoretical reason for this is similar to the one for having no Class IV-solutions in Table 4.3, that the probability of equality between two continous random variables is of a zero measure.

Fraction of systems		Case 1) $\mathcal{E}_i = \mathcal{E}_j$ all $i,\ j$	Case 2) $\mathcal{E}_i = \mathcal{E}_j > \mathcal{E}_k$ $\mathcal{E}_i = \mathcal{E}_j < \mathcal{E}_k$	Case 3) $\mathcal{E}_i > \mathcal{E}_j > \mathcal{E}_k$
$\mathcal{E}_i$ model	Uni$(0, 1)$, Indep.	0.00	0.00	1.00
	Uni$(0, 1)$ Tree	0.00	0.00	1.00
	Exp(2), Indep.	0.00	0.00	1.00
	Exp(2), Tree	0.00	0.00	1.00

Table 4.4: Empirical probability of balance of first-order energy uptake $\mathcal{E}_i$ as outlined in Section 3.2 for $N = 10^6$ systems.

4.2.2 Stable interior fixed points

Existence of the interior fixed point $\mathbf{x}^* = \frac{1}{1+p+q}(1,\ p,\ q)$ is determined by the signs of the sub-determinants (3.19)-(3.21), which gives the criterion

$$\text{sgn}(\Delta_1) = \text{sgn}(\Delta_2) = \text{sgn}(\Delta_3) \qquad (4.20)$$
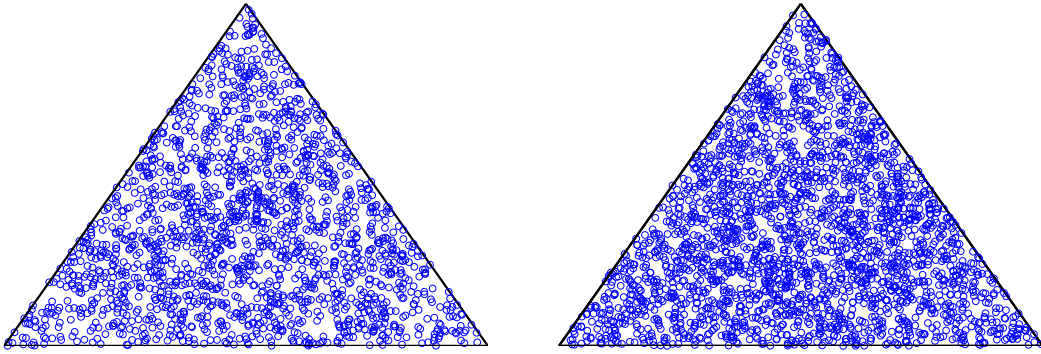
Figure 4.6: $N = 10^5$ interior fixed points for indepdent model. Left: Uniformly distributed. Right: Exponentially distributed.
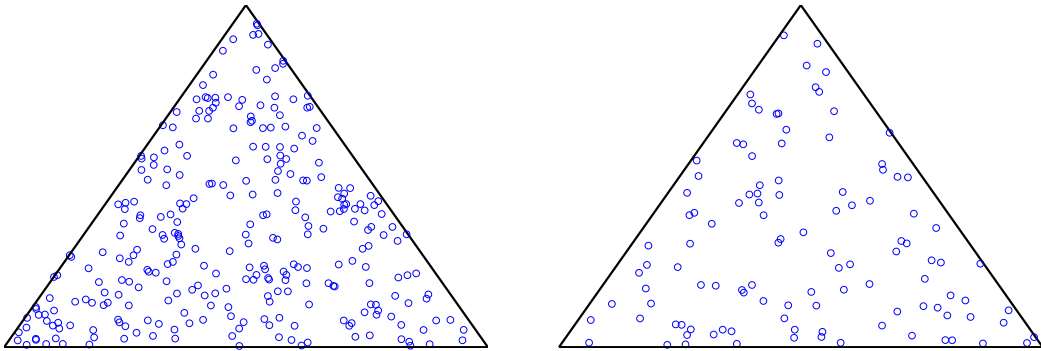
Figure 4.7: $N = 10^5$ interior fixed points for tree hierarchy model. Left: Uniformly distributed. Right: Exponentially distributed.

where sgn() denotes the sign function. The necessary criterion for permanence of the system is negative real parts of the eigenvalues (3.23) to the interior fixed point. By Corollary 7 of Bomze [2], we have

$$\alpha p + \beta q < 0 \tag{4.21}$$

Table 4.5 collects the results from simulations of the independent and tree-hierarchy model for uniformly and expontentially distributed random variables. For the probability of existence in the independent model, we note that the difference between the distributions is small whereas it is larger, relatively speaking, for the tree hierarchy models. This behaviour is also seen in Figures 4.6 and 4.7, where the scatter plot for systems with Exponentially distributed parameters in the latter figure is clearly less dense than the corresponding plot for systems with Uniformly distributed parameters in the former.

Probability		P(Existent) (4.20)	P(Coexistent) (4.21)	P(Coexistent|Existent) (4.20) & (4.21)
$\mathcal{E}_i$ model	Uni$(0,1)$, Indep.	7.063×10^{-2}	1.775×10^{-2}	0.251
	Uni$(0,1)$, Tree	1.240×10^{-2}	3.156×10^{-3}	0.255
	Exp(2), Indep.	8.303×10^{-2}	2.338×10^{-2}	0.282
	Exp(2), Tree	3.704×10^{-3}	8.780×10^{-4}	0.237

Table 4.5: Empirical probability of existence of a stable interior fixed point.

4.2.3 Cyclic trajectories

For existence of a cyclic fixed point, with a Class IV solution, the criterion (4.20) is not enough, as the subdeterminants Δ_i need to be positive as described by (3.34)-(3.36). For the simulated systems that have an interior fixed point, the cyclic property described by (3.37) is considered. Simulations of the system is found in the second column of Table 4.6. As expected from theory, no simulated system is cyclic, since this would require eigenvalues with zero real parts.

The criterion (3.37) forms a surface in the parameter space and we may consider the probability of having an interior fixed point given that the parameters lie on this plane. In other terms, we assume the criterion (3.37) of the cyclic property and investigate the probability of existence for the fixed point. The estimate probability of existence of an interior fixed point, given that it is cyclic, is computed from system simulations is found in Table 4.6. As seen when comparing the results to the probabilities of existence found in Table 4.5, the cyclic fixed points are slightly less likely in the independent model and more likely in the hierarchical.

Probability		P(Cyclic) (3.34)-(3.37)	P(Existent|Cyclic) (3.39)-(3.41)
$\mathcal{E}_i$ model	Uni$(0,1)$, Indep.	0.00	6.790×10^{-2}
	Uni$(0,1)$, Tree	0.00	2.736×10^{-2}
	Exp(2), Indep.	0.00	6.948×10^{-2}
	Exp(2), Tree	0.00	1.579×10^{-2}

Table 4.6: Empirical probability of a cyclic system by (3.34)-(3.37) as well as probability of existence of an interior fixed point, given that it is cyclic by criteria (3.39)-(3.41).

4.2.4   Pair-wise coexistence

For a pair-wise coexistent triplet, we require a stable interior fixed point as investigated in Section 4.2.2. In addition, we use the criteria found in Table 3.2, 3.3 or 3.4 for existence and semi-stability of the three, two or one edge fixed points. The criteria for stability are sufficient also for existence of the fixed points so that existence will not be reported for the systems in question. The results on stability and existence of the boundary fixed points are found in Table 4.7.

The simulation results for the criteria of existence of the stable interior fixed point are found in Table 4.5, which are used when computing the probability of permanence of the different versions of the pair-wise coexistence. The permanence results, which combine a stable interior fixed point with one to three semi-stable fixed points in the boundary of the simplex, are found in Table 4.8.

P(Boundary fixed points)		Three pairs (Table 3.2)	Two pairs (Table 3.3)	One pair (Table 3.4)
$\mathcal{E}_i$ model	Uni$(0,1)$, Indep.	1.174×10^{-2}	6.003×10^{-2}	2.248×10^{-1}
	Uni$(0,1)$, Tree	2.229×10^{-3}	1.183×10^{-2}	1.394×10^{-1}
	Exp(2), Indep.	1.107×10^{-2}	6.190×10^{-2}	2.295×10^{-1}
	Exp(2), Tree	6.410×10^{-4}	4.174×10^{-3}	9.397×10^{-2}

Table 4.7: Empirical probability of existence of three, two or one stable boundary fixed points (3.48)-(3.50), by criteria found in Table 3.2, 3.3 or 3.4.

P(Permanence)		**Three pairs** (Table 3.2)	**Two pairs** (Table 3.3)	**One pair** (Table 3.4)
$\mathcal{E}_i$ model	Uni$(0,1)$, Indep.	6.441×10^{-3}	5.370×10^{-3}	3.957×10^{-3}
	Uni$(0,1)$, Tree	1.097×10^{-3}	9.820×10^{-4}	7.280×10^{-4}
	Exp(2), Indep.	4.836×10^{-3}	8.812×10^{-3}	7.262×10^{-3}
	Exp(2), Tree	2.750×10^{-4}	2.950×10^{-4}	2.100×10^{-4}
P(Permanence|Boundary FPs)		**Three pairs**	**Two pairs**	**One pair**
$\mathcal{E}_i$ model	Uni$(0,1)$, Indep.	0.5486	8.946×10^{-2}	1.760×10^{-2}
	Uni$(0,1)$, Tree	0.4922	8.300×10^{-2}	5.222×10^{-3}
	Exp(2), Indep.	0.4757	0.1424	3.165×10^{-2}
	Exp(2), Tree	0.4290	7.068×10^{-2}	2.235×10^{-3}

Table 4.8: Top: Empirical probability of permanence, computed from the criteria in Table 3.2, 3.3 or 3.4 on fixed points in the interior and on the boundary of the simplex in systems with three, two and one coexistent pairs. Bottom: Probability of permanence given that stable boundary fixed points exist.

With respect to the existence results in Table 4.7, we see that the probability of existence is decreasing with the number of fixed points on the boundary. This is not fully reflected in the permanence results shown in the upper part of Table 4.8, where we see that three coexistent pairs is the most likely configuration for systems with Uniformly distributed parameters and that two coexistent pairs is most likely for Exponentially distributed parameters. This is due to correlation between the conditions for having a stable interior fixed point and the conditions for stable fixed points on the boundary.

We may also investigate the probability of permanence conditionally on the number of fixed points on the boundary of the simplex. Then we see that the systems with three coexistent pairs on the simplex boundary is indeed the most likely to be permanent.

4.2.5 Intransitivity and permanence

To properly define the clock-wise and anti-clockwise versions of intransitivity, we need that either the conditions (3.60)-(3.61) or (3.62)-(3.63) hold for all pairs $(\mathbf{x}_i, \mathbf{x}_{i+1})$ where we as usual consider the indices as modulo 3. The results of the simulations are collected in Table 4.9, where we see that the tree hierarchy model is less likely to be intransitive and permanent and also note that the probability of permanence is less than or on the order of one permanent system per thousand. Finally, note that approximately half of the intransitive systems are permanent. This corresponds well to theory, as the intransitive systems that do not have an interior fixed point (cf. phase portrait 46 of Bomze [2]) constitute a zero-measure set which is also the case

for the intransitive system with a center fixed point (cf. Section 4.2.3 and phase portrait 16 of Bomze [2]). The only systems with an interior fixed point that have a non-zero probability either have positive eigenvalues so that the fixed point is unstable or have negative eigenvalues and a stable fixed point, which is the coxistent case.

Probability		Intransitivity (Table 3.5)	Intrans. & permanent Table 3.5 & (3.66)	Permanent fraction
$\mathcal{E}_i$ model	Uni$(0,1)$, Indep.	2.341×10^{-3}	1.168×10^{-3}	0.4989
	Uni$(0,1)$, Tree	4.300×10^{-4}	2.140×10^{-4}	0.4977
	Exp(2), Indep.	2.417×10^{-3}	1.200×10^{-3}	0.4965
	Exp(2), Tree	1.380×10^{-4}	7.700×10^{-5}	0.5580

Table 4.9: Probability of permanence in intransitive scenario by criteria (3.66) and Table 3.5.

4.2.6 Comparison of coexistent systems

To compare the different forms of coexistence, we will now repeat the permanence results presented in Section 4.2.2-4.2.5 and also compute the fraction that each different form of coexistence covers of the whole set of permanent systems. We will not repeat the trivial results of zero probability for cyclic systems, to save some space in the tables.

First, we notice that the intransitive scenario is an order of magnitude less likely than even the least likely version of the pair-wise coexistence scenarios. Also, the fraction of intransitive systems in the set of systems with stable interior fixed points is largely constant over the four different models for the parameters. Second, the pair-wise coexistence scenarios were discussed in Section 4.2.4 and we only add that the cases with three or two coexistent pairs occupy some two thirds of the systems with a stable interior fixed point for systems with Uni$(0, 1)$-distributed parameters. In the case where the parameters are Exp(2)-distributed, we have that two or one coexistent pair are most likely for independent parameters and cover more than two thirds of the systems with stable interior fixed points, whereas the tree hierarchy is more similar to the systems with Uniform parameters. As a last note, we see that the sum of pair-wise coexistent and intransitive systems do not cover the full set of systems with interior fixed points. This is due to non-permanent systems that have a stable interior fixed point that can only be reached from some states in the simplex, like Bomze phase portraits 12-13 [2].

Probability	Stable interior fixed point (Table 4.5)	Pair-wise coexistent and permanent (Table 4.8)			Intransitive and permanent (Table 4.9)
		Three pairs	Two pairs	One pair	
Uni(0, 1), Indep.	1.78×10^{-2}	6.44×10^{-3}	5.37×10^{-3}	3.96×10^{-3}	1.17×10^{-3}
Uni(0, 1), Tree	3.16×10^{-3}	1.10×10^{-3}	9.82×10^{-4}	7.28×10^{-4}	2.14×10^{-4}
Exp(2), Indep.	2.34×10^{-2}	4.84×10^{-3}	8.81×10^{-3}	7.26×10^{-3}	1.20×10^{-3}
Exp(2), Tree	8.78×10^{-4}	2.75×10^{-4}	2.95×10^{-4}	2.10×10^{-4}	7.70×10^{-5}
Fraction of stable interior fixed point	Stable interior fixed point	Pair-wise coexistent and permanent			Intransitive and permanent
		Three pairs	Two pairs	One pair	
Uni(0, 1), Indep.	1.00	0.363	0.302	0.223	0.066
Uni(0, 1), Tree	1.00	0.347	0.311	0.231	0.068
Exp(2), Indep.	1.00	0.207	0.377	0.311	0.051
Exp(2), Tree	1.00	0.313	0.336	0.239	0.088

Table 4.10: Probability of permanence in general, pair-wise coexistence and intransitive scenarios, collected from Table 4.5, 4.8 and 4.9.

We may also study the fraction of the investigated systems that are permanent, i.e., the probability of permanence conditionally on existence of the system. The results are collected in Table 4.11. First, we note that there is a pattern to the pair-wise coexistent systems in that the probability of permanence is increasing with the number of coexistent pairs. This pattern is the same for both models and distributions for the interactions parameters. We also note that the probability of permanence in triplets with three coexistent pairs is by far larger than the probability for triplets with two or one coexistent pairs. Finally, although intransitive systems are unlikely to exist when the interactions parameters are random (as shown in Table 4.9), close to half of the intransitive systems are permanent. This means that the intransitive property, and not the permanence, is the limiting factor. The converse is true for systems with one or two coexistent pairs on the boundary, as these systems are fairly likely to exist (Table 4.7) but have a low conditional probability of permanence.

Fraction of systems that are permanent	Pair-wise coexistent and permanent			Intransitive and permanent
	Three pairs	Two pairs	One pair	
		(Table 4.8)		(Table 4.9)
Uni(0, 1), Indep.	0.549	8.95×10^{-2}	1.76×10^{-2}	0.499
Uni(0, 1), Tree	0.492	8.30×10^{-2}	5.22×10^{-3}	0.498
Exp(2), Indep.	0.476	0.142	3.17×10^{-2}	0.497
Exp(2), Tree	0.429	7.07×10^{-2}	2.24×10^{-3}	0.558

Table 4.11: Fraction of permanent systems, collected from Table 4.8 and 4.9.

Finding an analytical expression for the probability of permanence as a function of η, which was used in the two-species case, was deemed impractical in the three-species case since the dimensionality of the inequalities that determine permanence is high. Rather, the criteria for stable interior fixed points are evaluated numerically for $\eta \in [0, 1]$ and graphs of the probability functions for the independent and tree hierarchy models are shown Appendix E. A zero value of η corresponds to a zero nutrient uptake κ in relation to the nutrient inflow γ, where no coexistence is possible. This property features in the simulated curves, where all of the estimated probabilities are increasing functions of η with $\text{P(Permanence)}\big|_{\eta=0} = 0$. The highest probability of permanence is attained for $\eta = 1$, which corresponds to the results of Pfeiffer & Bonhoeffer [18] who found that coexistence is most likely for low dilution rates in the chemostat.

The η-dependence forms a similar pattern, and we only note that the systems with three coexistent pairs on the non-corner boundary have an interesting feature, as seen in Figure 4.8. Where the rest of the graphs have a lower probability of permanence for systems with Uniformly distributed parameters for all values of η, the system with three coexistent pairs have point of equality in the probability of permanence for Exponentially and Uniformly distributed parameters. The point is located at $\eta \approx 0.55$ and for larger η-values, systems with Uniformly distributed parameters are more probable to be permanent.
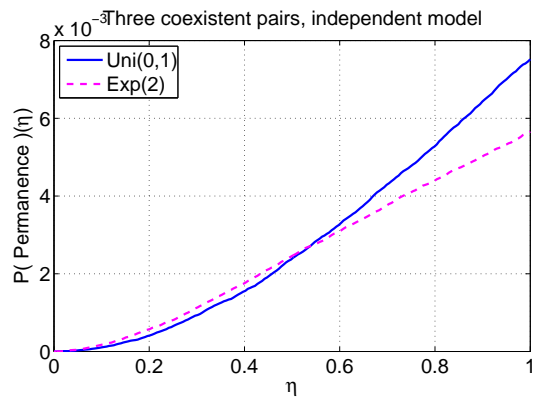
Figure 4.8: Probability of permanence by the criteria in Table 3.2 for three coexistent pairs as function of η, independent model

5

Discussion

5.1 Methods

The series-expansion model proposed by Lundh & Gerlee is a general model of cross-feeding in a system with a high inflow of energy and different time-scales for the metabolism and the population dynamics. It does not cover more than two levels of metabolism in the form used in this project but may be extended as such [16]. The basis of the model is the replicator equation, which models a well-mixed and infinite population of species involved in frequency-dependent selection without considering species evolution or spatial differences in the mixture [2, 10, 14, 16]. For modelling of finite populations, Markov chains or Moran processes are often used for modelling of stochastic interactions between individuals [22, 23].

To study statistical properties of the replicator system, we consider the parameters $\mathcal{E}_i$, $\mathcal{E}_{ij}$ that model the energy uptake of a species [16] as random variables and used two example distributions for the parameters. To model individual energy uptake parameters require probability distributions that are defined on $\mathbb{R}^+$, as any energy uptake is by necessity positive. For this, the Uni(0,1) distribution is chosen to investigate the properties of the system under the assumption that any energy uptake is equally likely when normalised onto the [0,1]-interval. This is contrasted to the case where smaller amounts of energy are more likely than larger, which is modelled as an Exp(λ)-distribution. In the simulations, the parameter $\lambda = 2$ is chosen to ensure a mean value of $\frac{1}{2}$, the same mean as for a random variable from the Uni(0,1)-distribution. Other possible distributions are the log-normal and the gamma distributions, where a certain interval for the extracted energy may be specified [11]. If one would like to consider the difference in energy uptake between species or between metabolites — rather than individual interactions parameters — then it is possible to use probability distributions that are defined for the whole real line. This approach may be used if the individual parameters are not known.

5.2 Parameter models

Two schemes are used for the random energy uptake parameters, the independent where any species is allowed to extract any amount of energy from any metabolite and, in particular, may extract more energy from a derived metabolite than from the primary nutrient. This is the most general case of cross-feeding, where different species may be specialised on different nutrients. To investigate the case where a species is not able to extract more energy further down in the metabolic chain, the tree hierarchy model with the condition $\mathcal{E}_{ij} < \mathcal{E}_i$ is used as an alternative. In the simulations, the hierarchical model was implemented as the more specific relation $\mathcal{E}_{ij} = r_{ij}\mathcal{E}_i$, where $r_{ij} \sim \text{Uni}(0, 1)$. In the performed simulations, the tree hierarchy model exhibits a lower probability of permanence since the first-order interactions

are more important and these tend to supress coexistence. The systems with only first-order terms discussed in Section 3.2.1 were permanent only on a zero-measure set, and would otherwise tend to a state of domination of one of the involved species. This is also hinted at in the scatter plots in Figure 4.2 and 4.5 of the two-species systems, where the bounded second-order interactions causes the coordinates ξ_α, ξ_β to cluster in the second and fourth quadrants corresponding to systems with trajectories that tend to corners.

5.3   Two-species coexistence

The derived analytic expressions (2.11), (2.15), (2.33) and (2.41) for the probability of permanence are more complex for the tree hierarchy model than for the independent model. As seen in the the algebraic expressions and visualised in the graphs of the probabilities, the behaviour of the probability as a function of η is also different. Where the independent model in Figure 2.2 shows increasing functions with negative curvature, the tree model in Figure 2.5 show functions with positive and nearly flat curvature. In addition, the tree hierarchy model functions take lower values on the interval η.

The analytic results are compared to simulations, where systems are generated by drawing random parameters according to one of the models. The coexistence properties are determined from the criteria $\xi_\alpha > 0$, $\xi_\beta > 0$ and the distribution of inner fixed points is computed from Eq. (17) of Lundh & Gerlee [16]. We find that the simulations correspond to the analytical results, which is taken as an indicator of the feasibility of numerical simulations in the three-species case.

5.4   Three-species system

The derived coexistence criteria for three-species systems are evaluated numerically over a sweep of η-values and the general behaviour is that the probability of permanence is an increasing function of η. In the independent model, the probability of permanence for a given η is larger for the Exp(2)-distributed interactions parameters than for systems with Uni(0, 1)-parameters. The notable exception is the case for three coexistent pairs, where the curves for the probability intersect. The case for the tree hierarchy model is the opposite: systems with uniformly distributed interactions parameters have a larger probability of permanence than those with exponentially distributed parameters.

Analytical expressions of the probability of permanence were considered infeasible in the three-species systems due to the dimensionality of the inequalities that determined the permanent subspaces. Rather, the three-species system was investigated numerically by drawing random samples from the two distributions and according to the independent and hierarchical models.

5.5   From pairs to triplets

Having established that the replicator system on normal form (investigated thoroughly by Bomze [2, 3]) is equivalent to the affine system with a fitness function

based on series-expansion as introduced by Lundh & Gerlee, we find that the possible dynamics of the series-expansion replicator system is the same as the dynamics of a system with a payoff matrix on normal form. This fact shows that the information on pair-wise interactions of the constituent species is not enough to draw any deterministic conclusions on the triplet coexistence, as there are multiple three-species systems with the same pair-wise dynamics but different stability properties of any interior fixed points. For the permanent systems investigated, the permanent intransitive system (Bomze phase portrait 17) has the same pair-wise properties as the non-permanent phase portrait with number 46 [2]. The pair-wise coexistent systems with Bomze phase portraits 7, 9 and 15 with three, two and one coexistent pairs, respectively, have the corresponding non-permanent systems with the same behaviour on the simplex boundary in phase portraits 35, 10 and 41 [2, 3]. Furthermore, any system with a stable inner fixed point has a mirror image in a system with the same pair-wise interactions but with an unstable inner fixed point.

However, triplet coexistence is more or less likely to occur in the three-species systems, depending on the pair-wise interactions of the systems. We find that nearly half of the systems with three coexistent pairs and intransitive systems are permanent, where the corresponding numbers for systems with one and two coexistent pairs are closer to one percent and ten percent, respectively.

6

Conclusions

The main questions in this project was to investigate what conclusions on permanence in three-species systems that could be drawn from known coexistence properties in the corresponding two-species systems. From the simulations, we find that intransitivity and three-pair coexistence are more strongly correlated with permanence than two- or one-pair coexistence. For the intransitive systems, there is a near 50% probability of permanence and the same holds for systems with three coexistent pairs on the simplex boundary. There can, however, be no deterministic conclusions on triplet permanence from pair-wise interactions. This is due to the result that the affine fitness function (1.10) is equivalent to the linear (1.2) and that triplet permanence in systems with a linear fitness function depends on stability of an inner fixed point.

Coexistence criteria are derived for the possible modes of coexistence in two- and three-species systems. The parameter η that relates the nutrient uptake κ to the nutrient inflow rate γ is central for the present model, and the general behaviour is that the probability of permanence increases with the parameter η.

Out of the investigated scenarios, a permanent system that exhibit pair-wise coexistence is the most likely form of permanence. Furthermore, the subgroup of pair-wise coexistence with three coexistent pairs on the boundary is the most likely for systems with Uni(0, 1)-distributed parameters. For systems with Exp(2)-distributed parameters, the case is less clear with differing behaviour in the independent and tree models.

Bibliography

[1] Belenguer, A. et al., Two Routes of Metabolic Cross-Feeding Between *Bifidobacterium adolescentis* and Butyrate-Producing Anaerobes from the Human Gut, *Applied and Environmental Microbiology*, **72**, pp. 3593-3599, 2006.

[2] Bomze, I. M., Lotka-Volterra Equation and Replicator Dynamics: A Two-Dimensional Classification, *Biological Cybernetics*, **48**, pp. 201-211, 1983.

[3] Bomze, I. M., Lotka-Volterra Equation and Replicator Dynamics: New Issues in Classification, *Biological Cybernetics*, **72**, pp. 447-453, 1995.

[4] Bull, J. J. & Harcombe, W. R., Population Dynamics Constrain the Cooperative Evolution of Cross-Feeding, *PLoS ONE*, **4**, e4115, 2009.

[5] Costa, E., Perez, J. & Kreft, J.-U., Why is metabolic labour divided in nitrification?, *Trends in Microbiology*, **14**, pp. 213-219, 2006.

[6] Doebeli, M., A Model for the Evolutionary Dynamics of Cross-Feeding Polymorphisms in Microorganisms, *Popul Ecol*, **44**, pp. 59-70, 2002.

[7] Estrela, S. & Gudelj, I., Evolution of cooperative cross-feeding could be less challenging than originally thought, *PLoS ONE*, **5**, e14121, 2010.

[8] Gerlee, P. & Lundh, T., Productivity and Diversity in a Cross-Feeding Population of Artificial Organisms, *Evolution*, **64**, pp. 2716-2730, 2010.

[9] Gerstung, M., Nakhoul, H. & Beerenwinkel, N., Evolutionary games with affine fitness functions: Applications to cancer, *Dynamical Games and Applications*, **1**, pp. 370-385, 2011.

[10] Gokhale, C. S., Traulsen, A. & Levin, S. A., Evolutionary Games in the Multiverse, *Proceedings of the National Academy of Sciences*, **107**, pp. 5500-5504, 2010.

[11] Grimmett, G., Stirzaker, D., *Probability and Random Processes*, Oxford University Press, Oxford, UK, 2001.

[12] Hallam, S. J., et al., Reverse methanogenesis: testing the hypothesis with environmental genomics, *Science*, **305**, pp. 1457-1462, 2004.

[13] Harcombe, W. R. et al., Metabolic resource allocation in individual microbes determines ecosystem interactions and spatial dynamics, *Cell Reports*, **7**, pp. 1104-1115, 2014.

[14] Hofbauer, J. & Sigmund, K., *Evolutionary Games and Population Dynamics*, Cambridge University Press, Cambridge, 2002.

[15] Katsuyama, C., et al., Complementary Cooperation Between Two Syntrophic Bacteria in Pesticide Degradation, *J. Theor. Biol.*, **256**, pp. 644-654, 2009.

[16] Lundh, T. & Gerlee, P., Cross-Feeding Dynamics Described by a Series Expansion of the Replicator Equation, *Bull Math Biol*, **75**, pp. 709-724, 2013.

[17] Pernthaler, A., et al., Diverse Syntrophic Parterships From Deep-Sea Methane Vents Revealed by Direct Cell Capture and metagenomics, *Proceedings of the National Academy of Sciences USA*, **105**, pp. 7052-7057, 2008.

[18] Pfeiffer, T. & Bonhoeffer, S., Evolution of Cross-Feeding in Microbial Populations, *American Society of Naturalists*, **163**, pp. E126-E135, 2004.

[19] Rice, J. A., *Mathematical statistics and data analysis*, Thomson Brooks/Cole, Belmont, Calif., 2007.

[20] Stadler, P. F. & Schuster, P., Dynamics of small autocatalytic networks – 1. Bifurcations, permanence and exclusion, *Bull. Math. Biol.*, **52**, pp. 485-508, 1990.

[21] Teschl, G., *Ordinary Differential Equations and Dynamical Systems*, American Mathematical Society, Providence, R.I, 2012.

[22] Traulsen, A., Pacheco, J. M. & Nowak, M. A., Pairwise comparison and selection temperature in evolutionary game dynamics, *J. Theor. Biol.*, **246**, pp.522-529, 2007.

[23] Traulsen, A., Shoresh, N. & Nowak, M. A., Analytical results for individual and group selection of any intensity, *Bull. Math. Biol.*, **70**, pp.1410-1424, 2008.

A

Comparison of fitness functions

The fitness function used by Bomze is formed from the payoff matrix

$$A = \begin{bmatrix} 0 & 0 & 0 \\ a & b & c \\ d & e & f \end{bmatrix} \tag{A.1}$$

which has a zero first row due to it being mapped from the equivalent Lotka–Volterra system [2]:

$$\begin{cases} \dot{x} = x(a + bx + cy) \\ \dot{y} = y(d + ex + fy) \end{cases}.$$

Since the replicator dynamics are unchanged under column-wise addition and subraction, we have that (A.1) may be written on normal form as

$$A = \begin{bmatrix} 0 & -b & -f \\ a & 0 & c - f \\ d & e - b & 0 \end{bmatrix}. \tag{A.2}$$

This structure of the payoff matrix was however not used for the example system in Section 3 for aestethic reasons.

The replicator system derived by Lundh & Gerlee [16] is shown [9] to be equivalent to a system with a fitness function based on the matrix

$$E = \gamma\eta \begin{bmatrix} \mathcal{E}_1 + \eta\mathcal{E}_{11} & \mathcal{E}_1 + \eta\mathcal{E}_{21} & \mathcal{E}_1 + \eta\mathcal{E}_{31} \\ \mathcal{E}_2 + \eta\mathcal{E}_{12} & \mathcal{E}_2 + \eta\mathcal{E}_{22} & \mathcal{E}_2 + \eta\mathcal{E}_{32} \\ \mathcal{E}_3 + \eta\mathcal{E}_{13} & \mathcal{E}_3 + \eta\mathcal{E}_{23} & \mathcal{E}_3 + \eta\mathcal{E}_{33} \end{bmatrix}, \tag{A.3}$$

which by the column-wise subraction transformation is equivalent to the normal form

$$E = \gamma\eta \begin{bmatrix} 0 & \lambda_{21} - \lambda_{22} & \lambda_{31} - \lambda_{33} \\ \lambda_{12} - \lambda_{11} & 0 & \lambda_{32} - \lambda_{33} \\ \lambda_{13} - \lambda_{11} & \lambda_{23} - \lambda_{22} & 0 \end{bmatrix}, \tag{A.4}$$

or the Lotka–Volterra form of the payoff matrix (A.1)

$$E = \gamma\eta \begin{bmatrix} 0 & 0 & 0 \\ \lambda_{12} - \lambda_{11} & \lambda_{22} - \lambda_{21} & \lambda_{32} - \lambda_{31} \\ \lambda_{13} - \lambda_{11} & \lambda_{23} - \lambda_{21} & \lambda_{33} - \lambda_{31} \end{bmatrix}, \tag{A.5}$$

I

where we recall the definition

$$\lambda_{ji} = \mathcal{E}_i + \eta \mathcal{E}_{ji}. \tag{A.6}$$

Hence, in order to map the affine system (1.10) used by Lundh & Gerlee [16] to the results of Bomze [2] that uses a homogenous fitness equation (1.2), we define the elements of the payoff matrix (A.1) as (A.5).

B

Analytic probability
$\mathbf{P}(\xi_\alpha > 0, \ \xi_\beta > 0)$

B.1 Derivation of distributions from difference of random variables

As a step towards simplification of the expressions (1.20) and (1.21), note that the sum of two independent random variables is distributed as the convolution of the respective distribution functions [19], i.e., for $X \sim f_X(x)$ and $Y \sim f_Y(y)$ we have that the random variable $Z = X + Y$ is distributed as

$$f_{X+Y}(z) = (f_X \star f_Y)(z) = \int_{\mathbb{R}} f_X(z - t) f_Y(t) \ dt. \tag{B.1}$$

B.1.1 Triangular distribution from difference of uniform variables

In order to calculate the distribution of the difference $Z = \mathcal{E}_\alpha - \mathcal{E}_\beta = \mathcal{E}_\alpha + (-\mathcal{E}_\beta)$, we use the fact that for $\mathcal{E}_\alpha, \ \mathcal{E}_\beta \sim \mathrm{Uni}(0, 1)$, the negative $-\mathcal{E}_\beta \sim \mathrm{Uni}(-1, 0)$. Hence, when $f_{\mathcal{E}_\alpha}(t) = \mathcal{I}_{t \in [0,1]}$ and $f_{-\mathcal{E}_\beta}(t) = \mathcal{I}_{t \in [-1,0]}$ and the indicator function $\mathcal{I}_{t \in S}$ is defined for a set $S \subset \mathbb{R}$ as

$$\mathcal{I}_{t \in S} = \begin{cases} 1, & \text{if } x \in S \\ 0, & \text{otherwise} \end{cases}, \tag{B.2}$$

we have that the distribution $f_Z(z) = (f_{\mathcal{E}_\alpha} \star f_{-\mathcal{E}_\beta})(z)$. This convolution of the distribution functions is straightforward. Use the fact that $f_{-\mathcal{E}_\beta}(t) = \mathcal{I}_{t \in [-1,0]}$ in (B.1) to see that

$$f_Z(z) = \int_{-1}^{0} f_{\mathcal{E}_\alpha}(z - t) \ dt. \tag{B.3}$$

A substitution of variables

$$\begin{cases} s = z - t \\ ds = -dt \end{cases}$$

gives that (B.3) is equal to

$$f_Z(z) = \int_{z}^{z+1} f_{\mathcal{E}_\alpha}(s) \ ds. \tag{B.4}$$

The integration limits imply that the indicator funtion $f_{\mathcal{E}_\alpha}(s) = \mathcal{I}_{s\in[0,1]}$ is non-zero in two cases, as visualised in Figure B.1, namely

$$
f_Z(z) = \begin{cases} 0 & \text{for } z < -1 \text{ or } z > 1 \\ \int\limits_{0}^{z+1} 1\ ds & \text{for } z \in [-1, 0) \\ \int\limits_{z}^{1} 1\ ds & \text{for } z \in [0, 1] \end{cases} .
\tag{B.5}
$$

In conclusion, we have that

$$
f_Z(z) = \begin{cases} 0 & \text{for } z \notin [-1, 1] \\ 1 + z & \text{for } z \in [-1, 0) \\ 1 - z & \text{for } z \in [0, 1] \end{cases} ,
\tag{B.6}
$$

which is the distribution function of the triangle distribution.

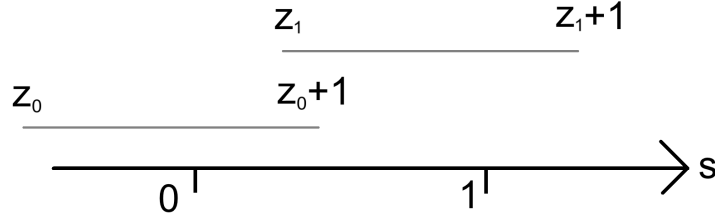**Figure B.1:** The two cases of z-s overlap in (B.5).

B.1.2 Laplace distribution from difference of exponential variables

For the exponentially distributed uptake parameters, we have the rate parameter $\lambda = 2$ so that $\mathcal{E}_i,\ \mathcal{E}_{ij} \sim \text{Exp}(2)$ in the simulations. For clarity, the derivations will however consider a general λ. As a first step towards showing that the distribution of the difference of two exponentially distributed parameters is Laplacian, define the random variables

$$
\begin{align}
X &= \mathcal{E}_{\alpha\alpha} - \mathcal{E}_{\alpha\beta}, \tag{B.7} \\
Y &= \mathcal{E}_{\beta\alpha} - \mathcal{E}_{\beta\beta}, \tag{B.8} \\
Z &= \mathcal{E}_\alpha - \mathcal{E}_\alpha. \tag{B.9}
\end{align}
$$

Note that the definition (B.1) refers to a sum of random variables, whence we first need to know how the negative of $\mathcal{E}_{\alpha\beta}$ is distributed. For the exponentially distributed $\mathcal{E}_{\alpha\beta}$, we have that $-\mathcal{E}_{\alpha\beta}$ have the distribution function

$$
f_{-\mathcal{E}_{\alpha\beta}}(t) = \begin{cases} \lambda e^{\lambda t}, & t \leq 0 \\ 0, & t > 0 \end{cases}
\tag{B.10}
$$

when λ, as stated, is the rate parameter of the exponential distribution. Also $-\mathcal{E}_{\beta\beta}$ and $-\mathcal{E}_\alpha$ have the functional form (B.10). Then, as described by (B.1) in the section

preamble, we have that the random variable Z is distributed as

$$f_Z(z) = \int_{\mathbb{R}} f_{\mathcal{E}_{\alpha\alpha}}(z - t) f_{-\mathcal{E}_{\alpha\beta}}(t) \; dt$$
$$= \lambda \int_{\mathbb{R}^-} f_{\mathcal{E}_{\alpha\alpha}}(z - t) e^{\lambda t} \; dt, \tag{B.11}$$

where the non-zero part of $f_{\mathcal{E}_{\alpha\alpha}}(z - t)$ requires $z - t > 0$. We see that there are two possibilities when $t < 0$, either that $z > 0$ so that the condition is true by default and we have

$$f_Z(z) = \lambda^2 \int_{-\infty}^{0} e^{-\lambda(z-t)} e^{\lambda t} \; dt$$
$$= \lambda^2 e^{-\lambda z} \left[\frac{1}{2\lambda} e^{2\lambda t} \right]_{t=-\infty}^{0}$$
$$= \frac{\lambda}{2} e^{-\lambda z}. \tag{B.12}$$

When z is negative, we have that $z > t$ so that

$$f_Z(z) = \lambda^2 \int_{-\infty}^{z} e^{-\lambda(z-t)} e^{\lambda t} \; dt$$
$$= \lambda^2 e^{-\lambda z} \left[\frac{1}{2\lambda} e^{2\lambda t} \right]_{t=-\infty}^{z}$$
$$= \frac{\lambda}{2} e^{\lambda z}. \tag{B.13}$$

The two cases may be collected into a single density function

$$f_Z(z) = \frac{\lambda}{2} e^{-\lambda|z|}, \tag{B.14}$$

which is defined for all real z and known as the density for the Laplace distribution [11] with location parameter $a = 0$ (which would otherwise have been found in the exponent as $|z - a|$) and rate parameter λ. The same holds for the variables X and Y.

B.2 Calculation of P($\xi_\alpha > 0$, $\xi_\beta > 0$)

Below are the details of the calculations of the probabilities (2.11), (2.15), (2.33) and (2.41).

B.2.1 Independent, uniformly distributed parameters

We are now to find an analytical expression for the probability of having a permanent system as described by the coordinates ξ_α (1.20) and ξ_β (1.21). The probability was found to be described by the integral (2.7), which we now repeat for convenience

$$P(\xi_\alpha > 0, \xi_\beta > 0) = \int_{-1}^{1} \int_{-1}^{1} \int_{-1}^{1} f_{X,Y,Z}(x, y, z) \mathcal{I}_{\{\eta x - z > 0\}} \mathcal{I}_{\{\eta y + z > 0\}} \; dz dy dx. \tag{B.15}$$

B. Analytic probability $P(\xi_\alpha > 0, \; \xi_\beta > 0)$

It is beneficial to decompose the region $x \in [-1, 1]$, $y \in [-1, 1]$ into its four main quadrants

$$Q_1 = \{ \; 0 < x \leq 1, \; 0 < y \leq 1 \} \tag{B.16}$$

$$Q_2 = \{ -1 < x \leq 0, \; 0 < y \leq 1 \} \tag{B.17}$$

$$Q_3 = \{ -1 < x \leq 0, -1 < y \leq 0 \} \tag{B.18}$$

$$Q_4 = \{ \; 0 < x \leq 1, -1 < y \leq 0 \} \tag{B.19}$$

Then, the probability (B.15) with the idependence assumption (2.8) that leads to the separability of the joint distribution, is expressed as the sum of four integrals

$$P(\xi_\alpha > 0, \xi_\beta > 0) = I_1 + I_2 + I_3 + I_4, \tag{B.20}$$

where the integrals I_1 through I_4 are defined as

$$I_1 = \int_0^1 f_X(x) \int_0^1 f_Y(y) \int_{-1}^1 f_Z(z) \mathcal{I}_{\{\eta x - z > 0\}}(x, z) \mathcal{I}_{\{\eta y + z > 0\}}(y, z) \; dz dy dx \tag{B.21}$$

$$I_2 = \int_{-1}^0 f_X(x) \int_0^1 f_Y(y) \int_{-1}^1 f_Z(z) \mathcal{I}_{\{\eta x - z > 0\}}(x, z) \mathcal{I}_{\{\eta y + z > 0\}}(y, z) \; dz dy dx \tag{B.22}$$

$$I_3 = \int_{-1}^0 f_X(x) \int_{-1}^0 f_Y(y) \int_{-1}^1 f_Z(z) \mathcal{I}_{\{\eta x - z > 0\}}(x, z) \mathcal{I}_{\{\eta y + z > 0\}}(y, z) \; dz dy dx \tag{B.23}$$

$$I_4 = \int_0^1 f_X(x) \int_{-1}^0 f_Y(y) \int_{-1}^1 f_Z(z) \mathcal{I}_{\{\eta x - z > 0\}}(x, z) \mathcal{I}_{\{\eta y + z > 0\}}(y, z) \; dz dy dx \tag{B.24}$$

Recall now that the distribution functions $f_X(x)$, $f_Y(y)$ and $f_Z(z)$ describe the triangle distribution (B.6) and that the product of the indicator function can be expressed as the condition

$$\mathcal{I}_{\{\eta x - z > 0\}}(x, z) \mathcal{I}_{\{\eta y + z > 0\}}(y, z) = \mathcal{I}_{\{-\eta y < z < \eta x\}}(x, y, z),$$

where it is also implied that $-y < x$. These two facts allow for the following simplification:

$$I_1 = \int_0^1 (1 - x) \int_0^1 (1 - y) \int_{-1}^1 f_Z(z) \mathcal{I}_{\{-\eta y < z < \eta x\}}(x, y, z) \; dz dy dx \tag{B.25}$$

$$I_2 = \int_{-1}^0 (1 + x) \int_0^1 (1 - y) \int_{-1}^1 f_Z(z) \mathcal{I}_{\{-\eta y < z < \eta x\}}(x, y, z) \; dz dy dx \tag{B.26}$$

$$I_3 = \int_{-1}^0 (1 + x) \int_{-1}^0 (1 + y) \int_{-1}^1 f_Z(z) \mathcal{I}_{\{-\eta y < z < \eta x\}}(x, y, z) \; dz dy dx \tag{B.27}$$

$$I_4 = \int_0^1 (1 - x) \int_{-1}^0 (1 + y) \int_{-1}^1 f_Z(z) \mathcal{I}_{\{-\eta y < z < \eta x\}}(x, y, z) \; dz dy dx \tag{B.28}$$

The indicator functions will behave differently in the four quadrants (B.16)-(B.19). In the first quadrant $Q_1 = \{x > 0,\ y > 0\}$, the condition provided by $\mathcal{I}_{\{-\eta y < z < \eta x\}}(x, y, z)$ are straightforward, since the implicit inequality $-y < x$ is trivial for $x > 0,\ y > 0$. Hence, I_1 of (B.25) can be expressed as

$$I_1 = \int_0^1 (1-x) \int_0^1 (1-y) \int_{-\eta y}^{\eta x} f_Z(z)\ dz dy dx,$$

and for f_Z as of (B.6) and $y > 0$, we have that

$$I_1 = \int_0^1 (1-x) \int_0^1 (1-y) \left(\int_{-\eta y}^0 (1+z)\ dz + \int_0^{\eta x} (1-z)\ dz \right) dy dx,$$

which by calculation gives

$$I_1 = \frac{\eta}{6}\left(1 - \frac{\eta}{4}\right). \tag{B.29}$$

In the second quadrant $Q_2 = \{x < 0,\ y > 0\}$, we have that $-y < x$ as long as $-x < y$, by which we may express I_2 of (B.26) as

$$I_2 = \int_{-1}^0 (1+x) \int_{-x}^1 (1-y) \int_{-\eta y}^{\eta x} f_Z(z)\ dz dy dx.$$

While $-1 < -y < x < 0$, we have that $z \in [-\eta y, \eta x]$ is negative (for positive η, which is assumed) and hence that $f_Z(z) = 1 + z$ so that

$$I_2 = \int_{-1}^0 (1+x) \int_{-x}^1 (1-y) \int_{-\eta y}^{\eta x} (1+z)\ dz dy dx, \tag{B.30}$$

which is evaluated to

$$I_2 = \frac{\eta}{30}\left(1 - \frac{3\eta}{8}\right). \tag{B.31}$$

For the third quadrant $Q_3 = \{x < 0,\ y < 0\}$, it is enough to note that no numbers $x < 0,\ y < 0$ can fulfil $-y < x$. Hence,

$$I_3 = 0. \tag{B.32}$$

Consider now the last quadrant $Q_4 = \{x > 0,\ y < 0\}$, where $-y < x$ is realised when $-x < y$ as in the second quadrant. However, $z \in [-\eta y, \eta x]$ is now positive so that $f_Z(z) = 1 - z$. We will now claim that $I_4 = I_2$ by a symmetry argument. First, define a new set of variables as

$$\begin{cases} \tilde{x} = y, & d\tilde{x} = dy \\ \tilde{y} = x, & d\tilde{y} = dx \\ \tilde{z} = -z & d\tilde{z} = -dz \end{cases},$$

VII

so that

$$I_4 = \int\limits_0^1 (1-x) \int\limits_{-x}^0 (1+y) \int\limits_{-\eta y}^{\eta x} (1-z) \ dzdydx$$

$$= -\int\limits_0^1 (1-\tilde{y}) \int\limits_{-\tilde{y}}^0 (1+\tilde{x}) \int\limits_{\eta\tilde{x}}^{-\eta\tilde{y}} (1+\tilde{z}) \ d\tilde{z}d\tilde{x}d\tilde{y}.$$

Now, reverse the order of integration for $\tilde{x}$ and $\tilde{y}$ and adjust the integration limits of $\tilde{z}$ so that

$$I_4 = \int\limits_{-\tilde{y}}^0 (1+\tilde{x}) \int\limits_0^1 (1-\tilde{y}) \int\limits_{-\eta\tilde{y}}^{\eta\tilde{x}} (1+\tilde{z}) \ d\tilde{z}d\tilde{y}d\tilde{x}. \tag{B.33}$$

The integral limits of $\tilde{x}$ and $\tilde{y}$ in (B.33) are seemingly different from those of x and y in (B.30). They are however equivalent since the bounds $-1 < -y < x < 0$ of the $\tilde{x}$ integral in (B.33) are the same as the bounds $0 < -x < y < 1$ present in the y-integral in (B.30). Hence,

$$I_4 = \frac{\eta}{30}\left(1 - \frac{3\eta}{8}\right), \tag{B.34}$$

and the probability (B.20) may be computed from (B.29), (B.31), (B.32) and (B.34) as $P(\xi_\alpha > 0, \xi_\beta > 0) = I_1 + I_2 + I_3 + I_4$. We find

$$P(\xi_\alpha > 0, \xi_\beta > 0) = \frac{\eta}{30}(7 - 2\eta). \tag{B.35}$$

B.2.2 Independent, exponentially distributed parameters

Having defined new random variables to model the difference between the exponentially distributed energy uptake parameters as

$$X = \mathcal{E}_{\alpha\beta} - \mathcal{E}_{\alpha\alpha} \sim \text{Laplace}(0, \ \lambda) \tag{B.36}$$
$$Y = \mathcal{E}_{\beta\alpha} - \mathcal{E}_{\beta\beta} \sim \text{Laplace}(0, \ \lambda) \tag{B.37}$$
$$Z = \mathcal{E}_\alpha - \mathcal{E}_\beta \sim \text{Laplace}(0, \ \lambda) \tag{B.38}$$

where the Laplace probability density function is (B.14). The joint density function is

$$f_{X,Y,Z}(x,y,z) = \frac{\lambda}{2}e^{-\lambda|x|}\frac{\lambda}{2}e^{-\lambda|y|}\frac{\lambda}{2}e^{-\lambda|z|} \tag{B.39}$$

for real $x, \ y, \ z$ and we may define the probability of permanence as

$$P(\xi_\alpha > 0, \xi_\beta > 0) = \frac{\lambda^2}{4}\int_\mathbb{R} e^{-\lambda|x|}\int_\mathbb{R} e^{-\lambda|y|}\int_\mathbb{R} \frac{\lambda}{2}e^{-\lambda|z|}\mathcal{I}_{\{\eta x-z>0\}}\mathcal{I}_{\{\eta y+z>0\}} \ dzdydx. \tag{B.40}$$

The innermost integral over $z \in \mathbb{R}$ will have its integration limits defined by x and y so that we may define it as the function

$$I_z(x,y) = \frac{\lambda}{2}\int\limits_{-\eta y}^{\eta x} e^{-\lambda|z|} \ dz, \tag{B.41}$$

the evaluation of which depending on whether x and y are positive or negative. The function is piecewise defined on the four main quadrants of $\mathbb{R}^2$ as

$$
I_z(x, y) = \frac{\lambda}{2}
\begin{cases}
\int\limits_{-\eta y}^{0} e^{\lambda z}\, dz + \int\limits_{0}^{\eta x} e^{-\lambda z}\, dz, & -y < 0 < x \\
\int\limits_{-\eta y}^{\eta x} e^{\lambda z}\, dz, & -y < x < 0 \\
0, & x < 0 < -y \\
\int\limits_{-\eta y}^{\eta x} e^{-\lambda z}\, dz, & 0 < -y < x
\end{cases}
\tag{B.42}
$$

so that, when evaluating the integrals, we get

$$
I_z(x, y) = \frac{1}{2}
\begin{cases}
2 - e^{-\lambda\eta y} - e^{-\lambda\eta x}, & -y < 0 < x \\
e^{\lambda\eta x} - e^{-\lambda\eta y}, & -y < x < 0 \\
0, & x < 0 < -y \\
e^{\lambda\eta y} - e^{-\lambda\eta x}, & 0 < -y < x
\end{cases}
\tag{B.43}
$$

As in the uniformly distributed case, we split the probability integral (B.40) into its components defined on the $(x,\ y)$ quadrants so that the piecewise density functions (B.14) are well-defined. Note that the cases of the piecewise (B.43) is sorted on the proper form, where the first quadrant have variable values $x > 0$, $y > 0$, the second having $x < 0$, $y > 0$ etc. We have the terms

$$
I_1 = \frac{\lambda^2}{8} \int_{\mathbb{R}+} e^{-\lambda x} \int_{\mathbb{R}+} e^{-\lambda y} \left(2 - e^{-\lambda\eta y} - e^{-\lambda\eta x} \right) dy\, dx
\tag{B.44}
$$

$$
I_2 = \frac{\lambda^2}{8} \int_{\mathbb{R}-} e^{\lambda x} \int_{\mathbb{R}+} e^{-\lambda y} \left(e^{\lambda\eta x} - e^{-\lambda\eta y} \right) dy\, dx
\tag{B.45}
$$

$$
I_3 = 0
\tag{B.46}
$$

$$
I_4 = \frac{\lambda^2}{8} \int_{\mathbb{R}+} e^{-\lambda x} \int_{\mathbb{R}-} e^{\lambda y} \left(e^{\lambda\eta y} - e^{-\lambda\eta x} \right) dy\, dx
\tag{B.47}
$$

and it is a straightforward calculation to find

$$
I_1 = \frac{\eta}{2\lambda(1 + \eta)},
\tag{B.48}
$$

$$
I_2 = \frac{\eta}{4\lambda(2 + \eta)(1 + \eta)},
\tag{B.49}
$$

$$
I_3 = 0,
\tag{B.50}
$$

$$
I_4 = \frac{\eta}{4\lambda(2 + \eta)(1 + \eta)}.
\tag{B.51}
$$

The probability as defined as the sum of the terms (B.48)-(B.51) so that

$$
\mathrm{P}(\xi_\alpha > 0, \xi_\beta > 0) = \frac{\eta(3 + \eta)}{2\lambda(2 + \eta)(1 + \eta)}.
\tag{B.52}
$$

B.2.3 Tree hierarchy, uniformly distributed

Recall the definition (2.30) of the probability of permanence

$$\mathrm{P}(\xi_\alpha > 0, \xi_\beta > 0) = \int\limits_0^1 \int\limits_0^1 \int\limits_{1-\eta}^{1+\eta} \int\limits_{1-\eta}^{1+\eta} f_{S,T,X,Y}(s,t,x,y)\mathcal{I}_{\{\xi_\alpha > 0, \xi_\beta > 0\}} \ dy dx dt ds, \quad \text{(B.53)}$$

the joint distribution (2.29)

$$f_{S,T,X,Y}(s,t,x,y) = f_S(s)f_T(t)f_X(x)f_Y(y), \quad \text{(B.54)}$$

and the indicator function (2.28)

$$\mathcal{I}_{\{\xi_\alpha > 0, \xi_\beta > 0\}} = \mathcal{I}_{\{T > SX\}}\mathcal{I}_{\{S > TY\}} \quad \text{(B.55)}$$

Defined for the tree hierarchy model, where $\mathcal{E}_{ij} = r_{ij}\mathcal{E}_i$. Now use the definition of uniform probability densities

$$f_S(s) = 1, \ s \in [0,1],$$
$$f_T(t) = 1, \ t \in [0,1],$$

to simplify the joint probability (B.54) into

$$f_{S,T,X,Y}(s,t,x,y) = f_X(x)f_Y(y)\mathcal{I}_{s \in [0,1], \ t \in [0,1]}. \quad \text{(B.56)}$$

The probability (B.53) may then be defined as

$$\mathrm{P}(\xi_\alpha > 0, \xi_\beta > 0) = \int\limits_0^1 \int\limits_0^1 \left(\int\limits_{1-\eta}^{1+\eta} f_X(x)\mathcal{I}_{\{T > SX\}} \ dx \right) \left(\int\limits_{1-\eta}^{1+\eta} f_Y(y)\mathcal{I}_{\{S > TY\}} \ dy \right) dt ds.$$
$$\text{(B.57)}$$

For the present tree hierarchy model, we have the random variables $X, Y \sim \mathrm{Tri}(1 - \eta, \ 1 + \eta)$ with the density function

$$f_X(x) = \eta^{-2} \begin{cases} \eta + x - 1, & 1 - \eta < x \le 1 \\ \eta - x + 1, & 1 < x < 1 + \eta \\ 0, & x \notin [1 - \eta, \ 1 + \eta) \end{cases}. \quad \text{(B.58)}$$

Similar to the procedure in the previous section, define the probability integral as the sum of integrals over the the sub-intervals $[1 - \eta, \ 1]$ and $[1, \ 1 + \eta]$ of x and y

$$\mathrm{P}(\xi_\alpha > 0, \xi_\beta > 0) = I_1 + I_2 + I_3 + I_4, \quad \text{(B.59)}$$

X

so that the piecewise linear distribution functions $f_X(x)$ and $f_Y(y)$ (2.27) are well defined. The integral terms are

$$I_1 = \int_0^1 \int_0^1 \left(\eta^{-2} \int_1^{1+\eta} (\eta - x + 1) \mathcal{I}_{\{T > SX\}} \, dx \right) \left(\eta^{-2} \int_1^{1+\eta} (\eta - y + 1) \mathcal{I}_{\{S > TY\}} \, dy \right) dt ds,$$
(B.60)

$$I_2 = \int_0^1 \int_0^1 \left(\eta^{-2} \int_1^{1+\eta} (\eta - x + 1) \mathcal{I}_{\{T > SX\}} \, dx \right) \left(\eta^{-2} \int_{1-\eta}^1 (\eta + y - 1) \mathcal{I}_{\{S > TY\}} \, dy \right) dt ds,$$
(B.61)

$$I_3 = \int_0^1 \int_0^1 \left(\eta^{-2} \int_{1-\eta}^1 (\eta + x - 1) \mathcal{I}_{\{T > SX\}} \, dx \right) \left(\eta^{-2} \int_1^{1+\eta} (\eta - y + 1) \mathcal{I}_{\{S > TY\}} \, dy \right) dt ds,$$
(B.62)

$$I_4 = \int_0^1 \int_0^1 \left(\eta^{-2} \int_{1-\eta}^1 (\eta + x - 1) \mathcal{I}_{\{T > SX\}} \, dx \right) \left(\eta^{-2} \int_{1-\eta}^1 (\eta + y - 1) \mathcal{I}_{\{S > TY\}} \, dy \right) dt ds,$$
(B.63)

Next, we define the inner integrals over the x interval as the functions

$$J_+(s, t) = \eta^{-2} \int_1^{1+\eta} (\eta - x + 1) \mathcal{I}_{\{T > SX\}} \, dx \tag{B.64}$$

$$J_-(s, t) = \eta^{-2} \int_{1-\eta}^1 (\eta + x - 1) \mathcal{I}_{\{T > SX\}} \, dx \tag{B.65}$$

for $s \in [0, 1)$, $t \in [0, 1)$ and note that the integrals over the corresponding y intervals may be defined as $J_+(t, s)$ and $J_-(t, s)$ due to the symmetry of the indicator functions

$$J_+(t, s) = \eta^{-2} \int_1^{1+\eta} (\eta - y + 1) \mathcal{I}_{\{S > TY\}} \, dy, \tag{B.66}$$

$$J_-(t, s) = \eta^{-2} \int_{1-\eta}^1 (\eta + y - 1) \mathcal{I}_{\{S > TY\}} \, dy. \tag{B.67}$$

We will first consider (B.64), where the indicator function $\mathcal{I}_{\{T > SX\}}$ of (B.64) is determined by the relation of S and T, and — more specifically — whether t is larger or smaller than $(1 + \eta)t$. There are two cases where $\mathcal{I}_{\{T > SX\}}$ is non-zero:

$$t \in [sx, \ s(1 + \eta)] \Rightarrow T > SX \tag{B.68}$$
$$t > s(1 + \eta) \Rightarrow T > SX \tag{B.69}$$

for $x \in [1, \ 1 + \eta]$. We hence find the constraints

$$S < T < \min((1 + \eta)S, 1), \text{ when } s \in [0, 1) \tag{B.70}$$

when $t < (1 + \eta)s$, and

$$(1 + \eta)S < T < 1, \ \text{when} \ (1 + \eta)s < 1, \ s \in [0, 1). \tag{B.71}$$

for $t > (1 + \eta)s$. Evaluation of the J_+ integral of (B.64) under the conditions (B.70)-(B.71) give

$$J_+(s, t) = \frac{1}{2\eta^2 s^2} \begin{cases} (t - s)(s(2\eta + 1) - t), & s < t < (1 + \eta)s \\ \eta^2 s^2, & (1 + \eta)s < t < 1 \end{cases} \tag{B.72}$$

for $s \in [0, \ 1)$.

The corresponding division for (B.65) depends on the relation of t and s. When $t < s$, we have that the characteristic function $\mathcal{I}_{\{S > TX\}}$ is non-zero when

$$(1 - \eta)s < t < s \tag{B.73}$$

and for $t > s$ we have

$$s < t < 1 \tag{B.74}$$

for $s \in [0, 1)$. Evaluation of the J_- integral of (B.65) then yields

$$J_-(s, t) = \frac{1}{2\eta^2 s^2} \begin{cases} (t + \eta s)^2 + s^2(1 - 2\eta) - 2st, & (1 - \eta)s < t < s \\ \eta^2 s^2, & s < t < 1 \end{cases} \tag{B.75}$$

for $s \in [0, \ 1)$.

The first integral of the sum that constitutes the probability, (B.60), contains the product $J_+(s, t)J_+(t, s)$ which will be zero for all $s, t \in [0, 1)$ due to the involved indicator functions. First note that there is no overlap of the set $s < t < (1 + \eta)s$ of $J_+(s, t)$ with the sets $t < s < \min((1 + \eta)t, 1)$ and $(1 + \eta)t < s < 1$ of $J_+(t, s)$ and consider then the set $(1 + \eta)s < t < 1$ of $J_+(s, t)$ which does not overlap with the sets indicated by $J_+(t, s)$. We may draw the conclusion that the first integral is zero,

$$I_1 = 0. \tag{B.76}$$

In the second integral (B.61), we have the product $J_-(s, t)J_+(t, s)$ since $x \in [1 - \eta, \ 1)$ and $y \in [1, \ 1 + \eta)$. The products between indicator functions that arise are

$$\mathcal{I}_{\{(1-\eta)S < T < S\}}\mathcal{I}_{\{(1+\eta)T < S < 1\}} = \mathcal{I}_{\{(1-\eta)S < (1+\eta)T < S\}} \tag{B.77}$$

$$\mathcal{I}_{\{(1-\eta)S < T < S\}}\mathcal{I}_{\{T < S < \min((1+\eta)T, 1)\}} = \mathcal{I}_{\{(1-\eta)S < T < S\}} \tag{B.78}$$

$$\mathcal{I}_{\{S < T < 1\}}\mathcal{I}_{\{(1+\eta)T < S < 1\}} = \emptyset \tag{B.79}$$

$$\mathcal{I}_{\{S < T < 1\}}\mathcal{I}_{\{T < S < \min((1+\eta)T, 1)\}} = \emptyset \tag{B.80}$$

for $s, t \in [0, 1)$, meaning that the product

$$J_-(s, t)J_+(t, s) = \frac{1}{4\eta^4 t^2 s^2} \left((t + \eta s)^2 + s^2(1 - 2\eta) - 2st\right)\eta^2 t^2 \tag{B.81}$$

when $s, t \in \{0 < (1 - \eta)S < (1 + \eta)T < S < 1\}$ and

$$J_-(s, t)J_+(t, s) = \frac{1}{4\eta^4 t^2 s^2} \left((t + \eta s)^2 + s^2(1 - 2\eta) - 2st\right)(s - t)(t(2\eta + 1) - s) \tag{B.82}$$

XII

when $s, t \in \{0 < (1 - \eta)S < T < S < 1\}$. The integral (B.61) is split into

$$I_2 = \int_0^1 \frac{1}{4\eta^4 s^2} \left(\eta^2 \int_{s\frac{1-\eta}{1+\eta}}^{s\frac{1}{1+\eta}} \left((t + \eta s)^2 + s^2(1 - 2\eta) - 2st \right) dt \right.$$
$$\left. + \int_{s(1-\eta)}^s \frac{(s-t)(t(2\eta+1)-s)}{t^2} \left((t + \eta s)^2 + s^2(1 - 2\eta) - 2st \right) dt \right) ds, \tag{B.83}$$

and evaluated to

$$I_2 = \frac{-12 + 6\eta + 14\eta^2 - 6\eta^3 - 2\eta^4 + \eta^5}{24\eta^3(1 + \eta)} + \frac{2 - 3\eta^2 + \eta^4}{4\eta^4(1 + \eta)} \log(1 + \eta). \tag{B.84}$$

In the third integral (B.62), the domain is $(x, \, y) \in [1 - \eta, \, 1) \times [1 - \eta, \, 1)$ so that we have the product $J_-(s,t)J_-(t,s)$. The associated indicator functions are

$$\mathcal{I}_{\{(1-\eta)S<T<S\}}\mathcal{I}_{\{(1-\eta)T<S<T\}} = \emptyset \tag{B.85}$$
$$\mathcal{I}_{\{(1-\eta)S<T<S\}}\mathcal{I}_{\{T<S<1\}} = \mathcal{I}_{\{(1-\eta)S<T<S\}} \tag{B.86}$$
$$\mathcal{I}_{\{S<T<1\}}\mathcal{I}_{\{(1-\eta)T<S<T\}} = \mathcal{I}_{\{(1-\eta)T<S<T\}} \tag{B.87}$$
$$\mathcal{I}_{\{S<T<1\}}\mathcal{I}_{\{T<S<1\}} = \emptyset \tag{B.88}$$

so that the product has the functional form

$$J_-(s,t)J_-(t,s) = \frac{1}{4\eta^4} \begin{cases} \frac{1}{s^2}\left((t + \eta s)^2 + s^2(1 - 2\eta) - 2st\right), & (1-\eta)s < t < s \\ \frac{1}{t^2}\left((s + \eta t)^2 + t^2(1 - 2\eta) - 2st\right), & (1-\eta)t < s < t \end{cases} \tag{B.89}$$

where, as before, $s, \, t \in [0, 1)$. The symmetry of (B.89) shows that the integral (B.62) is

$$I_3 = \frac{1}{2\eta^2} \int_0^1 \int_{(1-\eta)s}^s \frac{1}{s^2} \left((t + \eta s)^2 + s^2(1 - 2\eta) - 2st \right) dtds \tag{B.90}$$

which is evaluated to

$$I_3 = \frac{\eta}{12}. \tag{B.91}$$

The fourth integral (B.63) over the domain $x \in [1, \, 1 + \eta)$ and $y \in [1 - \eta, \, 1)$ is symmetric in s and t to the second, and is hence equal to I_2 so that

$$I_4 = \frac{-12 + 6\eta + 14\eta^2 - 6\eta^3 - 2\eta^4 + \eta^5}{24\eta^3(1 + \eta)} + \frac{2 - 3\eta^2 + \eta^4}{4\eta^4(1 + \eta)} \log(1 + \eta). \tag{B.92}$$

Adding the integrals (B.76), (B.84), (B.91) and (B.92), we get

$$P(\xi_\alpha > 0, \xi_\beta > 0) = \frac{-12 + 6\eta + 14\eta^2 - 6\eta^3 - \eta^4 + 2\eta^5}{12\eta^3(1 + \eta)} + \frac{2 - 3\eta^2 + \eta^4}{2\eta^4(1 + \eta)} \log(1 + \eta). \tag{B.93}$$

B.2.4 Tree hierarchy, exponentially distributed

To compute the analytical probability of permanence in the tree-hierarchy model with exponentially distributed energy-uptake parameters $\mathcal{E}_i$, $\mathcal{E}_{ij}$, we define the variables

$$S = \mathcal{E}_\alpha \sim \mathrm{Exp}(\lambda), \tag{B.94}$$

$$T = \mathcal{E}_\beta \sim \mathrm{Exp}(\lambda), \tag{B.95}$$

$$X = 1 - \eta \left(r_{\alpha\beta} - r_{\alpha\alpha}\right) \sim \mathrm{Tri}(1 - \eta, 1 + \eta), \tag{B.96}$$

$$Y = 1 - \eta \left(r_{\beta\alpha} - r_{\beta\beta}\right) \sim \mathrm{Tri}(1 - \eta, 1 + \eta), \tag{B.97}$$

and recall the exponential distribution density functions

$$f_S(s) = \lambda e^{-\lambda s}, \ s \geq 0 \tag{B.98}$$

$$f_T(t) = \lambda e^{-\lambda t}, \ t \geq 0 \tag{B.99}$$

and the triangle density function

$$f_X(x) = \eta^{-2} \begin{cases} \eta + x - 1, & 1 - \eta < x \leq 1 \\ \eta - x + 1, & 1 < x < 1 + \eta \\ 0, & x \notin [1 - \eta, \ 1 + \eta) \end{cases} \tag{B.100}$$

that also holds for $Y \sim \mathrm{Tri}(1 - \eta, 1 + \eta)$. From the densities, we may define the probability of permanence based on the criteria (1.20), (1.21) as

$$\mathrm{P}(\xi_\alpha > 0, \xi_\beta > 0) = \int_{\mathbb{R}^+} f_S(s) \int_{\mathbb{R}^+} f_T(t) \Big(J_+(s,t) + J_-(s,t)\Big) \Big(J_+(t,s) + J_-(t,s)\Big) \, dt ds, \tag{B.101}$$

where we for convenience have defined the inner integrals

$$J_+(s,t) + J_-(s,t) = \int_{1-\eta}^{1+\eta} f_X(x) \mathcal{I}_{\{T > SX\}} \, dx \tag{B.102}$$

$$J_+(t,s) + J_-(t,s) = \int_{1-\eta}^{1+\eta} f_Y(y) \mathcal{I}_{\{S > TY\}} \, dy \tag{B.103}$$

taking the functions

$$J_+(s,t) = \frac{1}{2\eta^2 s^2} \begin{cases} (t - s)\left(s(2\eta + 1) - t\right), & s < t < (1 + \eta)s \\ \eta^2 s^2, & (1 + \eta)s < t \end{cases} \tag{B.104}$$

from (B.64) and

$$J_-(s,t) = \frac{1}{2\eta^2 s^2} \begin{cases} \left((t + \eta s)^2 + s^2(1 - 2\eta) - 2st\right), & (1 - \eta)s < t < s \\ \eta^2 s^2, & s < t \end{cases} \tag{B.105}$$

from (B.65). Note that both functions are defined for all positive s and t, whereas (B.64) and (B.65) were only defined for $s, \ t \in [0, 1)$.

We decompose the probability (B.101) into the four terms

$$I_1 = \int_{\mathbb{R}+} f_S(s) \int_{\mathbb{R}+} f_T(t) J_+(s,t) J_+(t,s) \ dt ds \tag{B.106}$$

$$I_2 = \int_{\mathbb{R}+} f_S(s) \int_{\mathbb{R}+} f_T(t) J_-(s,t) J_+(t,s) \ dt ds \tag{B.107}$$

$$I_3 = \int_{\mathbb{R}+} f_S(s) \int_{\mathbb{R}+} f_T(t) J_-(s,t) J_-(t,s) \ dt ds \tag{B.108}$$

$$I_4 = \int_{\mathbb{R}+} f_S(s) \int_{\mathbb{R}+} f_T(t) J_+(s,t) J_-(t,s) \ dt ds \tag{B.109}$$

analogously to the four quadrants (B.48)-(B.51) used to compute the probability of permanence in the independent model.

For the first integral, (B.106), recall (see the paragraph leading up to (B.76)) that we have that $J_+(s,t) J_+(t,s) = 0$ in the derivation of the tree-hierarchy model with uniformly distributed parameters. This is due to no overlap in the regions of definition for s and t and leads to

$$I_1 = 0. \tag{B.110}$$

For the second integral, (B.107), we have derived that

$$J_-(s,t) J_+(t,s) = \frac{1}{4\eta^4 t^2 s^2} \left((t + \eta s)^2 + s^2(1 - 2\eta) - 2st \right) \eta^2 t^2 \tag{B.111}$$

when $(1 - \eta)s < (1 + \eta)t < s$ and

$$J_-(s,t) J_+(t,s) = \frac{1}{4\eta^4 t^2 s^2} \left((t + \eta s)^2 + s^2(1 - 2\eta) - 2st \right) (s - t)(t(2\eta + 1) - s) \tag{B.112}$$

when $(1-\eta)s < t < s$. The derivations of the expressions are found in the paragraphs leading up to (B.81) and (B.82), respectively. Based on these results, we split (B.107) further into

$$I_2 = \int_{\mathbb{R}+} f_S(s) \frac{1}{4\eta^4 s^2} \left(\eta^2 \int_{s\frac{1-\eta}{1+\eta}}^{s\frac{1}{1+\eta}} \lambda e^{-\lambda t} \left(\left((t + \eta s)^2 + s^2(1 - 2\eta) - 2st \right) \right) dt \right.$$

$$\left. + \int_{s(1-\eta)}^{s} \lambda e^{-\lambda t} \left(\left((t + \eta s)^2 + s^2(1 - 2\eta) - 2st \right) (s - t)(t(2\eta + 1) - s) \right) dt \right) ds, \tag{B.113}$$

and find that

$$I_2 = \frac{1}{4\eta^4} \left(4\eta^2(2 - \eta) \coth^{-1} \left(\frac{\eta^2 - 2\eta - 4}{\eta^2} \right) + \eta(2 - \eta)(\eta^2 - 3) + \left(6 + 8\eta - 4\eta^2 \right) \log(1 + \eta) \right.$$

$$\left. + 2\eta(2 - \eta)(4 + \eta) \log(2) - 2\eta(2 - \eta)(4 + \eta) \log(2 + \eta) \right) \tag{B.114}$$

The third integral, I_3 of (B.108), contains the product $J_-(s,t) J_-(t,s)$, which was found to be

$$J_-(s,t) J_-(t,s) = \frac{1}{4\eta^4} \begin{cases} \frac{1}{s^2} \left((t + \eta s)^2 + s^2(1 - 2\eta) - 2st \right), & (1 - \eta)s < t < s \\ \frac{1}{t^2} \left((s + \eta t)^2 + t^2(1 - 2\eta) - 2st \right), & (1 - \eta)t < s < t \end{cases} \tag{B.115}$$

B. Analytic probability $P(\xi_\alpha > 0, \ \xi_\beta > 0)$

so that due to the symmetry, we have

$$I_3 = \frac{1}{2\eta^4} \int_{\mathbb{R}^+} f_S(s) \int_{(1-\eta)s}^{s} f_T(t) \frac{1}{s^2} \left((t + \eta s)^2 + s^2(1 - 2\eta) - 2st \right) \, dt ds \qquad \text{(B.116)}$$

which is evaluated to

$$I_3 = \frac{1}{4\eta^2} \left(-\eta^2 + 4\eta - 4(2 - \eta) \log(2) + 4(2 - \eta) \log(2 - \eta) \right) \qquad \text{(B.117)}$$

By symmetry in s and t, we see that the product $J_+(s,t)J_-(t,s)$ present in the fourth integral (B.109) will cause the integral to be equal to the one in the second case. We have

$$I_4 = \frac{1}{4\eta^4} \left(4\eta^2(2 - \eta) \coth^{-1} \left(\frac{\eta^2 - 2\eta - 4}{\eta^2} \right) + \eta(2 - \eta)(\eta^2 - 3) \right.$$
$$+ \left(6 + 8\eta - 4\eta^2 \right) \log(1 + \eta)$$
$$\left. + 2\eta(2 - \eta)(4 + \eta) \log(2) - 2\eta(2 - \eta)(4 + \eta) \log(2 + \eta) \right) \qquad \text{(B.118)}$$

The sum of the integrals finds the probability of permanence

$$P(\xi_\alpha > 0, \xi_\beta > 0) = \frac{-12 + 6\eta + 8\eta^2 - 3\eta^3}{4\eta^3} + \frac{2(2 - \eta)}{\eta^2} \coth^{-1} \left(\frac{\eta^2 - 2\eta - 4}{\eta^2} \right)$$
$$+ \frac{1}{\eta^4} \left((3 + 4\eta - \eta^2) \log(1 + \eta) + \eta^2(2 - \eta) \log(2 - \eta) \right.$$
$$\left. - \eta(2 - \eta)(4 + \eta) \log(2 + \eta) + 4\eta(2 - \eta) \log(2) \right) \qquad \text{(B.119)}$$

XVI

C

Proof: d-order series dynamics described by $(d+1)$-order tensor

In Section 3.2.3, we found that the affine fitness function (1.10) is equivalent to the linear fitness function (1.2), which is easily generalised to higher dimensions. To derive and prove this, we use the series expansion with $d+1$ orders of metabolisation of Lundh & Gerlee [16], and also use the notation where $I = i_1 i_2 \cdots i_d$ is the d-th order multi-index of the tensor $\mathcal{E}_I$, Ii denotes the concatenation of I with the index i and where $x_I = \prod\limits_{k=1}^{d} x_{i_k}$. We claim that the fitness of a species

$$\phi_i(\mathbf{x}) = \gamma\eta\mathcal{E}_i + \gamma\eta^2 \sum_{i_1} x_{i_1}\mathcal{E}_{i_1 i} + \gamma\eta^3 \sum_{i_2}\sum_{i_1} x_{i_2}x_{i_1}\mathcal{E}_{i_2 i_1 i} + \cdots + \gamma\eta^{d+1}\sum_{i_1}\sum_{i_2}\cdots\sum_{i_d} x_I \mathcal{E}_{Ii}, \tag{C.1}$$

can be described by a $(d+1)$-th order tensor

$$E_{Ii} = \gamma\eta\mathcal{E}_i + \gamma\eta^2\mathcal{E}_{i_1 i} + \cdots + \gamma\eta^{d+1}\mathcal{E}_{Ii}. \tag{C.2}$$

so that

$$\phi_i(\mathbf{x}) = \sum_{i_d}\sum_{i_{d-1}}\cdots\sum_{i_1} x_I E_{Ii}. \tag{C.3}$$

The dynamics of the replicator system based on the series expansion with $d+1$ orders of metabolisation is hence determined by the dynamics of an equivalent replicator system based on a $(d+1)$-th order tensor. The latter may be interpreted as an n-strategy, $d+1$-player game, the dynamics of which is investigated by Gokhale & Traulsen [10].

For proving the claim, assume that the fitness of a species is described by the d-th order series expansion (C.1) of the metabolism, as described by Lundh & Gerlee [16]. Also, recall the notation I for the multi-index — the concatenation of d indices — and the convention that $x_I = x_{i_d}x_{i_{d-1}}\cdots x_{i_2}x_{i_1}$. The proof is adapted from Stadler [20] and relies on the fact that the sum of species frequencies over all indices in a multi-index, consisting of a finite number of indices i_1, $i_2, \ldots,$ i_d, is unity. This is also used when proving the bound of the error of the series expansion in Lundh & Gerlee [16] and is easily motivated

$$\sum_{i_d}\sum_{i_{d-1}}\cdots\sum_{i_1} x_I = \sum_{i_d}\sum_{i_{d-1}}\cdots\sum_{i_1}\left(x_{i_d}x_{i_{d-1}}\cdots x_{i_1}\right) = \sum_{i_d} x_{i_d}\sum_{i_{d-1}} x_{i_{d-1}}\cdots\sum_{i_1} x_{i_1} = 1. \tag{C.4}$$

C. Proof: d-order series dynamics described by $(d+1)$-order tensor

Using this information, we may decouple the fitness function as

$$
\begin{aligned}
\phi_i(\mathbf{x}) &= \gamma\eta\mathcal{E}_i + \gamma\eta^2 \sum_{i_1} x_{i_1}\mathcal{E}_{i_1 i} + \cdots + \gamma\eta^{d+1} \sum_{i_d}\sum_{i_{d-1}}\cdots\sum_{i_1} x_I \mathcal{E}_{Ii} = \left\{ \sum_{i_d} x_{i_d} = 1 \right\} \\
&= \gamma\eta \sum_{i_d} x_{i_d}\mathcal{E}_i + \gamma\eta^2 \sum_{i_d}\sum_{i_1} x_{i_d}x_{i_1}\mathcal{E}_{i_1 i} + \cdots + \gamma\eta^{d+1}\sum_{i_d}\sum_{i_{d-1}}\cdots\sum_{i_1} x_I \mathcal{E}_{Ii} \\
&= \sum_{i_d} x_{i_d}\left(\gamma\eta\mathcal{E}_i + \gamma\eta^2 \sum_{i_1} x_{i_1}\mathcal{E}_{i_1 i} + \cdots + \gamma\eta^{d+1}\sum_{i_{d-1}}\cdots\sum_{i_1}(x_{i_{d-1}}\cdots x_{i_1})\mathcal{E}_{Ii}\right) \\
&= \left\{ \sum_{i_{d-1}} x_{i_{d-1}} = 1 \right\} \\
&= \sum_{i_d} x_{i_d}\left(\gamma\eta\sum_{i_{d-1}} x_{i_{d-1}}\mathcal{E}_i + \cdots + \gamma\eta^{d+1}\sum_{i_{d-1}}\cdots\sum_{i_1}(x_{i_{d-1}}\cdots x_{i_1})\mathcal{E}_{Ii}\right) \\
&= \sum_{i_d}\sum_{i_{d-1}} x_{i_d}x_{i_{d-1}}\left(\gamma\eta\mathcal{E}_i + \gamma\eta^2 \sum_{i_1} x_{i_1}\mathcal{E}_{i_1 i} + \cdots + \gamma\eta^{d+1}\sum_{i_{d-2}}\cdots\sum_{i_1}(x_{i_{d-2}}\cdots x_{i_1})\mathcal{E}_{Ii}\right) \\
&\;\;\vdots \\
&= \sum_{i_d}\sum_{i_{d-1}}\cdots\sum_{i_1} x_I\left(\gamma\eta\mathcal{E}_i + \gamma\eta^2\mathcal{E}_{i_1 i} + \cdots + \gamma\eta^{d+1}\mathcal{E}_{Ii}\right) \\
&= \sum_{i_d}\sum_{i_{d-1}}\cdots\sum_{i_1} x_I E_{Ii} \\
&= \widetilde{\phi}_i(\mathbf{x}).
\end{aligned}
$$

Hence, we may conclude that the dynamics of a replicator system with a series-expansion fitness function as derived by Lundh & Gerlee [16] is captured in the dynamics of an effective tensor of order $d+1$.

D

Bounding ellipse of $(\xi_\alpha,\ \xi_\beta)$

For the two-species system, recall that the coordinates are defined as

$$\xi_\alpha = \eta X - Z \tag{D.1}$$
$$\xi_\beta = \eta Y + Z \tag{D.2}$$

where their components X, Y and Z are defined and distributed as

$$X_u = \mathcal{E}_{\alpha\beta} - \mathcal{E}_{\alpha\alpha} \sim \text{Tri}(-1,\ 1) \tag{D.3}$$
$$Y_u = \mathcal{E}_{\beta\alpha} - \mathcal{E}_{\beta\beta} \sim \text{Tri}(-1,\ 1) \tag{D.4}$$
$$Z_u = \mathcal{E}_\alpha - \mathcal{E}_\beta \sim \text{Tri}(-1,\ 1) \tag{D.5}$$

when $\mathcal{E}_i,\ \mathcal{E}_{ij} \sim \text{Uni}(0,\ 1)$-distributed and

$$X_e = \mathcal{E}_{\alpha\beta} - \mathcal{E}_{\alpha\alpha} \sim \text{Laplace}(0, \lambda) \tag{D.6}$$
$$Y_e = \mathcal{E}_{\beta\alpha} - \mathcal{E}_{\beta\beta} \sim \text{Laplace}(0, \lambda) \tag{D.7}$$
$$Z_e = \mathcal{E}_\alpha - \mathcal{E}_\beta \sim \text{Laplace}(0, \lambda) \tag{D.8}$$

when $\mathcal{E}_i,\ \mathcal{E}_{ij} \sim \text{Exp}(\lambda)$.
The bounding ellipse, written on general form as

$$\left(\frac{x\cos(\theta) - y\sin(\theta)}{a}\right)^2 + \left(\frac{x\sin(\theta) + y\cos(\theta)}{b}\right)^2 = 1. \tag{D.9}$$

is defined by the minor axis of length b and the major axis of length a and slanted by an angle θ to the x-axis. From the definitions (D.1) and (D.2), we see that ξ_α and ξ_β are negatively correlated so that the ellipse is slanted by $-\frac{\pi}{4}$. We see that minor axis need to be located on the axis where

$$\xi_\alpha = \xi_\beta \tag{D.10}$$

so that we have

$$Z = \frac{\eta}{2}(X - Y) \tag{D.11}$$

from the definitions (D.1), (D.2). Hence

$$\xi_i = \frac{\eta}{2}(X + Y) \tag{D.12}$$

for $i = \alpha,\ \beta$. On the major axis, we have that

$$\xi_\alpha = -\xi_\beta, \tag{D.13}$$

so that

$$X = -Y, \tag{D.14}$$

from which we find

$$\xi_\alpha = \eta X - Z \tag{D.15}$$
$$\xi_\beta = -\xi_\alpha. \tag{D.16}$$

D.1   Uni$(0,\ 1)$-distributed parameters

We note that all of the component variables X_u, Y_u and Z_u that form ξ_α, ξ_β are bounded within the interval $(-1\ 1)$. Then, we have that the coordinates (D.12) are bounded as

$$\xi_i \in (-\eta,\ \eta) \tag{D.17}$$

on the minor axis, which lead to the extreme points $(\xi_\alpha,\ \xi_\beta) = (-\eta,\ -\eta)$ and $(\xi_\alpha,\ \xi_\beta) = (\eta,\ \eta)$. On the major axis, the coordinates (D.15), (D.16) are bounded as

$$\xi_\alpha \in (-(1+\eta),\ 1+\eta) \tag{D.18}$$
$$\xi_\beta \in (-(1+\eta),\ 1+\eta) \tag{D.19}$$

leading the points $(-(1+\eta),\ 1+\eta)$ and $(1+\eta,\ -(1+\eta))$ at the extremes in the top left and bottom right corners of the graph. Finally, the slanting angle θ is implicit in the definitions (D.1) and (D.2).

In conclusion, the scatter plot of $(\xi_\alpha,\ \xi_\beta)$ is bounded by the ellipse (D.9) with the axes lengths a, b and the slanting angle θ as

$$a = \sqrt{2}(1+\eta) \tag{D.20}$$
$$b = \sqrt{2}\eta \tag{D.21}$$
$$\theta = -\frac{\pi}{4}. \tag{D.22}$$

D.2   Exp(λ)-distributed parameters

The Laplace(λ)-distributed components X, Y and Z, that form the parameters (D.1) and (D.2), are not bounded. The probability of exceeding a given quantile does however decay exponentially which means that for a given sample size, we are not likely to see values above a certain level. To find these extreme values, define first a probability threshold α so that

$$P(\Xi \leq \xi^*) = F_\Xi(\xi^*) = 1 - \alpha, \tag{D.23}$$

i.e., that the probability of $\Xi \in \{\xi_\alpha,\ \xi_\beta\}$ being larger than the threshold ξ^* is less than α. To find the quantiles that define the major and minor axes of the ellipse, we need the joint distributions that define the ξ_i coordinates under the assumptions (D.10) and (D.13). As in the uniform case, we have that $\xi_\alpha = \xi_\beta = \Xi_m$ on the minor axis (index m on all variables related to the *minor* axis) so that

$$\Xi_m = \frac{\eta}{2}(X + Y) \tag{D.24}$$

where the sum $X + Y$ of the Laplace(λ)-distributed X, Y is distributed as

$$f_{X+Y}(s) = \int_\mathbb{R} f_X(s-t)f_Y(t)\ dt = \frac{\lambda}{4}e^{-\lambda|s|}(1 + \lambda|s|) \tag{D.25}$$

XX

when the probability densities f_X, f_Y are the Laplace density (B.14) since we have the general result that the sum of two independent random variables is distributed as the convolution of the respective distribution functions [11]. Then, joint CDF is

$$F_{X+Y}(z) = \int_{-\infty}^{z} f_{X+Y}(s) \, ds = \begin{cases} \frac{1}{4}\left(4 - (2 + \lambda z)e^{-\lambda z}\right), & z > 0 \\ \frac{1}{4}(2 - \lambda z)e^{\lambda z}, & z < 0 \end{cases} \tag{D.26}$$

Hence, when we define Ξ_m as (D.24), we have that the probability (D.23) is

$$F_{X+Y}\left(\frac{2\xi_m}{\eta}\right) = 1 - \alpha \tag{D.27}$$

for some quantile $\xi_m > 0$. The substitution $z = \frac{2\xi_m}{\eta}$ into (D.26) is due to the definition (D.24). This is simplified into

$$(1 + \frac{\lambda}{\eta}\xi_m)e^{-\frac{2\lambda}{\eta}\xi_m} = 2\alpha, \ \xi_m > 0 \tag{D.28}$$

and the (numerical) solution $\xi_m(\alpha)$ for $\lambda = 2$ is shown in Figure 4.4.
For the major axis, all related variables are indexed by M and we have $\xi_\alpha = -\xi_\beta \equiv \Xi_M$, where

$$\Xi_M = \eta X - Z \tag{D.29}$$

which is distributed as

$$f_{\Xi_M}(s) = \int_{\mathbb{R}} \frac{1}{\eta} f_X\left(\frac{s-t}{\eta}\right) f_{-Z}(t) \, dt \tag{D.30}$$

since an η-scaled random variable ηX is distributed as $\frac{1}{\eta} f_X(\frac{x}{\eta})$. Evaluation of the integral shows that

$$f_{\Xi_M}(s) = \frac{\lambda}{2(1 - \eta^2)}\left(e^{-\lambda|s|} - \eta e^{-\frac{\lambda}{\eta}|s|}\right) \tag{D.31}$$

so that the CDF becomes

$$F_{\Xi_M}(z) = \frac{1}{2(1 - \eta^2)}\begin{cases} e^{\lambda z} - \eta^2 e^{\frac{\lambda}{\eta}z}, & z < 0 \\ 2(1 - \eta^2) - e^{-\lambda z} + \eta^2 e^{-\frac{\lambda}{\eta}z}, & z > 0 \end{cases}. \tag{D.32}$$

Simplification of $F_{\Xi_M}(\xi_M) = 1 - \alpha$ under the assumption $\xi_M > 0$ shows

$$e^{-\lambda\xi_M} - \eta^2 e^{-\frac{\lambda}{\eta}\xi_M} = 2\alpha(1 - \eta^2) \tag{D.33}$$

and the solution $\xi_M(\alpha)$ is shown in Figure 4.4.

E

Three-species permanence as function of η

Due to the high dimensionality of the inequalities that form criteria for coexistence in three-species systems, the analytical approach that was used in Section 2 to evaluate the probability of permanence as a function of η is not used for three-species systems. Rather, the dependence of the probabilities on η is evaluated numerically. For each $\eta_k \in [0, 1]$ in a suitably fine grid of nodes η_k, $k = 1, 2, \ldots, N_\eta$, we draw $N = 10^6$ random samples of each $\mathcal{E}_i$ and $\mathcal{E}_{ij}$ according to the models and distributions under consideration. Then, the probability of permanence is estimated as the number of permanent systems divided by the total number of sampled systems.
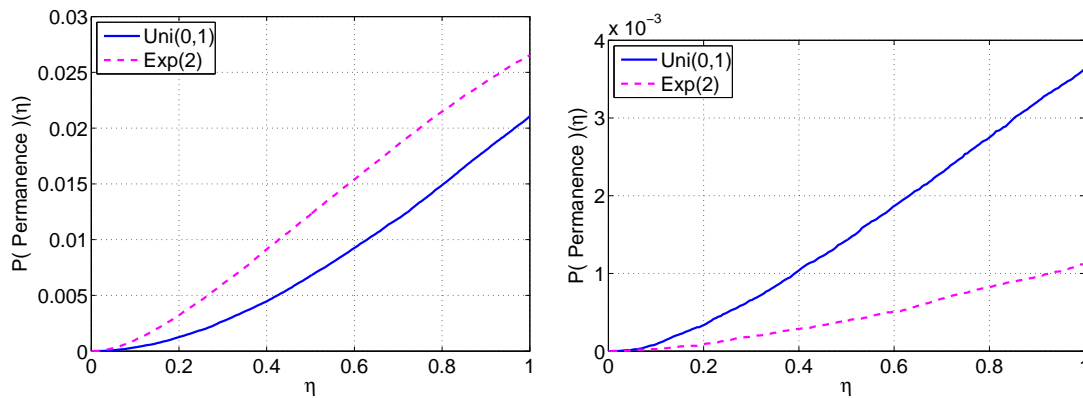
Figure E.1: Probability of existence and stability of an interior fixed point by the criteria in Table 3.1, as function of η. Left: Independent model. Right: Tree hierarchy model.
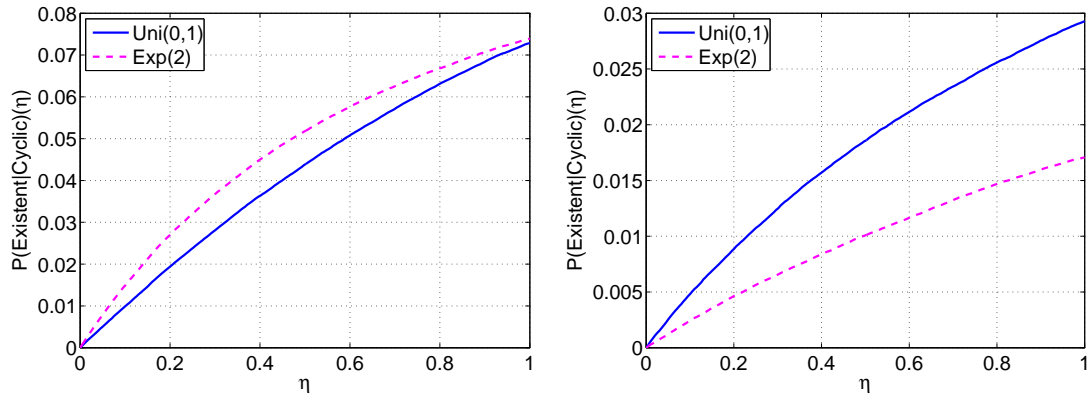
Figure E.2: Probability of existence of a fixed point in the interior of the simplex, given that it would be cyclic by criteria (3.39)-(3.41), as function of η. Left: Independent model. Right: Tree model.
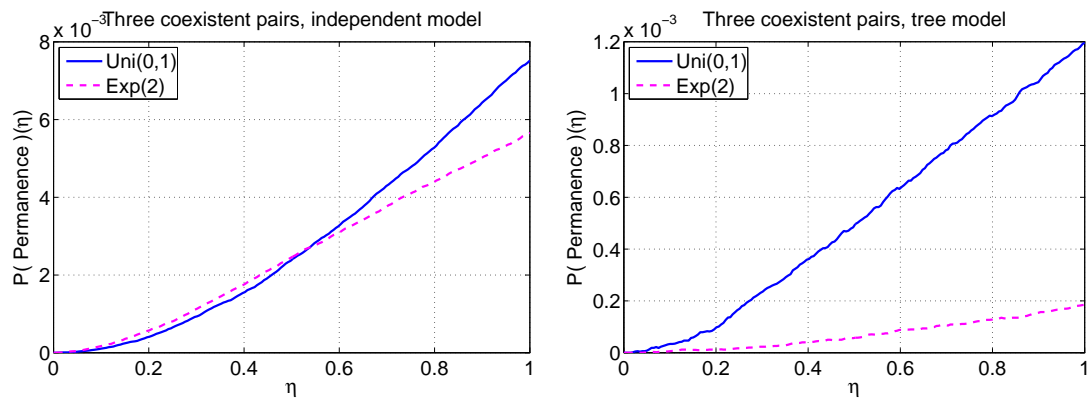

Figure E.3: Probability of permanence by the criteria in Table 3.2 for three coexistent pairs, as function of η. Left: Independent model. Right: Tree model.
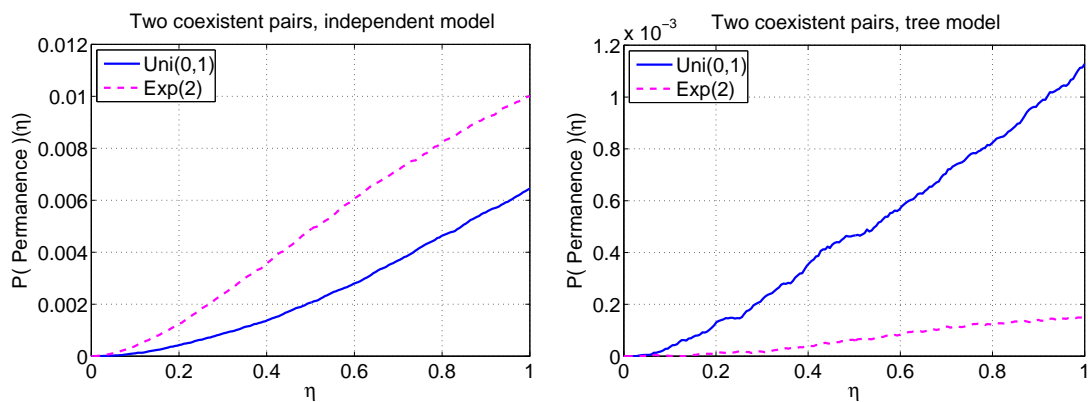

Figure E.4: Probability of permanence by the criteria in Table 3.3 for two coexistent pairs, as function of η. Left: Independent model. Right: Tree model.
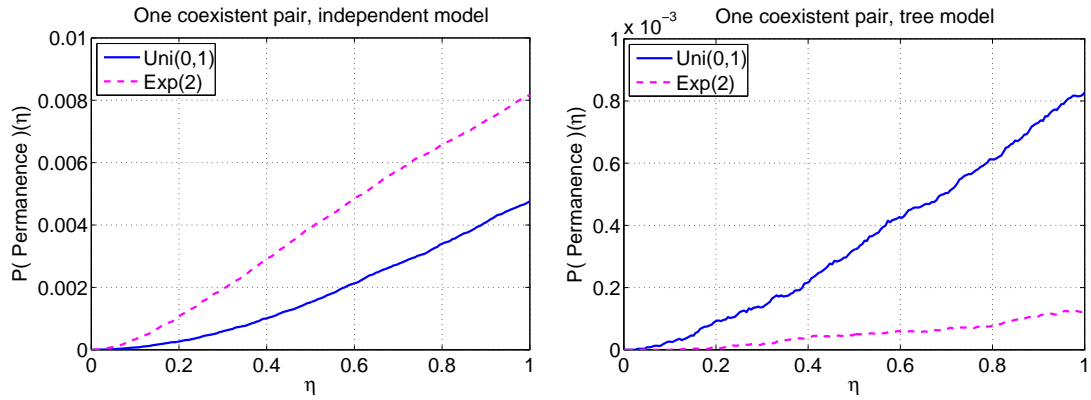
Figure E.5: Probability of permanence by the criteria in Table 3.4 for one coexistent pair, as function of η. Left: Independent model. Right: Tree model.
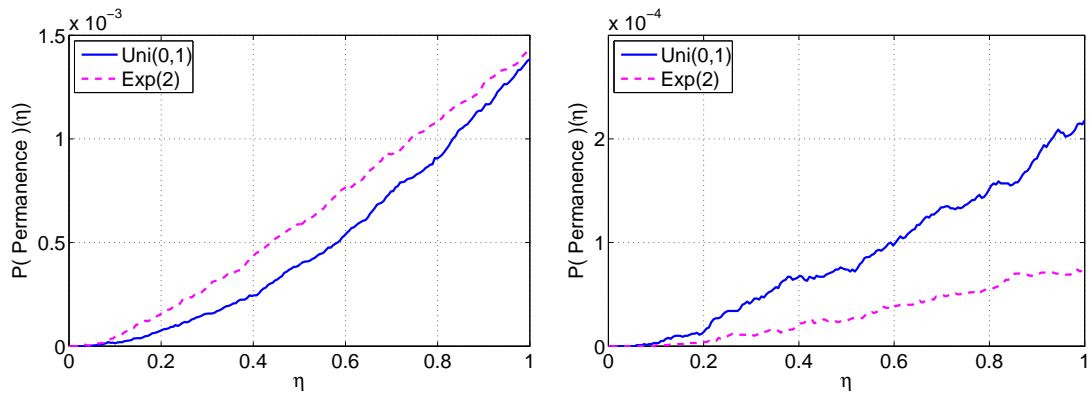

Figure E.6: Probability of permanence in intransitive system by the criteria in Table 3.5, as function of η. Left: Independent model. Right: Tree model.